論文 / 著書情報
Article / Book Information

題目(和文)	
Title(English)	Controlling the Orientation of Ultrathin Phthalocyanine Films by the Molecular-Beam Epitaxy Technique
著者(和文)	星肇
Author(English)	HAJIME HOSHI
出典(和文)	学位:博士(工学), 学位授与機関:東京工業大学, 報告番号:乙第2333号, 授与年月日:1992年3月31日, 学位の種別:論文博士, 審査員:
Citation(English)	Degree:Doctor of Engineering, Conferring organization: Tokyo Institute of Technology, Report number:乙第2333号, Conferred date:1992/3/31, Degree Type:Thesis doctor, Examiner:
学位種別(和文)	博士論文
Type(English)	Doctoral Thesis

Controlling the Orientation of Ultrathin Phthalocyanine Films by the Molecular-Beam Epitaxy Technique

Thesis for a Doctorate

at the

Tokyo Institute of Technology

by

Hajime Hoshi

1992

ACKNOWLEDGMENT

The present work has been carried out under the supervision of Professor Yusei Maruyama (Institute for Molecular Science). The author would like to express sincere gratitude to him for his continual interest and valuable suggestions.

The author would like to express his heartfelt thanks to Professor Riichirô Chûjô (Tokyo Institute of Technology) for his kind reading of the manuscript and valuable suggestions.

The author would like to thank Professor Atsuo Fukuda, Professor Isao Ando, Professor Yoshio Inoue, Associate Professor Yoshio Okahata, and Associate Professor Minoru Sakurai (Tokyo Institute of Technology) for refereeing the thesis.

The author wishes to express his indebtedness to Drs. Tamotsu Inabe and Hideki Masuda (Institute for Molecular Science) for their help of preparation of materials, and to Messrs. Akio Oba and Hiroshi Maebashi (National Institute for Physiological Sciences) for the use of electron microscope, and to Mr. Yoichiro Kawai (Toyota Motor Company) for performing x-ray diffraction measurements. The author is grateful to Dr. Anthony J. Dann (British Telecom) for his collaboration and helpful discussion.

The author thanks all the members of laboratory of Professor Maruyama for their advices and support.

CONTENTS

ABBREVIATIONS

EDP	electron diffraction pattern
FTIR	Fourier-transform infrared
LEED	low-energy electron diffraction
MBE	molecular-beam epitaxy
Pc	phthalocyanine
AlPcCl	chloroaluminum phthalocyanine
$(AlPcF)_n$	fluoro-bridged aluminum phthalocyanine polymer
LiPc	lithium phthalocyanine
$LuPc_2$	lutetium diphthalocyanine
MPc	metal phthalocyanine
VOPc	vanadyl phthalocyanine
RHEED	reflection high-energy electron diffraction
SEM	scanning electron microscopy
TEM	transmission electron microscopy
UHV	ultrahigh-vacuum
XPS	x-ray photoelectron spectroscopy
XRD	x-ray diffraction

CHAPTER 1 GENERAL INTRODUCTION

1-1. MOTIVATION OF CONTROLLING THE STRUCTURES OF ULTRATHIN ORGANIC FILMS

Controlling the structures of molecular or atomic assemblies leads to controlling their functions. The development of the technique for the structural control has been one of the main subjects in material science. The states of assemblies, which are to be controlled, are well represented by two simple indices. The first one is crystallinity, whose influence on the properties has been well known. The crystal growth technique has become important. The second index is size of the system. This classifies the systems into bulk, films, and clusters. Many researchers have been trying to find the differences in their properties derived from small size (film or cluster), but only a little knowledge has been obtained. The difficulty in progress of the study arises from the lack of the technique that enables us to control both crystallinity and size at once.

In ultrathin films, which are expected to become the models of two-dimensional systems and advantageous forms to device applications, inorganic semiconductor system has been most extensively studied. In this system, Esaki *et al.*'s development of the molecular-beam epitaxy (MBE) technique, which is vacuum deposition under ultrahigh-vacuum ($<10^{-9}$ Torr), has overcome the difficulty. The MBE technique has opened up the new system of the crystalline ultrathin films and led to

the discovery of new phenomenon called quantum Hall effect and the realization of new devices such as high electron mobility transistors and quantum well lasers.[1-3] The attainment in inorganic semiconductor has stimulated the researchers' interest in ultrathin films. The MBE technique has been successfully applied to metal system as well.[4]

Recently, ultrathin organic films have received much attention. Various functions of organic molecules promise well for the realization of future electronic and optical devices.[5] In this system, structural control, crystallinity and thickness, are essential as well. Previous studies about thick organic films have shown that the crystallinity has much influence on the electronic and optical properties.[6] Because of the difficulty in preparation, researchers have not reached satisfactory studies of ultrathin organic films. In organic system, controlling techniques for ultrathin films has been less sophisticated than those in inorganic and metal systems. This situation motivates the present study. The main subject of the thesis is thus to develop a technique of controlling ultrathin organic films. For that purpose, the MBE technique is established. Considering the success in inorganic and metal systems, the MBE technique is promissing in organic system as well, though such trials have been very rare.

In the next section, previous techniques used to prepare ultrathin organic films will be reviewed, and the problems inherent in organic system will be presented.

1-2. PRESENT SITUATION OF PREPARING ULTRATHIN ORGANIC FILMS

In academic side, two types of technique are mainly used to prepare ultrathin organic films. One is Langmuir-Blodgett (LB) film technique, and the other is vacuum deposition technique. LB technique has been the most widely used technique to prepare ultrathin organic films.[7] Organic amphiphilic molecules are developed on the surface of water to form monomolecular films, which are picked up on a substrate. The advantage of LB technique is easy controllability of thickness. However, it has disadvantages as well. To form LB films, special types of molecules must be synthesized. The use of solvent may introduce ingredients in the resultant films.

Vacuum deposition technique overcomes the problem of ingredients, since this is dry process. This technique is applicable to the molecules that can be sublimed without decomposition. The base pressure usually used in organic system has been in the range of high-vacuum ($>10^{-6}$ Torr). It has been known that this technique can produce oriented organic films since a long time ago.[8] In particular, the films of linear molecules such as fatty acids, and planar molecules such as phthalocyanines have been extensively prepared and observed by electron microscopy.[9-12] The orientation found in these films was assumed to be derived from the following mechanism.[13,14] When a molecule is adsorbed on the surface of the substrate, it is fixed with specific orientation. This provides a nucleation site where the following molecules are

condensed into their crystal form. Thus, the resultant films consist of microcrystallites. The crystallinity of each microcrystalline is good. However, it seems difficult to orient each microcrystalline to form a single-crystalline film. For that purpose, more elaborate technique is required.

In inorganic and metal systems, it has been known that ultrahigh-vacuum ($<10^{-9}$ Torr) is a necessary condition to prepare high-quality ultrathin films, though organic films have been usually prepared under high-vacuum ($>10^{-6}$ Torr). The condition of ultrahigh-vacuum enables us to prepare clean surfaces of the substrates. As a result, it becomes possible that the deposited particles are oriented to match with the surface nets of the substrates. Crystal growth based on this phenomenon is called epitaxial growth, and it is a basis of the MBE technique that can produce single-crystalline ultrathin films. The application of this technique to organic system is promissing as well, though such studies have been very rare.

The principal difficulty of the MBE technique arises from the lack of the knowledge about the epitaxy. The condition of the epitaxial growth has not been well known. Since organic molecules are bigger and more complicated than the components of inorganic and metal systems, epitaxial growth is supposed to be more difficult to occur. It has been pointed out that organic molecules are too big to match with primitive nets of the usual substrate surfaces.[15]

So the following questions arise:

Is epitaxial growth possible ?

If possible, what is the condition ?

In 1977, Somorjai *et al.*'s group gave one answer. They deposited metal free-, copper-, and iron- phthalocyanines on clean copper surfaces, Cu(100) and Cu(111), under ultrahigh vacuum. The growth process was monitored by low-energy electron diffraction. New crystal structures of phthalocyanines was identified, which matched with the nets of the copper surfaces.[16] This observation shows that the MBE technique is promissing. However, they did not study the morphology of the films, since preparation of the thin films was not their purpose. This principle had not been applied to prepare ultrathin organic films until a few recent MBE studies have started.[17-19] The problems of realizing the epitaxy and controlling the structures are still unsolved.

The main subject of the present thesis is thus looking for the condition that provides high-quality ultrathin organic films by using the MBE technique.

Once the ultrathin films are prepared, the next step is to evaluate their quality. For that purpose, the electron microscopy technique developed by Kyoto university group has been known to be excellent.[20,21] Arrangements of the molecules such as phthalocyanine can be directly observed and even small defects in the crystals can be distinguished. Experimental technique to observe surface structure is developing at a high speed. Recently developed scanning tunneling microscopy is epoch-making, which succeeded in observing an isolated phthalocyanine molecule.[22] Though this technique is promissing, application to insulating organic molecules is still difficult at present. In this study,

ordinary electron microscopy is mainly used to analyze the structure of the films.

1-3. ADVANTAGES OF PHTHALOCYANINES

As described in the preceding section, this study aims to look for the conditions that provide high-quality ultrathin organic films by using the MBE technique.

The materials used in this study are phthalocyanines (Pc). Phthalocyanines have the advantages described in the following paragraphs.

Phthalocyanines are stable and sublimable without decomposition. This condition must be satisfied to prepare MBE films.[23]

Vapor-pressure of phthalocyanines is 10^{-14} Torr at room temperature, so they can be treated under ultrahigh-vacuum.[16]

The sublimation temperature of phthalocyanines under vacuum is about 400°C, so the deposited films are stable under ultrahigh-vacuum without resublimation.

Phthalocyanines are planar and highly symmetrical molecules. This will enhance the possibility of realizing the epitaxy.

The film structure of phthalocyanines can be directly observed by electron microscopy. Phthlocyanines have been known to resist being damaged by electron-beam, and many pictures have been taken by electron microscopy.[20,21]

The physical and chemical properties of phthalocyanines have attracted many researchers' attention. Some books and

reviews on phthalocyanines have been published.[24-27] Figure 1.1 shows the molecular structure of phthalocyanine, which is conjugated planar molecule. Various metal ions (M) coordinate at the center of phthalocyanine to form complexes (MPc), so various properties have been observed. More than 12000t phthalocyanine is being produced in Japan per year for the commercial use as pigments (blue-green color). Chemical and thermal stability is known to be good. The crystals of phthalocyanines have typical one-dimensional column structures, which consist of stacked phthalocyanine planes (Fig. 1.2). Phthalocyanines have been known to be one-dimensional electrical semiconductors. In some cases, even the metallic conduction has been realized.[28,29] Phthalocyanines have been known to show photoconduction,[30] electrochromism (from red to violet and *vice versa*),[31] large optical nonlinearity,[32,33] and so on. Preparation of high-quality ultrathin phthalocyanine films will contribute to advances in such studies.

1-4. SCOPE OF THE THESIS

The following phthalocyanine complexes are studied in the present thesis.

Fluoro-bridged aluminum phthalocyanine polymer, $(AlPcF)_n$, (Fig. 1.3), lutetium diphthalocyanine, $LuPc_2$, (Fig. 1.4), lithium phthalocyanine, LiPc, (Fig. 1.5), chloroaluminum phthalocyanine, AlPcCl, (Fig. 1.6), and vanadyl phthalocyanine, VOPc (Fig. 1.7).

The stacking structure is stabilized in polymer

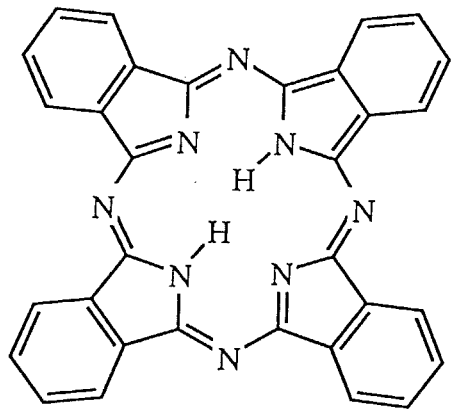

FIG. 1.1. Molecular structure of metal-free phthalocyanine.

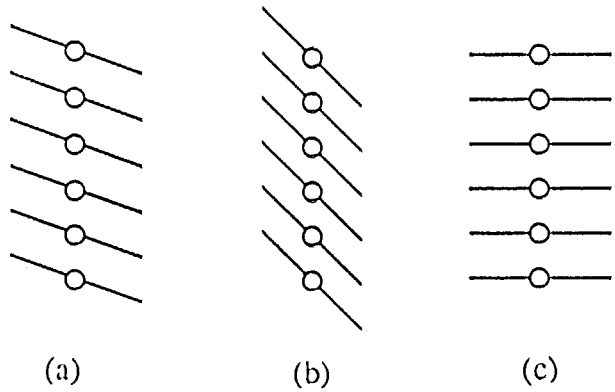

FIG. 1.2. Principal stacking geometries of phthalocyanines (a) α-form, (b) β-form, and (c) cofacial form.

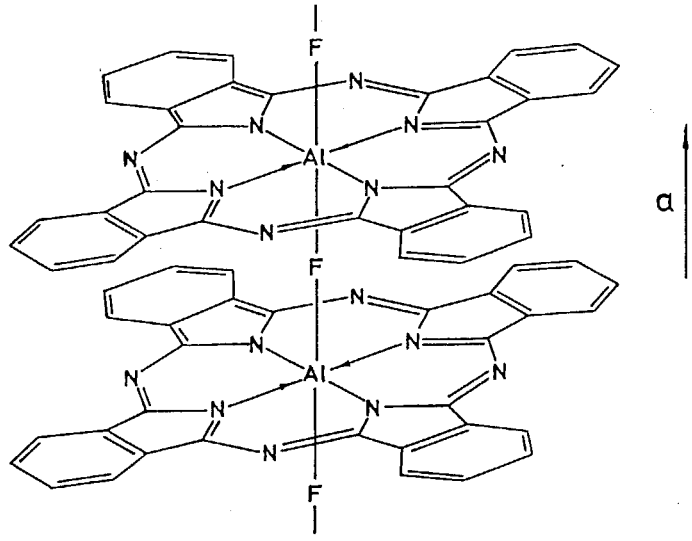

FIG. 1.3. Molecular structure of $(AlPcF)_n$.

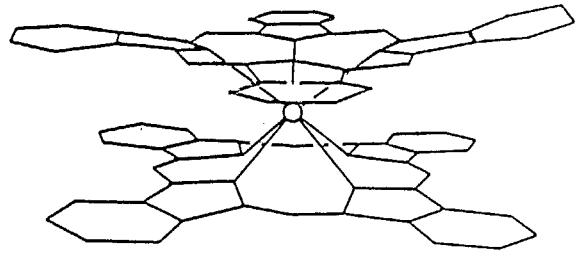

FIG. 1.4. Molecular structure of $LuPc_2$.

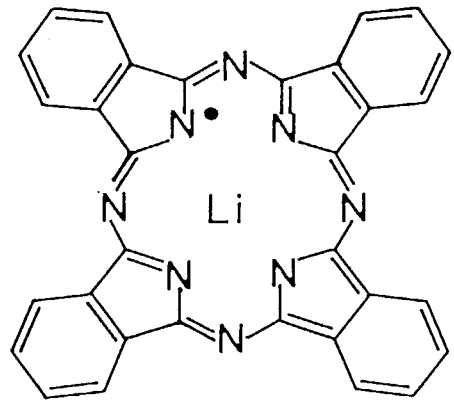

FIG. 1.5. Molecular structure of LiPc.

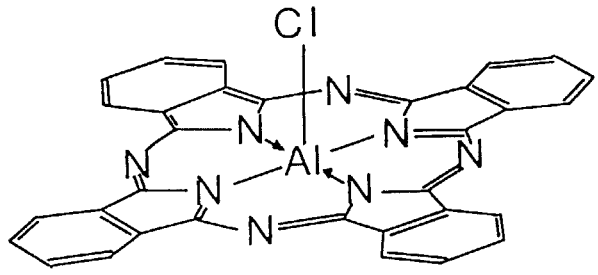

FIG. 1.6. Molecular structure of AlPcCl.

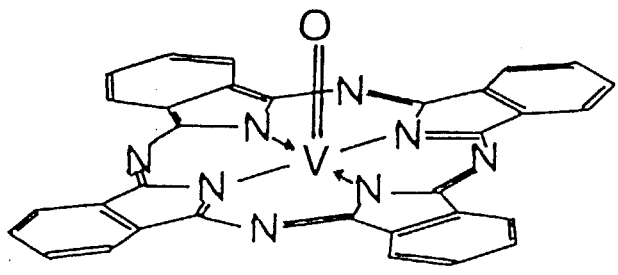

FIG. 1.7. Molecular structure of VOPc.

phthalocyanine, $(AlPcF)_n$, so highly stable films are expected to be obtained. In chapter 2, the relation between growth conditions and the resultant structures of $(AlPcF)_n$ films is studied.

In chapter 3, ultraviolet / visible spectra are studied to know the effect of the film structure on the electronic states of $(AlPcF)_n$.

In chapter 4, dimeric phthalocyanine, $LuPc_2$, is studied. The effect of the phthalocyanine form on the resultant film structure is studied.

In chapter 5, monomeric phthalocyanine, LiPc, is studied. The effect of the phthalocyanine form on the resultant film structure is studied.

In chapter 6, monomeric phthalocyanines, AlPcCl and VOPc, that have protrudent atoms on the phthalocyanine planes are studied. The effects of the protrudent atoms on the resultant film structures are studied.

In chapter 7, the results of this study are summarized.

REFERENCES

[1]Nihonbutsurigakkai, *Handotaichokoshi no butsuri to sonooyo* (Baifukan, Tokyo, 1984).

[2]M. Konagai, *Handotaichokoshi nyumon* (Baifukan, Tokyo, 1987).

[3]E. Corcoran, Scientific American **263**(5), 74 (1990).

[4]T. Shinjo, Kotaibutsuri **21**, 582 (1986).

[5]A. Yabe, Y. Taniguchi, H. Masuhara, and H. Matsuda, *Yukichohakumaku nyumon* (Baifukan, Tokyo, 1989).

[6]Y. Maruyama and H. Inokuchi, Kagaku to kogyo **40**, 826 (1987).

[7]Proc. 4th Int. Conf. LB Films, Thin solid Films **178-180** (1989).

[8]See, for example, H. Inokuchi, H. Kuroda, and H. Akamatsu, Bull. Chem. Soc. Jpn. **34**, 749 (1961).

[9]M. Okada and T. Kanaji, *Hyomen no kagaku* (Otsuki Shoten, Tokyo, 1986).

[10]K. Inaoka, K. Yase, K. Sato, and M. Okada, Hyomen **24**, 61 (1986).

[11]M. Ashida, Hyomen **25**, 207 (1987).

[12]K. Inaoka and K. Yase, *Shinkuchu de bunshi o naraberu-yukijochakumaku* (Kyoritsu shuppan, Tokyo, 1989).

[13]M. Ashida, Bull. Chem. Soc. Jpn. **39**, 2625 (1966).

[14]M. Ashida, Bull. Chem. Soc. Jpn. **39**, 2632 (1966).

[15]M. Hara, H. Sasabe, and A.Yamada, Seni to kogyo **45**, 210 (1989).

[16]J. C. Buchholz and G. A. Somorjai, J. Chem. Phys. **66**, 573 (1977).

[17]A. Yamada, K. Shigehara, and M. Hara, Synth. Met. **18**, 821 (1987).

[18]M. Komiyama, Y. Sakakibara, and H. Hirai, Thin Solid Films **151**, L109 (1987).

[19]M. Hara, H. Sasabe, A. Yamada, and A. F. Garito, Jpn. J. Appl. Phys. **28**, L310 (1989).

[20]N. Uyeda, Nihon kessho gakkaishi **25**, 51 (1983).

[21]N. Uyeda, Dyes and Pigments **6**, 115 (1985).

[22]P. H. Lippel, R. J. Wilson, M. D. Miller, Ch. Woll, and S. Chiang, Phys. Rev. Lett. **62**, 171 (1989).

[23]K. Isa, K. Sasaki, I. Murano, K. Fukui, and K. Mizuda, Nihon

kagakukaishi 615 (1985).

[24]E. Suito, Kinzokubutsuri seminar 1, 151 (1976).

[25]K. Kasuga and M. Tsutsui, Coord. Chem. Rev. **32**, 67 (1980).

[26]F. H. Moser and A. L. Thomas, *The Phthalocyanines* (CRC, Boca Raton, FL, 1983), Vol. 1-2.

[27]M. R. Willis, Mol. Cryst. Liq. Cryst. **171**, 217 (1989).

[28]T. J. Marks, Angew. Chem. Int. Ed. Engl. **29**, 857 (1990).

[29]Y. Orihashi and E. Tsuchida, in *Kobunshi sakutai*, edited by E. Tsuchida, N. Toshima, and H. Nishide (Gakkai shuppan center, Tokyo, 1990), Vol. 3, Chap. 3.

[30]See, for example, T. Tanaka and R. Hirohashi, Nihon kagakukaishi, 867 (1989).

[31]See, for example, G. C. S. Collins and D. J. Schiffrin, J. Electroanal. Chem. **139**, 335 (1982).

[32]Z. Z. Ho, C. Y. Ju, and W. M. Hetherington III, J. Appl. Phys. **62**, 716 (1987).

[33]T. Wada, S. Yamada, Y. Matsuoka, C. H. Grossman, K. Shigehara, H. Sasabe, A. Yamada, and A. F. Garito, in *Nonlinear Optics of Organics and Semiconductors*, edited by T. Kobayashi (Springer, Berlin, 1989), p. 292.

CHAPTER 2 EPITAXIAL GROWTH OF ULTRATHIN FILMS OF FLUORO-BRIDGED ALUMINUM PHTHALOCYANINE POLYMER

2-1. INTRODUCTION

The possibility of producing highly ordered, well-characterized ultrathin films of phthalocyanine-(Pc) based compounds is a prime objective of the research into future electronic or optoelectronic device applications utilizing this class of materials. The technique of vacuum evaporation is an excellent method for large-scale film growth, and most phthalocyanines are readily sublimable.

Initial studies of the structure of films prepared in this manner have shown that the orientation of the planar copper phthalocyanine molecule (CuPc) on various substrate surfaces is influenced by the nature of the substrate and its pretreatment.[1,2] In these reports, the pressure during evaporation was of the order of 10^{-5} Torr, and the rate of sublimation was relatively high (20-30 $\mathring{A}$ min^{-1}). As a result the films were largely composed of small crystal islands, and continuity was poor. High continuity is a neccessary criterion for future large-scale integration.

More recently the technique of ultrahigh-vacuum (UHV, $<10^{-9}$ Torr) deposition has been developed, which offers a precise control of sublimation rate and minimal incorporation of impurities during growth. Such control has permitted the preparation of high-quality CuPc films on amorphous quartz substrates.[3] X-ray diffraction studies indicate a single

orientation of the molecule with respect to the substrate surface, whereas higher-pressure vapor deposition results in mixed orientation films. A film of NiPc on indium tin oxide Nesa glass also grown under UHV was found to be very smooth and showed enhanced rectification characteristics when incorporated into a Schottky-barrier cell.[4]

The use of a single-crystal substrate, which can influence the resultant film structure, combined with a vacuum evaporation under UHV conditions is the basis of the molecular-beam epitaxy (MBE) technique.[5] A UHV low-energy electron diffraction (LEED) study of the deposition of H_2Pc, CuPc, and FePc on single-crystal Cu(100) and (111) substrates has shown that true epitaxial growth can occur in which the resultant structure consists of domains whose relative orientation is governed by the symmetry elements of the substrate.[6]

In an attempt to grow high-quality, continuous phthalocyanine films of a significant scale, the MBE technique is studied in this work. The cofacially stacked phthalocyanine polymer system $(AlPcF)_n$, where Al is the central metal aluminum atom and F is the bridging fluorine ligand, has interesting optical and electrical properties.[7,8] A variety of single-crystal substrates are used to determine the optimum choice for the preparation of single orientation, highly ordered films of the $(AlPcF)_n$ material. The role of substrate temperature on the growth process is also investigated.

2-2. EXPERIMENT

The $(AlPcF)_n$ material was synthesized by the established method of Linsky *et. al.*[9] Purification was carried out by twice sublimating at 10^{-6} Torr using a gradient sublimation system.[10] This gave highly pure material as confirmed by microanalysis: Mass % calculated for $C_{32}N_8H_{16}AlF$- C,68.8; H,2.9; N,20.1; F,3.4; Cl,0.0; found- C,68.83; H,2.69; N,19.97; F,3.26; Cl,0.0. The structure of the cofacially stacked system is shown in Fig. 2.1 with the crystal a-axis labeled by analogy to the known $(GaPcF)_n$ crystal structure.[11]

The substrates are prepared as follows. Single-crystal silicon(100) 15×15×0.5 mm^3 wafers were supplied by Hitachi Ltd. The cleaning of the surface was achieved by baking at 700 °C for 1 h in the MBE chamber. Fused quartz disks (17 mm diameter, 1 mm thick) were ultrasonically washed with detergent and distilled water and then baked under the same conditions. The alkali halide substrates of KCl, KBr, and KI were supplied as single-crystal blocks (15×15×15 mm^3) by Furuuchi Chemical Corporation. Cleavage of the blocks was carried out in an argon atmosphere using a razor blade. Subsequent baking in the MBE chamber at 500 °C for 30 min is known to produce high-quality surfaces.[12] The substrates were mounted onto an ultrasonically cleaned stainless-steel substrate holder for transfer into the main MBE chamber.

The MBE system was specially designed to be used for organic film growth (Fig. 2.2). It incorporates a sample transfer system so that the main chamber is maintained at 10^{-9}

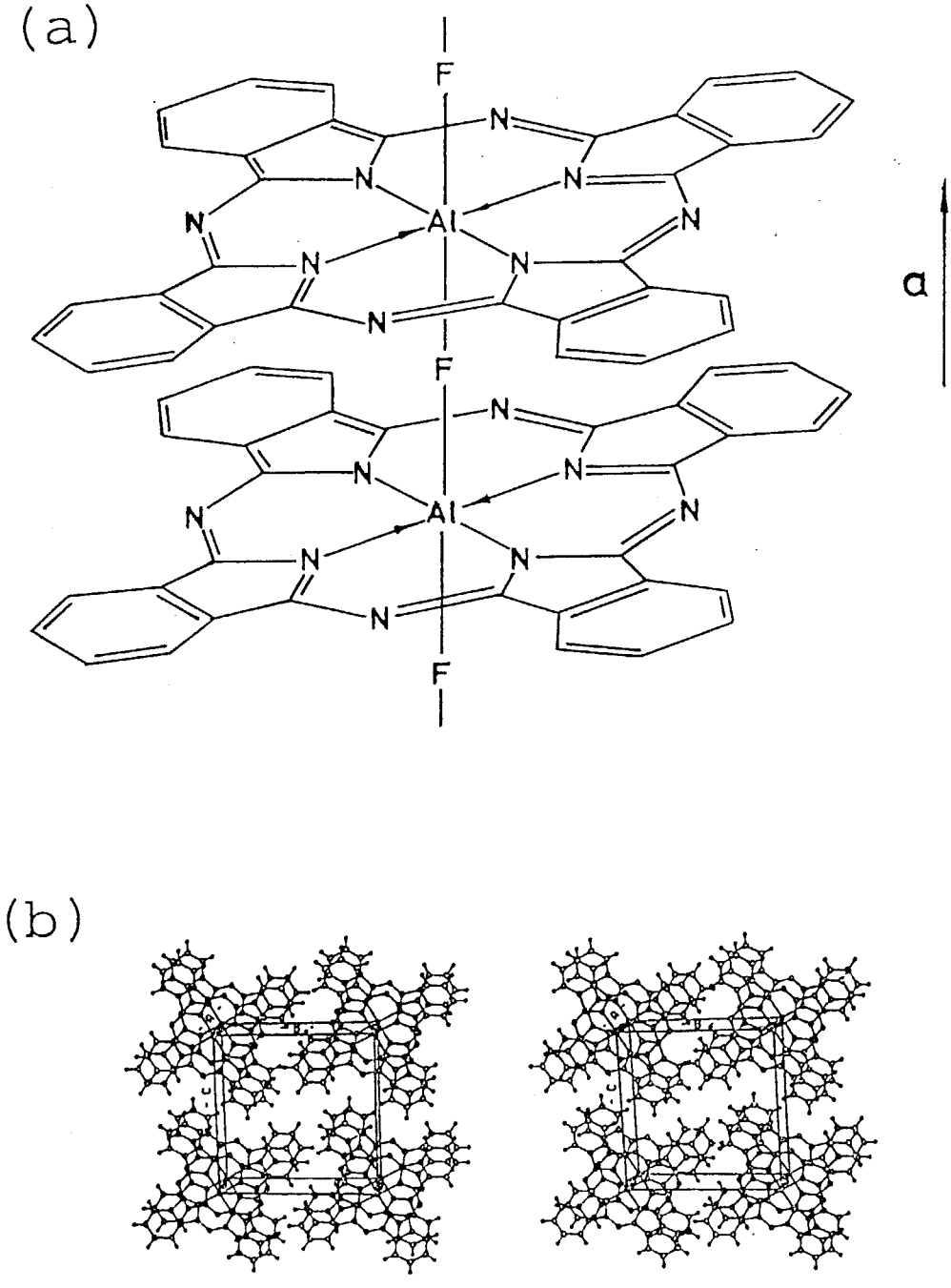

FIG. 2.1. (a) Molecular structure of $(AlPcF)_n$ and (b) the crystal structure of $(GaPcF)_n$ cited from ref. 11.

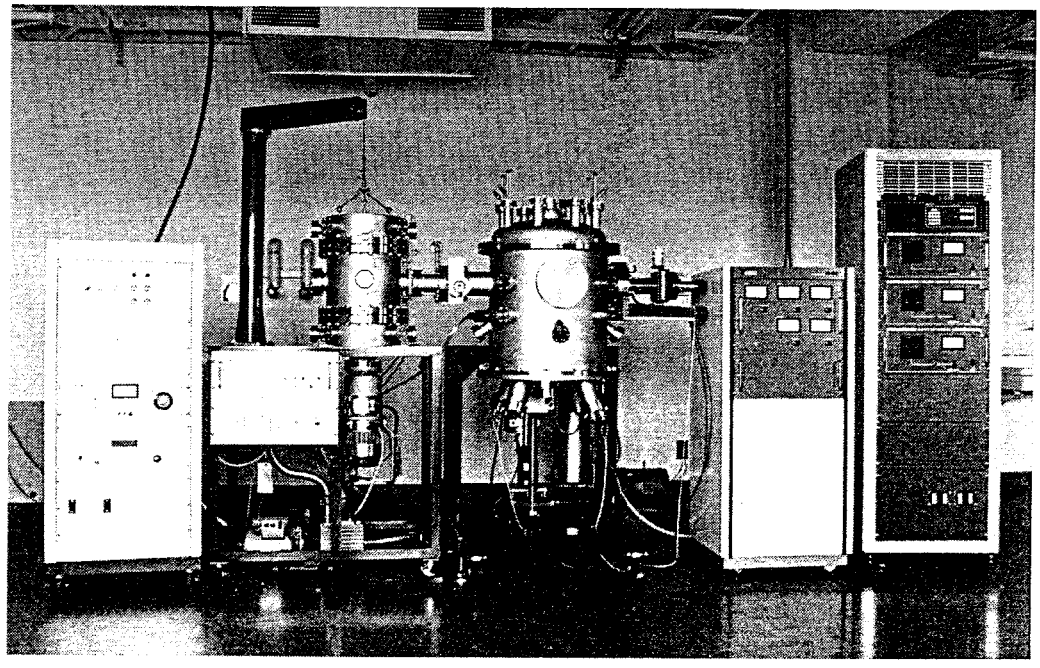

FIG. 2.2. The MBE system used in this experiment.

Torr or better by a cryopump coupled with an ionization pump. There are four separate Knudsen cell source compartments so that the deposition of multilayer heterogeneous films is possible. Film growth is monitored by an oscillating quartz-crystal system (Leybold-Heraeus Inficon IC6000). The distance from source to substrate holder in the chamber is 26 cm and the angle of incidence of impinging molecules is 25°. Substrate temperature can be varied from -170 to 750 °C. Low temperatures are made available by the flow of liquid nitrogen around the substrate holder. There is a mass spectrometer system (ULVAC MSQ400) that can monitor the residual gases and/or decomposition products during the evaporation.

Typical conditions for film growth are as follows; with base pressures of the order of 10^{-9} Torr or better the pressure during evaporation is usually 10^{-8} Torr or better. This results in a controlled growth rate of 0.02-0.03 $\mathring{A}\ s^{-1}$ using a Knudsen cell source temperature of 410 °C. The optimum thickness of the films for subsequent characterization was 100 $\mathring{A}$.

X-ray photoelectron spectroscopy (XPS) was carried out on films grown on silicon substrates by a VG Instruments ESCALAB MkII spectrometer using a Mg Kα source. The difficulty with charge buildup resulted in unwanted chemical shifts for samples grown on the highly resistive alkali halide substrates.

X-ray diffraction (XRD) studies were performed on a JEOL JSDX-60A2 instrument using a CuKα source. The sampling area was less than $2\times10\ mm^2$ and the angle of sample incidence was 1°.

Scanning electron microscopy (SEM) was carried out on a Hitachi S900 instrument. Because of charge buildup problem it was necessary to precoat the films with 15 Å of platinum using an ion sputterer in order to obtain satisfactory images.

Transmission electron microscopy (TEM) was studied using a Phillips EM400T instrument. The films were coated with carbon (15 Å) and then removed from the substrates by the wet stripping method. Water was used as the solvent for alkali halide and 0.1 *N* KOH was used for films on quartz and silicon. The samples withstood the damage by the electron beam, enabling the acquisition of good images and diffraction patterns with an accelerating voltage of 120 kV.

Fourier-transform infrared (FTIR) spectra were recorded on a Bomem DA3.002 spectrophotometer. Such an instrument was capable of giving excellent spectra of films of only 100 Å thickness after 1000 scans. In the case of films on silicon, the sample was first removed by the wet stripping method and then remounted onto a KCl substrate.

2-3 RESULTS AND DISCUSSION

The crystal structure of the ligand-bridged cofacially stacked polymeric phthalocyanines belongs to the triclinic space group of $P\bar{1}$. The three crystal axes are almost perpendicular, and the stacks form molecular columns, which appear as a square lattice when viewed along the a-axis. The phthalocyanine ring systems on successive metals are eclipsed.[13] Sublimation is assumed to occur by thermal

breakage of the weak fluorine bridge, which reforms during condensation. It is possible that dimer and oligomer sublimation produced by nonuniform bridge breaking may also occur. The high stability of the phthalocyanine molecule is well known[14] but possible decomposition was monitored. Mass spectra taken during the evaporation indicated that this occurs if the Knudsen cell source is overheated (>450 °C at 10^{-9} Torr). To avoid this and the subsequent deposition of unwanted material at the substrate surface, the source was maintained at or below 410 °C during all film preparation so that the phthalonitrile fragment peak at an *m/e* ratio of 128 was not detected.[15]

The XPS spectra of the films showed all the atomic peaks in the correct ratios [F_{1S}/N_{1S} = 0.35 (calc. 0.31) and Al_{2p}/F_{1S} = 0.18 (calc. 0.18)] [Fig. 2.3(a)]. It was concluded that no decomposition of the molecule occurs during condensation on the substrate. This was confirmed by the high-resolution C_{1s} spectrum, which is very characteristic of phthalocyanine and consists of three features; a peak at 289.2 eV due to phenyl carbons, one at 290.6 eV due to pyrrole carbons, and a π-π^* satellite at 292.7 eV [Fig. 2.3(b)].[16]

A. The structure of films on silicon(100) and quartz substrates

The structure of films grown on these substrates are similar to each other and so the following discussion of silicon substrate results is also applicable to quartz. The

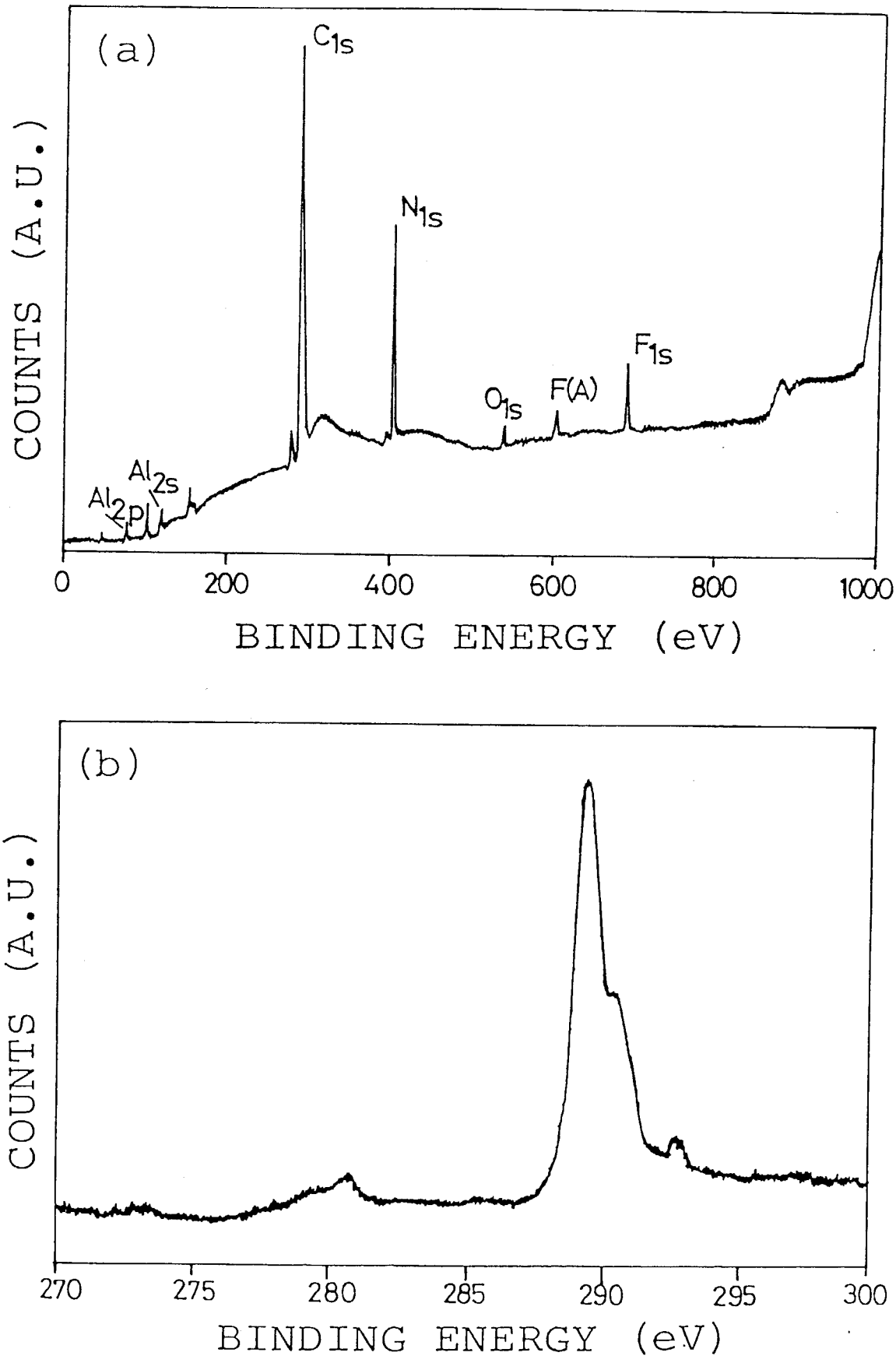

FIG. 2.3. The XPS spectra of an 85-Å $(AlPcF)_n$/Si deposited at 35 °C: (a) wide range and (b) C_{1s} region.

XRD patterns of these films consist of one peak centered at approximately 2θ = 6.0°, which corresponds to an interstack spacing of 14.7 Å (Fig. 2.4). The orientation of the phthalocyanine polymer thus occurs with the polymer backbone (a-axis) parallel to the substrate surface plane, and this distance represents the interstack dimension as depicted in the figure. The absence of any other peak in the pattern indicates that only this orientation predominates. This is also concluded from the transmission FTIR study in Fig. 2.5. The vibrational peak at 723±2 cm^{-1} is due to the C-H out-of-plane bending mode and so is expected to be intense compared to the C-N stretching at 1083 cm^{-1} and the C-H in-plane bending at 1123 cm^{-1}, when the plane of the molecule is perpendicular to the surface.[17]

The TEM image and electron diffraction pattern (EDP) are shown in Fig. 2.6. On very low-temperature substrates the films are very continuous, and it is difficult to observe any detailed structure. However, on higher-temperature substrates (e.g., 30 °C) the structure consists of randomly oriented crystallites. The EDP of such a film shows two intense but diffuse concentric rings at equivalent lattice spacings of 3.6 and 12.7 Å (by reference to a gold standard), which again confirms the parallel a-axis orientation. The diffuse ring pattern is a consequence of the crystallite disorder.

On 200 °C substrates these crystallites are much larger, and a wormlike structure is apparent [Fig. 2.7(a)]. The width of each worm is approximately 200 Å but with indefinite length. They are intermingled in a complex random network. It is

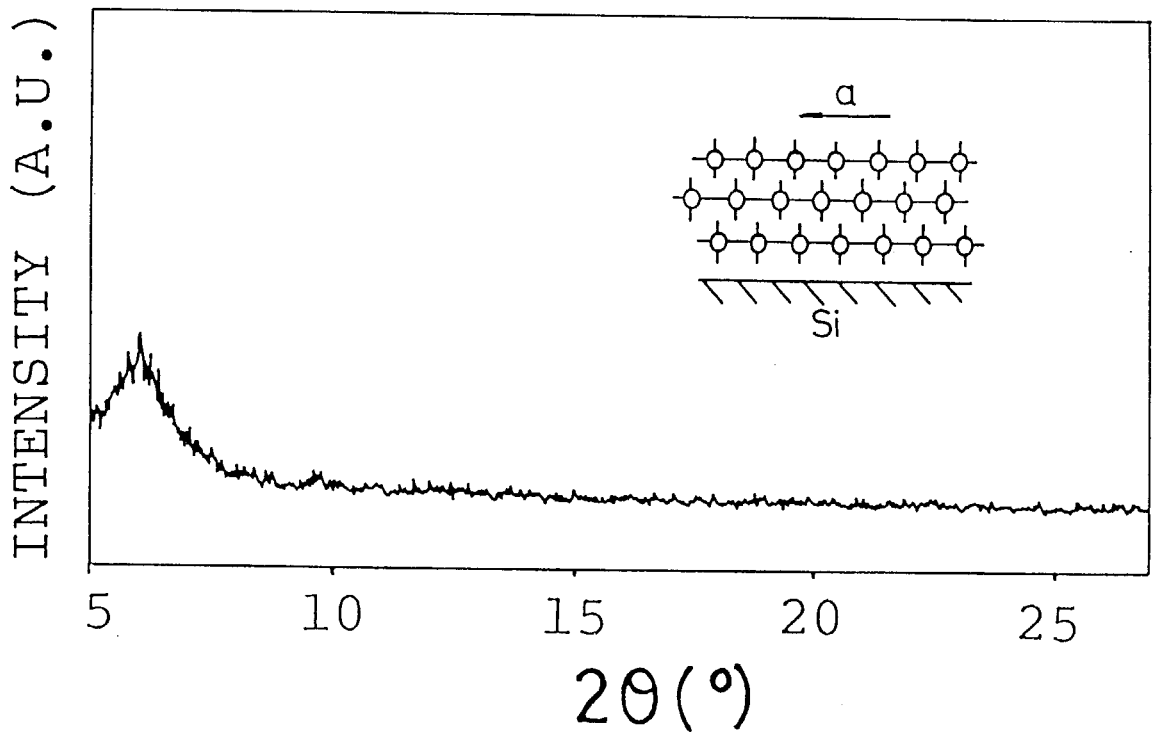

FIG. 2.4. The XRD pattern of an 85-Å $(AlPcF)_n$/Si deposited at 35 °C.

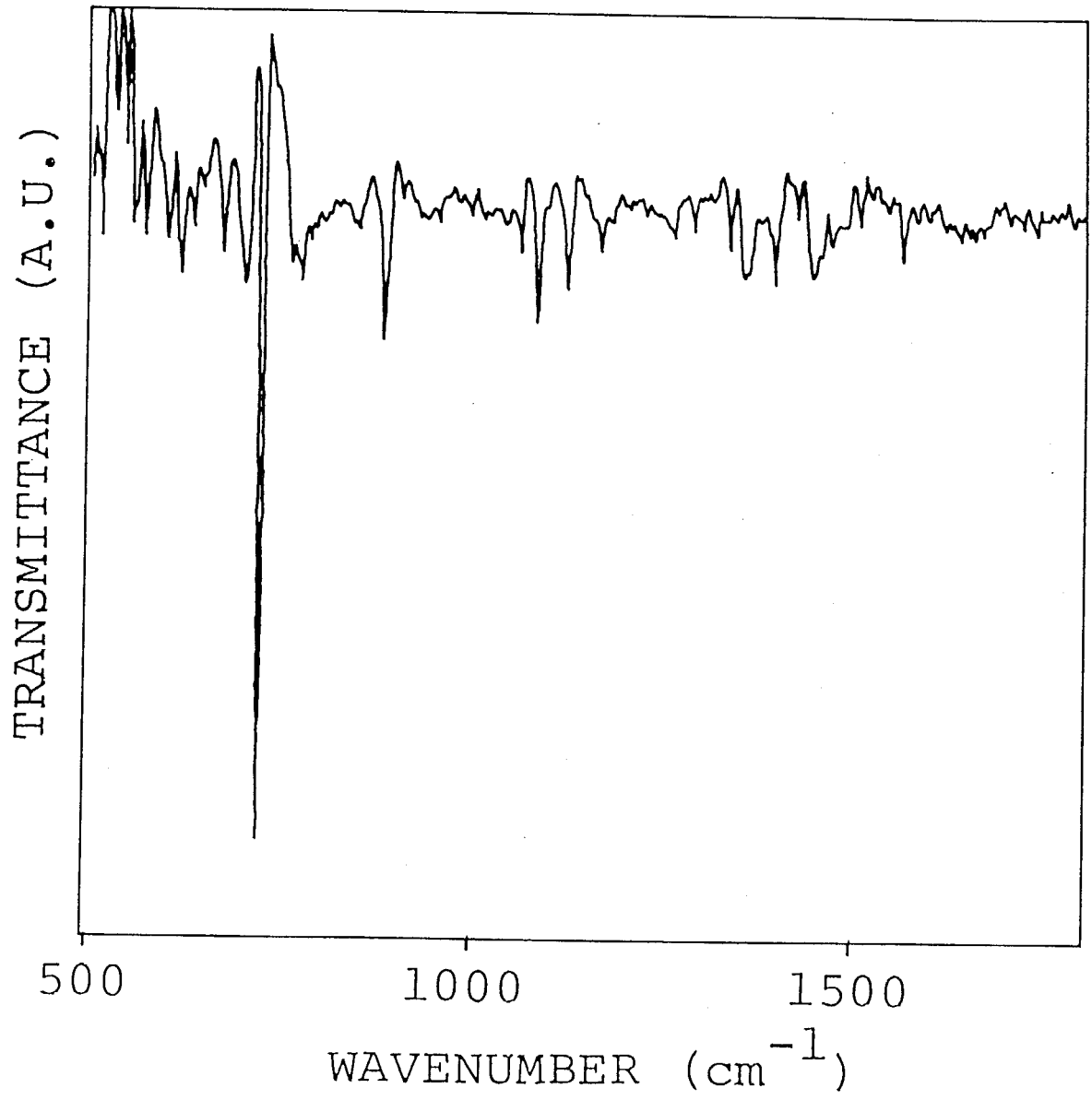

FIG. 2.5. The transmission FTIR spectrum of a 180-Å $(AlPcF)_n$/Si deposited at 200 °C.

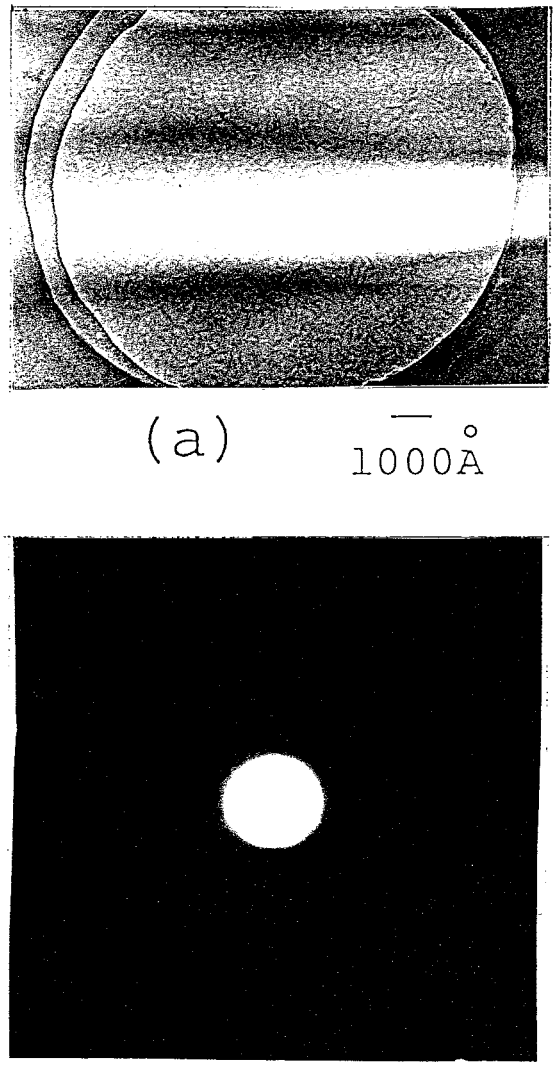

FIG. 2.6. (a) The TEM image of an 85-Å $(AlPcF)_n$/Si deposited at 35 °C and (b) the EDP of a 100-Å $(AlPcF)_n$/Si deposited at 27 °C.

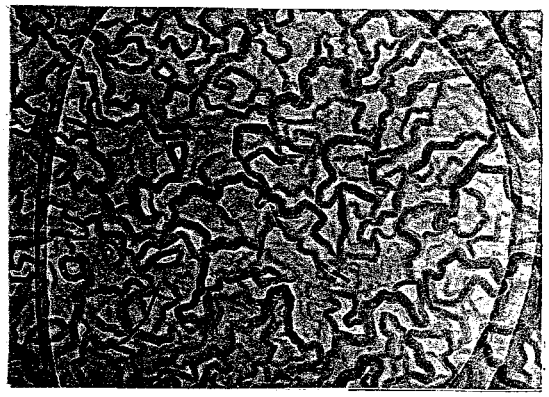

(a) 1000Å

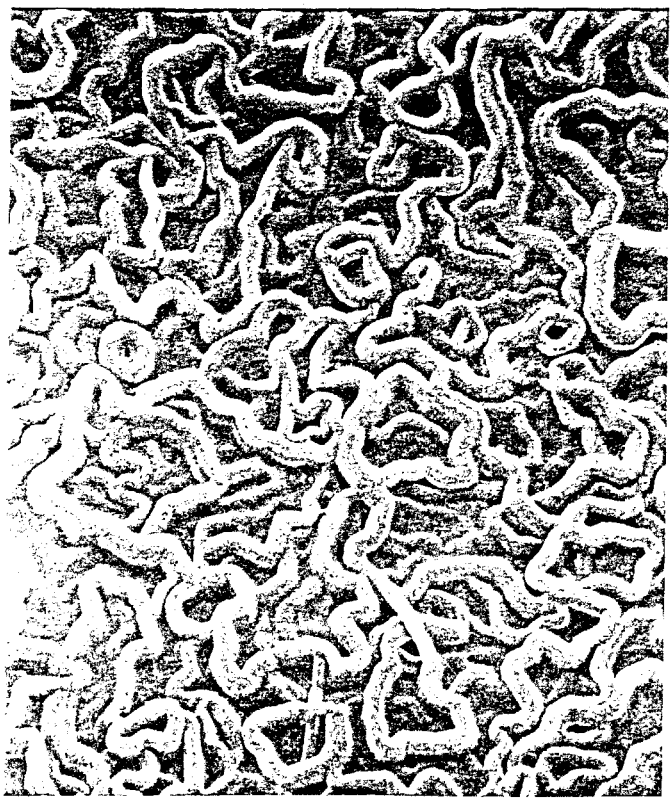

1000Å

(b)

FIG. 2.7. (a) The TEM image of a 200-Å $(AlPcF)_n$/Si deposited at 200 °C and (b) the SEM image of a 180-Å $(AlPcF)_n$/Si deposited at 200 °C.

important to note that the same structure is observed by SEM [Fig. 2.7(b)], and therefore the process of sample preparation by stripping or sputter coating does not result in significant damage to film structure. High-magnification TEM shows the ordered lattice images of the $(AlPcF)_n$ polymer backbones (assumed to be the black contrast lines) in each crystallite (Fig. 2.8). The bending of these crystallites shows that a high degree of flexibility of the polymer backbone is possible.

These results indicate that the substrate lattice plays almost no specific role in the growth of films on quartz and silicon(100). This may be because of the covalent nature of the substrates that precludes chemical and/or electrostatic interaction between any specific portion of the admolecule. On higher-temperature surfaces the admolecule mobility is much higher and larger crystallites result. On low-temperature surfaces the admolecule mobility is quenched at a faster rate and much smaller crystallites or amorphous structures are frozen in. The conclusion is that without some kind of interaction, epitaxial growth is not possible. However, the resultant films, particularly those on high-temperature substrates, have some merits in terms of mechanical robustness and flexibility.

B. The structure of films on alkali halide substrates

A single peak at 2θ = 24.8° in the XRD pattern of a film on KCl(100) corresponds to a d-spacing of 3.6 Å and indicates a perpendicular orientation of the a-axis polymer backbone on

FIG. 2.8. The TEM lattice image of a 200-Å $(AlPcF)_n$/Si deposited at 200 °C.

these substrates (Fig. 2.9). The FTIR spectra show that the C-H out-of-plane bending vibration at 726 ± 2 cm^{-1} is now significantly reduced in intensity (Fig. 2.10). SEM photos of films grown on KCl at room temperature are very different from the case of silicon and quartz. A mosaic crystallite domain structure covers the entire surface (Fig. 2.11). The appearance of steplike defects resulted from the inherent defects in the substrate crystal surfaces that were revealed by the cleavage process. Such defects may limit the size of crystallite and induce the formation of many grain boundaries, thereby increasing discontinuity.

The substrate temperature dependence of the structure of the films is shown in the TEM photographs of Figs. 2.12-14. At low temperatures the continuity is high and the films are smooth. However, on higher-temperature substrates the continuity becomes poor as large crystallite islands are formed. For example, for 400 Å-thick film on KCl at 240 °C, the island dimensions are of the order of 1000×1000 $Å^2$ and an SEM photograph clearly shows the monolithic structure of such an island (Fig. 2.15). Between islands there are large areas where little or no growth has occurred. On KBr and KI a similar temperature dependence is observed. There is an indication that preferential alignment of the islands occurs and that there is some similarity in the shape of the crystallites, particularly on KBr. It is clearly evident that a low-temperature substrate is better for film growth from the viewpoint of continuity.

High-magnification pictures reveal that each crystallite

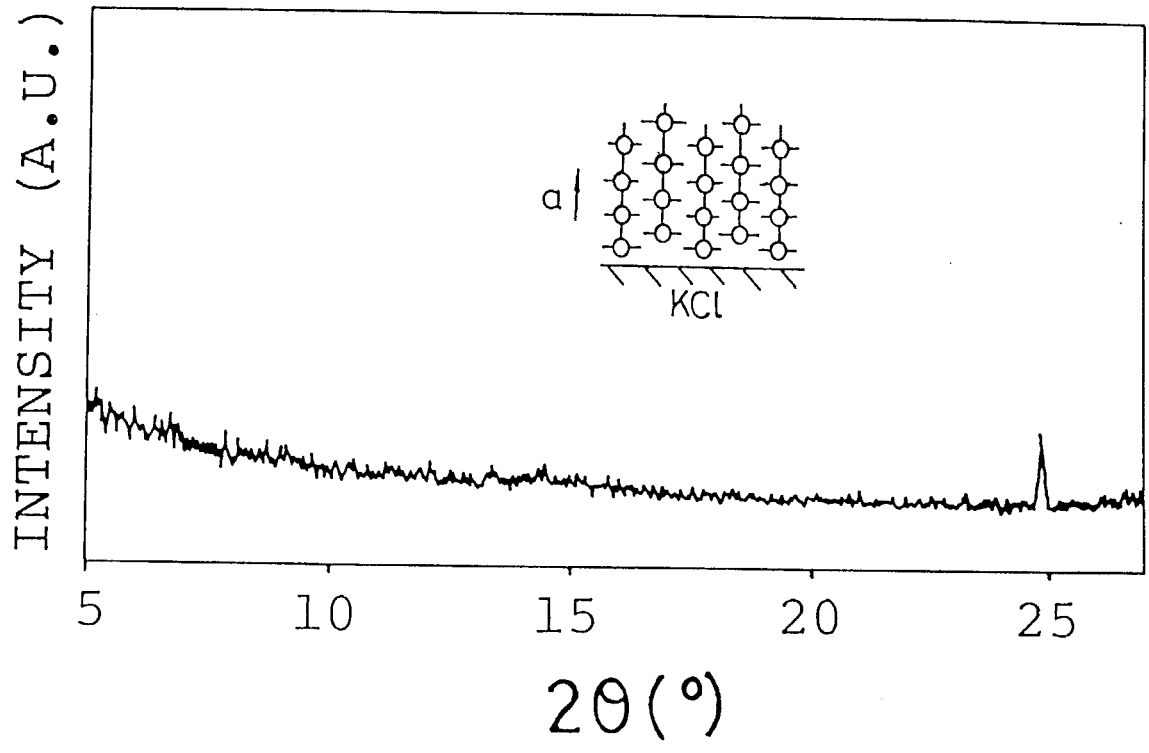

FIG. 2.9. The XRD pattern of a 200-Å $(AlPcF)_n$/KCl deposited at 200 °C.

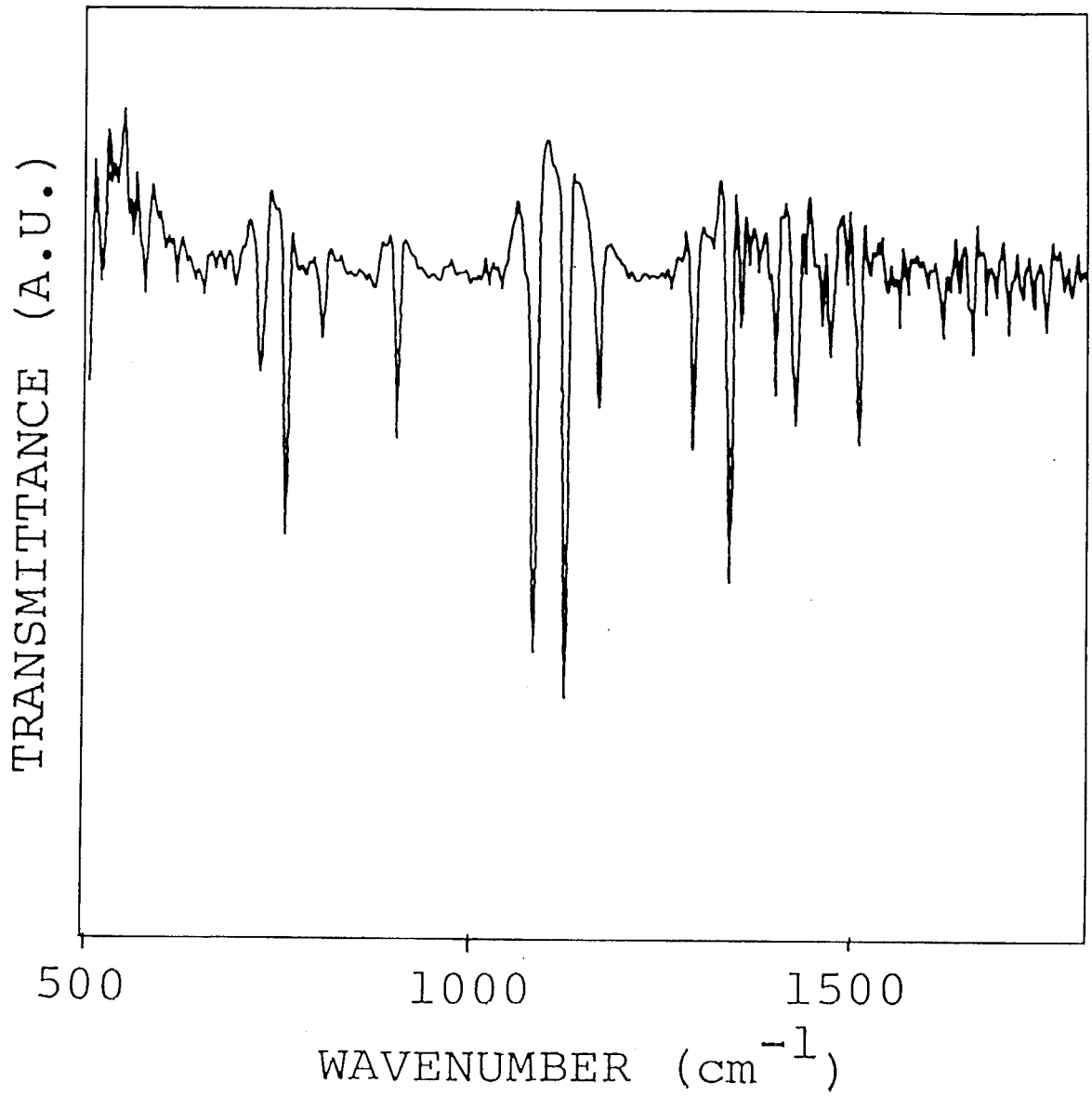

FIG. 2.10. The FTIR spectrum of a 100-Å $(AlPcF)_n$/KCl deposited at 28 °C and then annealed *in-situ* at 200 °C for 1 h.

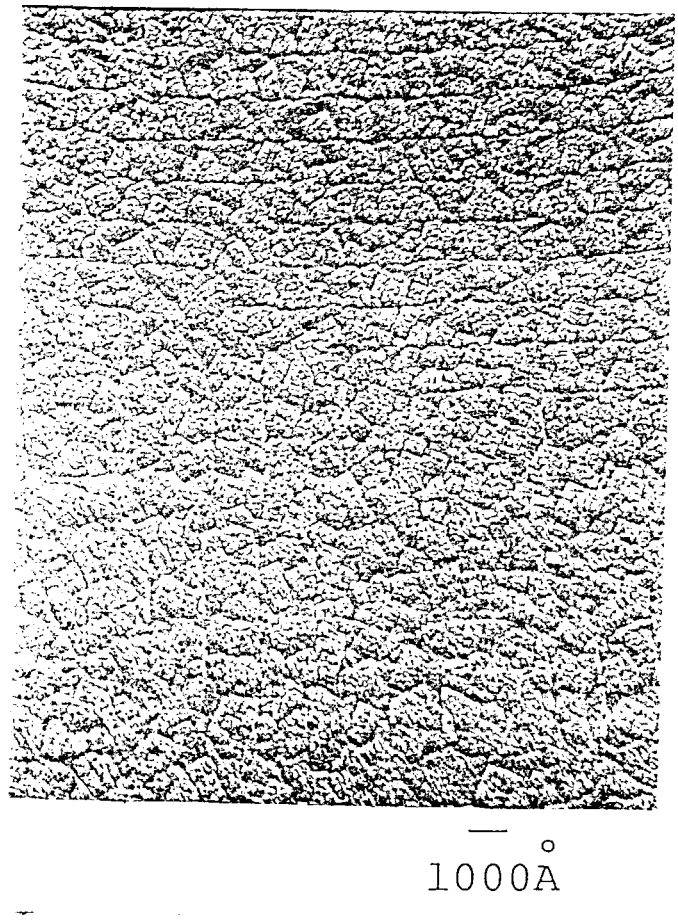

FIG. 2.11. The SEM image of a 100-Å $(AlPcF)_n$/KCl deposited at 27 °C.

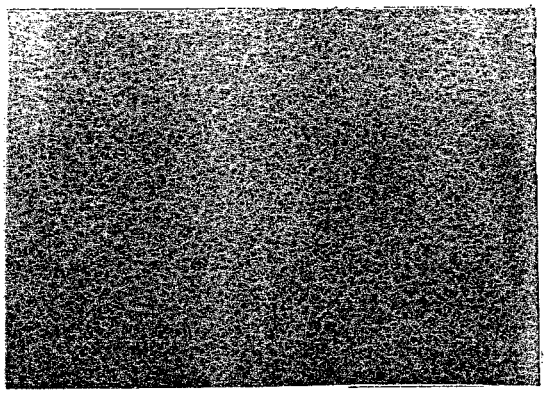

(a) 1000Å

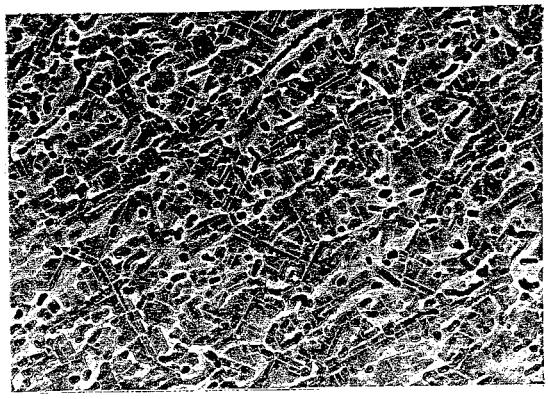

(d) 1000Å

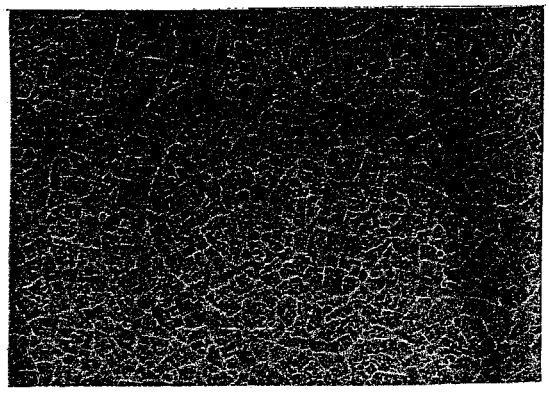

(b) 1000Å

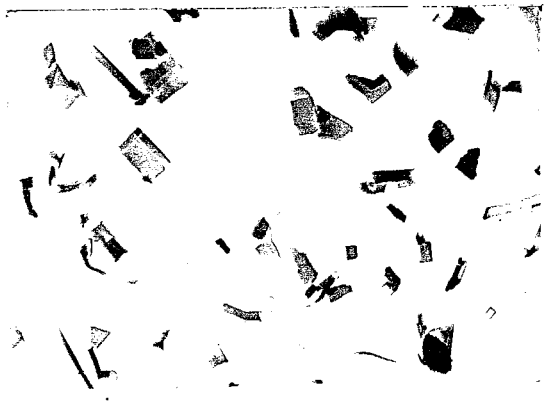

(e) 1000Å

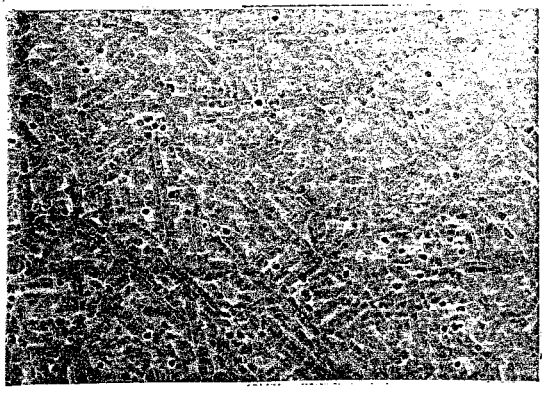

(c) 1000Å

FIG. 2.12. The TEM images of 100-Å $(AlPcF)_n$/KCl deposited at (a) -170 °C, (b) 27 °C, (c) 70 °C, (d) 100 °C, and (e) 200 °C.

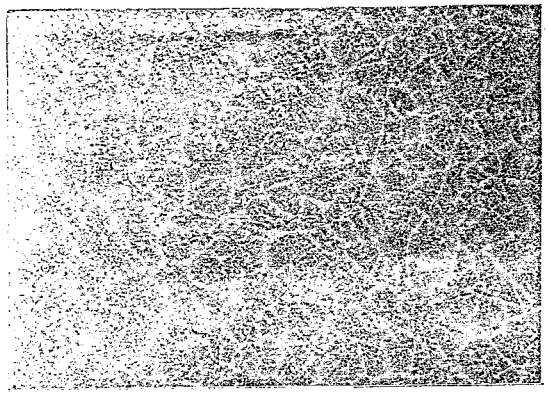

(a) 1000Å

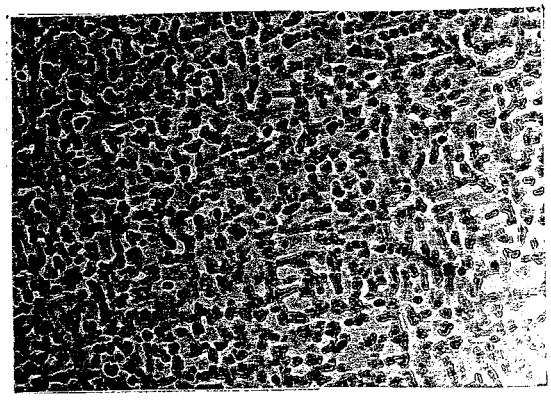

(d) 1000Å

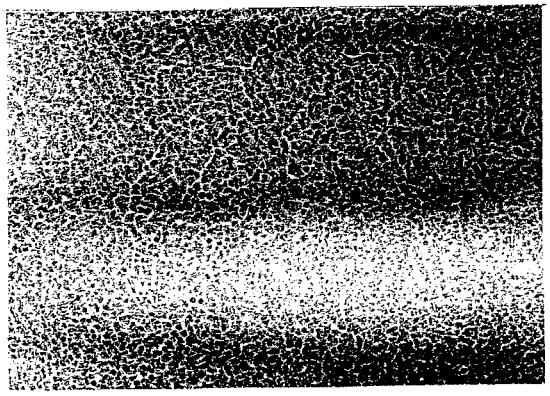

(b) 1000Å

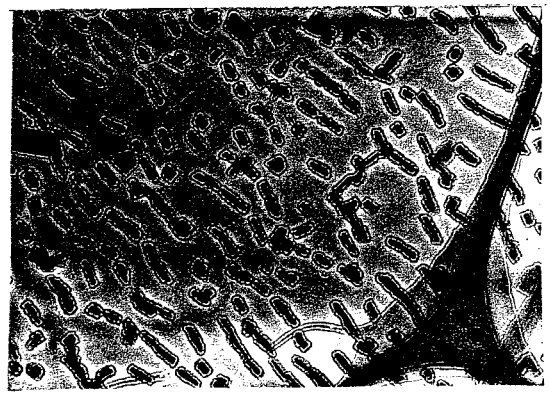

(e) 1000Å

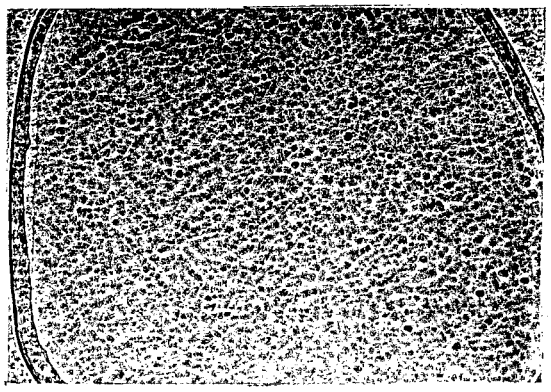

(c) 1000Å

FIG. 2.13. The TEM images of 100-Å $(AlPcF)_n$/KBr deposited at (a) -170 °C, (b) 30 °C, (c) 70 °C, (d) 100 °C, and (e) 200 °C.

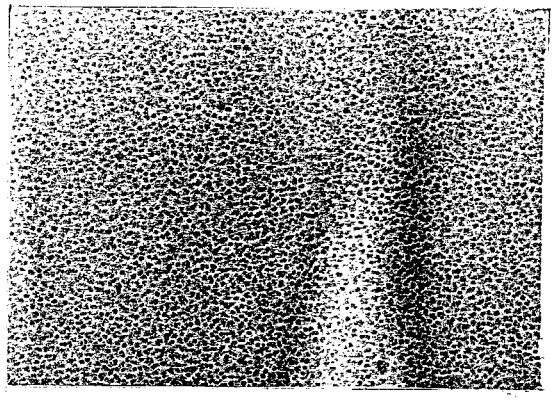

(a) 1000Å

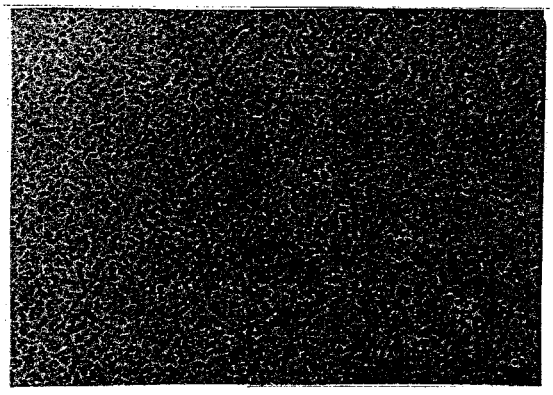

(b) 1000Å

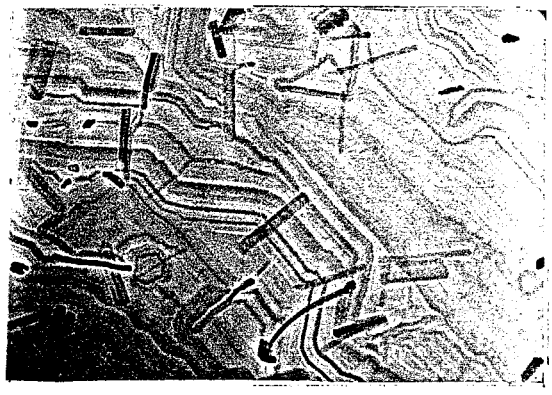

(c) 1000Å

FIG. 2.14. The TEM images of 100-Å $(AlPcF)_n$/KI deposited at (a) -170 °C, (b) 27 °C, and (c) 200 °C.

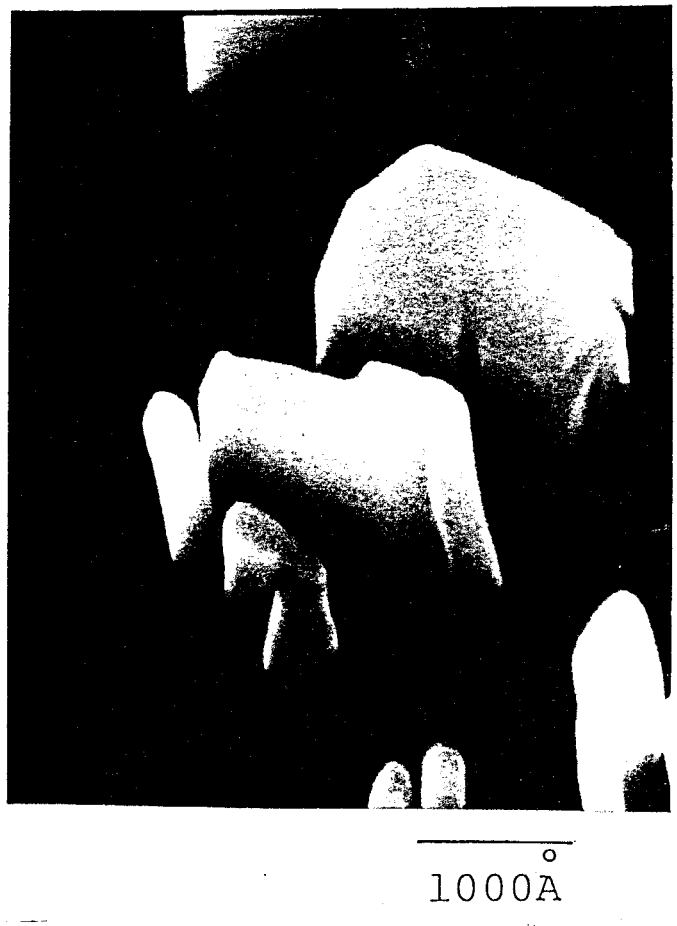

FIG. 2.15. The SEM image of a 400-Å $(AlPcF)_n$/KCl deposited at 240 °C.

consists of highly ordered square-lattice images [Fig. 2.16(a)]. This is the structure expected through viewing down the molecular columns formed by the polymer chain a-axis. It is assumed that each black dot is a phthalocyanine unit. The crystal structure is thus retained in the film.

Detailed examination shows that the relative orientation of the square-lattice images of different crystallites is influenced by the nature of the substrate. It is noted that on KCl a mutual angle of 37° between the square-lattice images of neighboring crystallites is found over the entire film [Fig. 2.16(a)]. This is confirmed by the EDP, which consists of two sets of four spots with an angle of 37° between them [Fig. 2.16(b)]. The four spots correspond to the square lattices of b and c axes. Also shown in this pattern are the square-lattice spots of the KCl substrate. This picture was obtained by semistripping the KCl from the film in the sample preparation, which enabled the direct observation of both film and substrate. Using the KCl lattice as a standard, the lattice dimensions of the phthalocyanine was calculated as b = c = 12.7 Å. In order to explain such a bidirectional crystallite orientation, it is neccesary to consider the mechanism of interaction of the substrate and admolecule.

If the center of the phthalocyanine ring of one AlPcF unit is assumed to be fixed on either the cation or the anion of the surface of the substrate, then in order to accommodate the next unit a distance of at least the size of the Pc ring is required (about 13 Å) since the strain energy will be too great otherwise. The most appropriate distance for the next

FIG. 2.16. (a) The TEM lattice image of a 100-Å $(AlPcF)_n$/KCl deposited at 70 °C and (b) the EDP of a 100-Å $(AlPcF)_n$/KCl deposited at -170 °C.

phthalocyanine to sit on a KCl(100) surface lies in the [021] or [012] directions with a vector length of 14.074 Å (Fig. 2.17). It is important to note that the angle between these vectors is also 37°. Such an agreement suggests that the growth axes of each crystallite is along either of these vector directions, and thus two congruent sets of square-lattice images in neighboring crystallites will result in such cases. In Wood's notation, these two square-lattices are denoted as KCl(100)($\sqrt{10}\times\sqrt{10}$)R$\pm$27°-$(AlPcF)_n$.[18]

On KBr, however, only a unidirectional orientation of lattice images is observed for all crystallites and the EDP of a semistripped film shows only four spots (calculated lattice dimensions: b = c = 12.7 Å) (Fig. 2.18). In this case the most appropriate distance on a KBr(100) surface is that of 13.992 Å which is in the [011] direction (Fig. 2.19). This square-lattice is denoted as KBr(100)(3×3)R45°-$(AlPcF)_n$. Because of the symmetry of such an axis there is only one possible orientation of the square-lattice images in all crystallites.

On KI, a unidirectional orientation is also found (Fig. 2.20). It was not possible to obtain a simultaneous pattern of the substrate lattice since KI is very hygroscopic. The interpretation is not so clear in this case since there is also a diffuse concentric ring pattern in the EDP corresponding to 3.6 Å, which indicates that there are some areas where the a-axis lies parallel to the substrate surface (the rings are more intense on films grown at higher substrate temperatures). The TEM study also confirmed that there is a larger degree of randomness in these films.

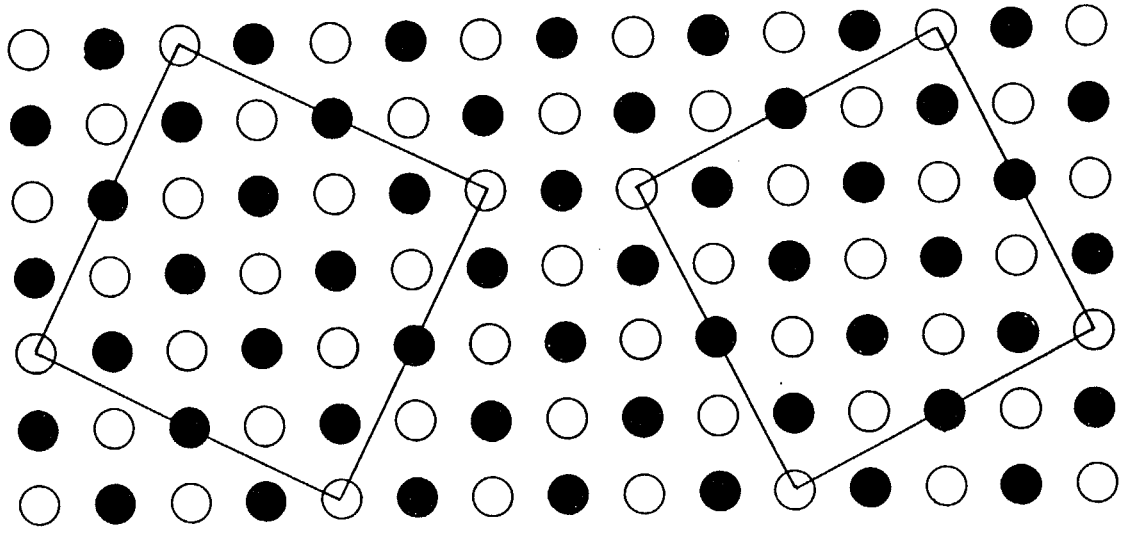

FIG. 2.17. The two possible models for accommodation of $(AlPcF)_n$ lattice on KCl(100).

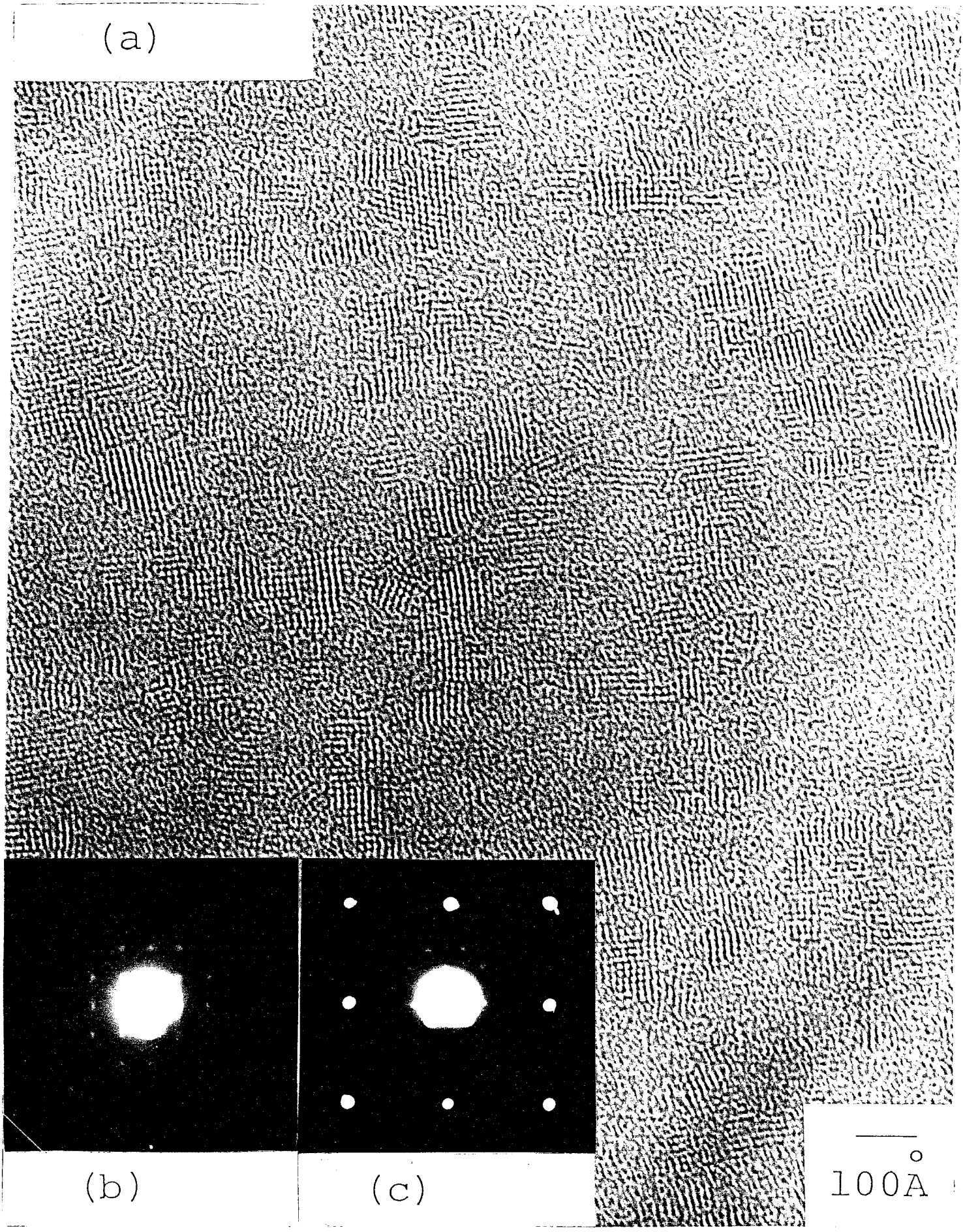

FIG. 2.18. (a) The TEM lattice image of a 100-Å $(AlPcF)_n$/KBr deposited at -170 °C, (b) the EDP of a 100-Å $(AlPcF)_n$/KBr deposited at -170 °C, and (c) the semistripped EDP of a 100-Å $(AlPcF)_n$/KBr deposited at -170 °C then annealed *in situ* at 200 °C for 24 h.

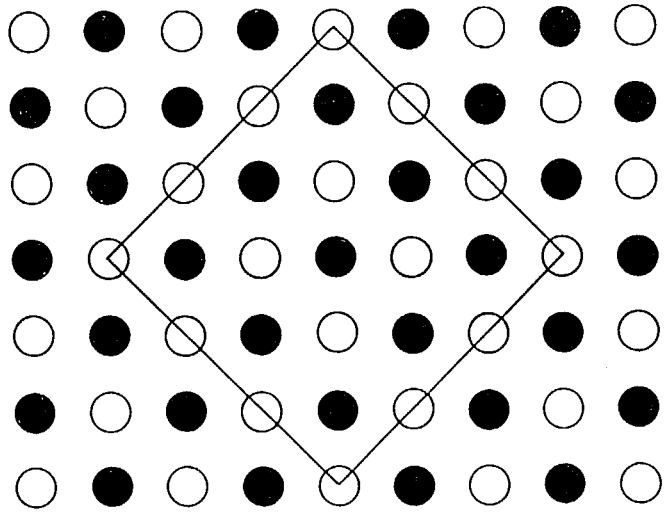

FIG. 2.19. The unique accommodation model of the $(AlPcF)_n$ lattice on KBr(100).

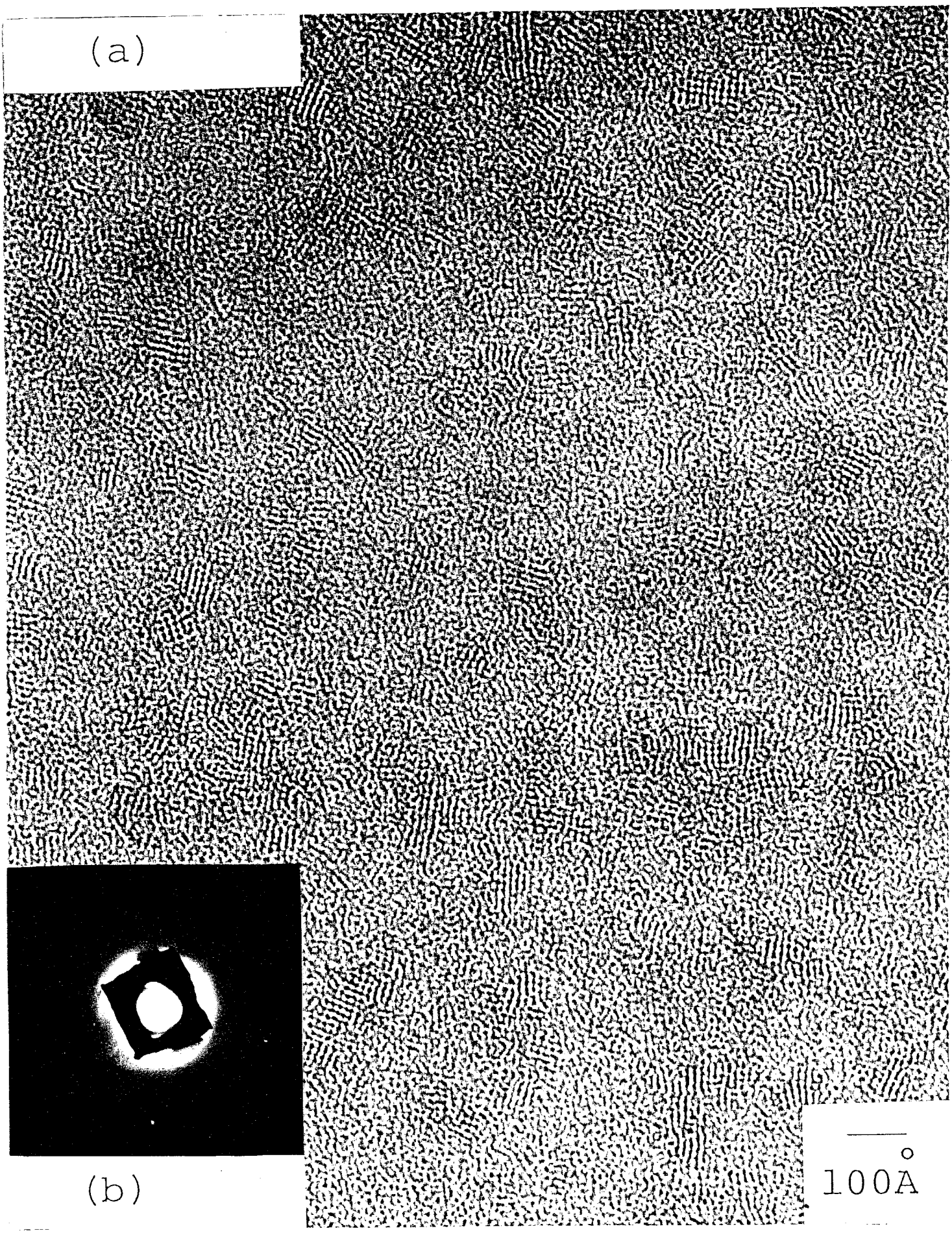

FIG. 2.20. The TEM lattice image of a 100-Å $(AlPcF)_n$/KI deposited at -170 °C and (b) the EDP of a 100-Å $(AlPcF)_n$/KI deposited at -170 °C.

The general degree of orientational order or homogeneity in the films is poorer on higher-temperature substrates in this series. The TEM lattice image and the EDP of the 200-Å film on KCl deposited at 200 °C illustrate this point (Fig. 2.21). The crystallinity in this film is high and the size of microcrystals is large, but the directionality of the lattice image and homogeneity are reduced, and consequently the degree of epitaxy proves to be lowered. A ring pattern corresponding to 3.6 Å in the EDP is suggestive of the orientation in which the a-axis is parallel to the substrate. This orientation is also recognized in the TEM picture as the long linear lattice images between the microcrystals. A similar behavior was observed on other substrates, and thus such an orientation may occur more favorably on higher-temperature substrates.

The growth process on alkali halides is influenced by a combination of two factors. The first is the electrostatic interaction between substrate and admolecule. The degree of ionicity of the substrates is of the following order: KCl > KBr > KI, and the strength of electrostatic interaction is thus expected to follow this order. The interaction provides a mechanism for fixing the initial phthalocyanine admolecules in the perpendicular a-axis orientation as they impinge on the surface. Growth of subsequent layers is driven by the molecule-molecule interaction. If the temperature of the substrate is high, the admolecule mobility is not quenched so readily, and crystallite islands are the result. If the molecule-substrate interaction is weak, then the initial layer may not be fixed, and growth of parallel a-axis orientation

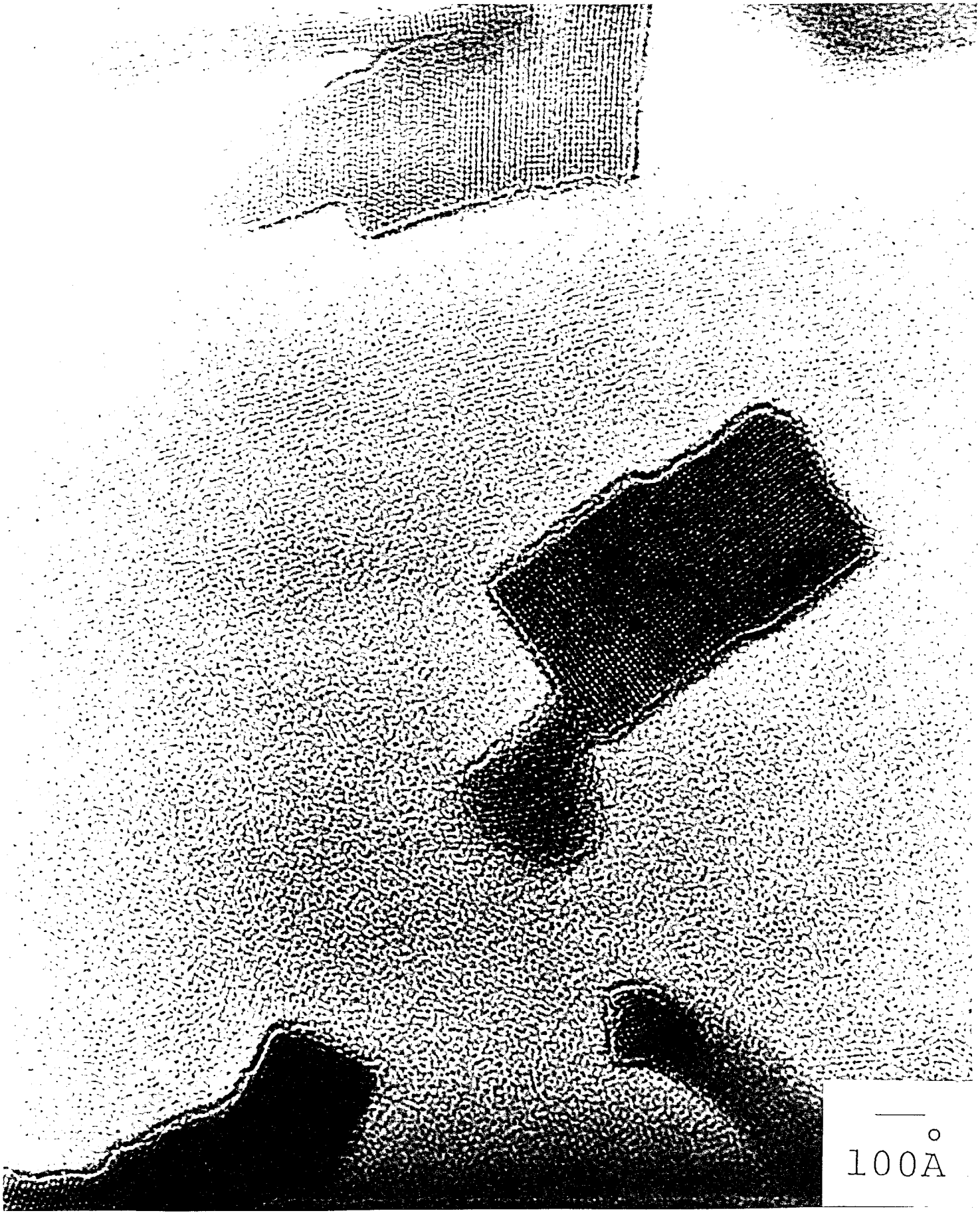

FIG. 2.21. The TEM lattice image of a 200-Å $(AlPcF)_n$/KCl deposited at 200 °C.

regions may occur as is the case on high-temperature substrates, particularly on KI. The small ionicity of this substrate is the reason for the randomness that occurs in the relative crystallite orientation.

The second factor is the growth axis symmetry of each substrate which governs the possible crystallite growth directions. The distances between aluminum ion centers in the above growth axes are different from the lattice dimensions calculated from the EDP (generally 12.7 Å - similar to the bulk-crystal value). This suggests that the formation of a pseudomorphic layer at the substrate-thin-film interface may occur. The lattice dimensions of this layer would match the substrate more perfectly. As the film thickness increases the dimensions would relax into the bulk-crystal value. The confirmation of such an effect could not be made in the present study since in the TEM method the films were stripped from the substrate, thus destroying any interface layer. However, this phenomena would have a large effect on the degree of order in a film. It is expected that the stabilization of the pseudolayer depends on the strength of the substrate-admolecule interaction, and therefore KCl is the best substrate to illustrate the effect.

2-4. SUMMARY

Epitaxial growth of the $(AlPcF)_n$ polymer films does not occur on the covalent substrates of silicon and quartz. The interaction that occurs between phthalocyanine and ionic

substrates results in an epitaxial relationship which manifests itself in the relative orientation of crystallite island regions. The most suitable substrate for the preparation of highly ordered epitaxial films is KCl(100) because of the high ionicity. However, the observed bidirectional crystallite orientation will increase the occurrence of grain boundaries and twinning that result from the merging of neighboring crystals. Because of this, KBr(100) is a more favorable substrate since the crystallite orientation is unidirectional.

The best-quality films in terms of continuity are those grown on very-low-temperature substrates. A film grown on KBr at -170° C shows an almost perfect single-crystal diffraction pattern over the electron-beam sampling area (5 μm). The controlled rate of growth of the films using the MBE technique enhances the ease of production of such highly continuous films. The inherent defects in the cleaved alkali halide substrates is a limiting factor to perfectly crystalline films over large areas, and methods of preparing defect-free surfaces should be investigated. However, this study has established some criteria for obtaining films with controlled orientation. In the next chapter, the effect of post-annealing of the as-deposited films is studied in order to increase crystallite size.

REFERENCES

[1]M. Ashida, N. Uyeda, and E. Suito, Bull. Chem. Soc. Jpn. 39, 2616 (1966).

[2]M. Ashida, Bull. Chem. Soc. Jpn. 39, 2632 (1966).

[3]M. Komiyama, Y. Sakakibara, and H. Hirai, Thin Solid Films **151**, L109 (1987).

[4]A. Yamada, K. Shigehara, and M. Hara, Synth. Met. **18**, 821 (1987).

[5]L. L. Chang, in *Handbook on Semiconductors*, edited by S. P. Keller (North-Holland, Amsterdam, 1980), Vol. 3.

[6]J. C. Buchholz and G. A. Somorjai, J. Chem. Phys. **66**, 573 (1977).

[7]Z. Z. Ho, C. Y. Ju, and W. M. Hetherington III, J. Appl. Phys. **62**, 716 (1987).

[8]R. S. Nohr, P. M. Kuznesof, K. J. Wynne, M. E. Kenney, and P. G. Siebenman, J. Am. Chem. Soc. **103**, 4371 (1981).

[9]J. P Linsky, T. R. Paul, R. S. Nohr, and M. E. Kenney, Inorg. Chem. **19**, 3131 (1980).

[10]H. J. Wagner, R. O. Loutfy, and C. K. Hsiao, J. Mater. Sci. **17**, 2781 (1982).

[11]K. J. Wynne, Inorg. Chem. **24**, 1339 (1985).

[12]I. Marklund and S. Andersson, Surf. Sci. **5**, 197 (1966).

[13]D. Djurado, C. Fabre, A. Hamwi, and J. C. Cousseins, Synth. Met. **22**, 121 (1987).

[14]F. H. Moser and A. L. Thomas, *The Phthalocyanines* (CRC Press, Florida, 1983), Vol. 1, p. 67 and references cited therein.

[15]H. C. Hill and R. I. Reed, Tetrahedron **20**, 1359 (1964).

[16]S. Maroie, M. Savy, and J. J. Verbist, Inorg. Chem. **18**, 2560 (1979).

[17]C. W. Dirk, T. Inabe, K. F. Schoch Jr., and T. J. Marks, J. Am. Chem. Soc. **105**, 1539 (1983).

[18]E. A. Wood, J. Appl. Phys. **35**, 1306 (1964).

CHAPTER 3 ULTRAVIOLET/VISIBLE SPECTRA OF ULTRATHIN FILMS OF FLUORO-BRIDGED ALUMINUM PHTHALOCYANINE POLYMER

3-1. INTRODUCTION

In the preceding chapter 2, the characterization of MBE-grown thin films of the fluoro-bridged aluminum phthalocyanine polymer, $(AlPcF)_n$, was presented.[1] It was clarified that on single-crystal alkali halide substrates, the orientation of the polymer chains was perpendicular to the surface. On KBr and KCl, epitaxial films were obtained which consisted of unidirectional and bidirectional crystallite orientations, respectively. By using low-temperature substrates (-170 °C), the continuity and long range order were increased, and the film was almost perfectly single crystal. It was suggested that a pseudomorphic region at the thin film-substrate interface may exist which is stabilized by the interaction between substrate and phthalocyanine molecule. On KI, the small ionicity resulted in a larger degree of disorder and irregularity of crystallite orientation, even at low temperature. Epitaxial growth did not occur on silicon and quartz. The polymer chains were oriented parallel to the surface and formed a wormlike structure.

In this chapter, the results of a uv/visible spectroscopic study of the MBE films are given. The effect of substrate identity, substrate temperature during deposition, and thickness of film is studied. Subsequent post-annealing of the films is carried out in order to observe expected increases in

crystallinity. The interesting spectroscopic behavior is discussed in terms of a qualitative hypothesis that supports the idea of a pseudomorphic layer region at the thin-film/substrate interface.

3-2. EXPERIMENT

The MBE film growth conditions are outlined in the preceding chapter.[1] Independent post-annealing of each sample was carried out *in-situ* at 10^{-9} Torr before removal from the chamber. The anneal time period was 2-24 h at temperatures of 70-200 °C. After annealing, the temperature was reduced at a rate of 1 °C min^{-1}. Characterization of the structure was carried out by transmission electron microscopy (TEM). The uv/visible spectra were recorded in air using a Hitachi U3400 spectrophotometer.

3-3. RESULTS

A. The spectra of the films on various substrates

The spectra of 100-Å $(AlPcF)_n$ films grown on various substrates at room temperature are shown in Fig. 3.1. It is apparent that there are three peaks which are consistent in all the spectra. The uv/visible absorption of phthalocyanines is well documented,[2-4] and these peaks can be assigned to three characteristic bands: the Q band, corresponding to the π - π^* transition that lies at about 635 nm; the B or Soret band (π -

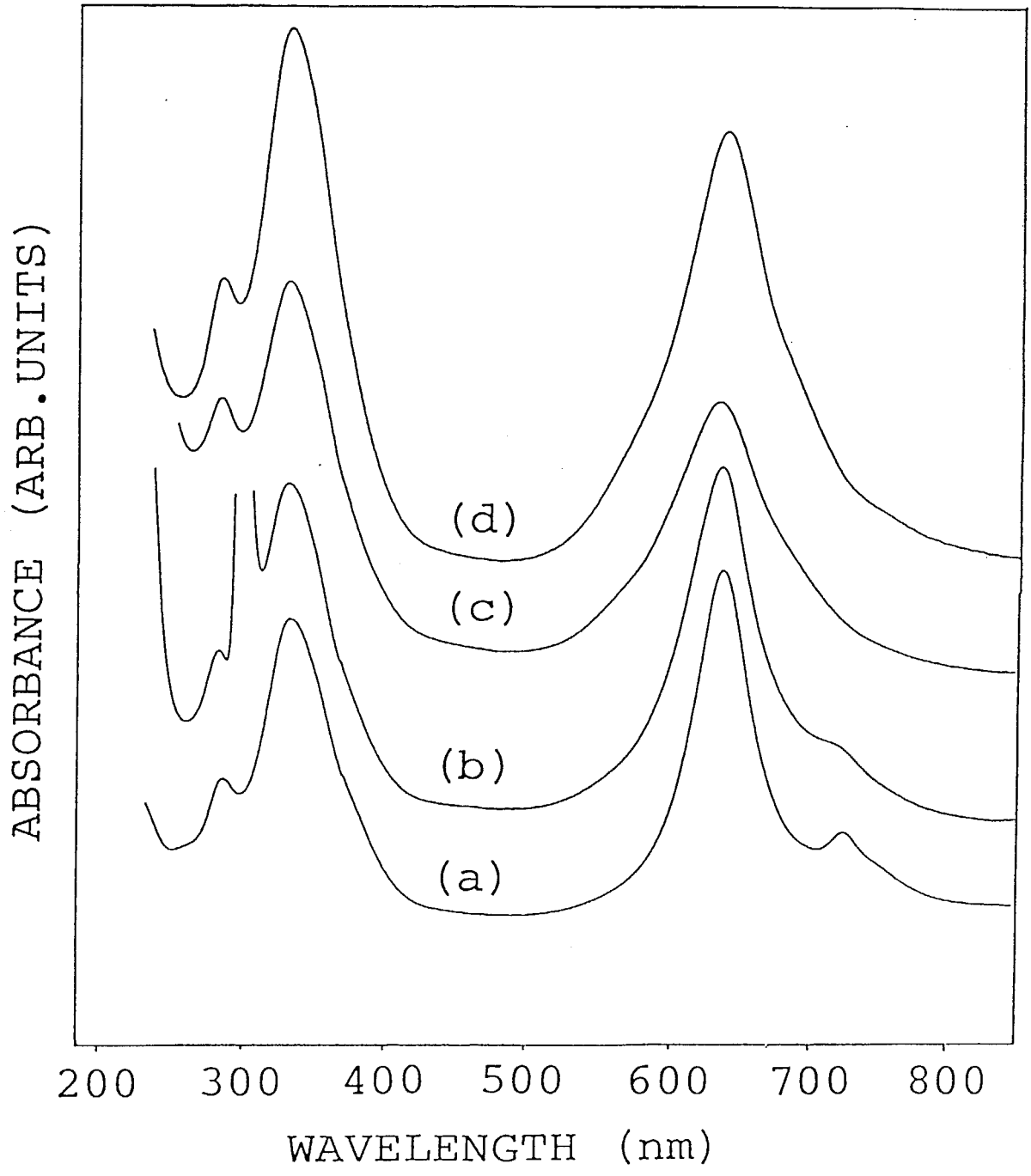

FIG. 3.1. The UV/visible spectra of 100-Å $(AlPcF)_n$ on various substrates deposited at room temperature: (a) KCl, (b) KBr, (c) KI, and (d) quartz.

π^*) at about 335 nm; and the N band at 285 nm. The phthalocyanine L and C bands cannot be assigned in all spectra due to masking by substrate absorption.

It is found that on KCl(100) substrates a new weak peak occurs at approximately 723 nm. New absorption is also present in films on KBr(100), although of reduced intensity and resembling a shoulder. On KI and quartz substrates, there is no evidence of any new absorption in this region.

A study of the structure of these MBE-grown films revealed that the degree of epitaxy was related to substrate type and followed the order KCl > KBr > KI > quartz, Si.[1] It is interesting to note that this order is in agreement with the order of the intensity of the new peak found on these substrates.

B. Substrate temperature dependence of the spectra

The spectra of 100-Å films grown on KCl(100) at various substrate temperatures are shown in Fig. 3.2. It is clear that on higher-temperature substrates, the new absorption becomes a shoulder at 100 °C and completely disappears at 200 °C. On a low-temperature substrate (-170 °C), the new absorption is slightly increased in intensity and a second new peak appears at approximately 759 nm. The results for KBr(100) are analogous, although again the new peaks are lower in intensity (Fig. 3.3). The sharp peak at 301 nm was also found in a blank KBr substrate. In the case of KI, there were no new peaks even on substrates at low temperatures.

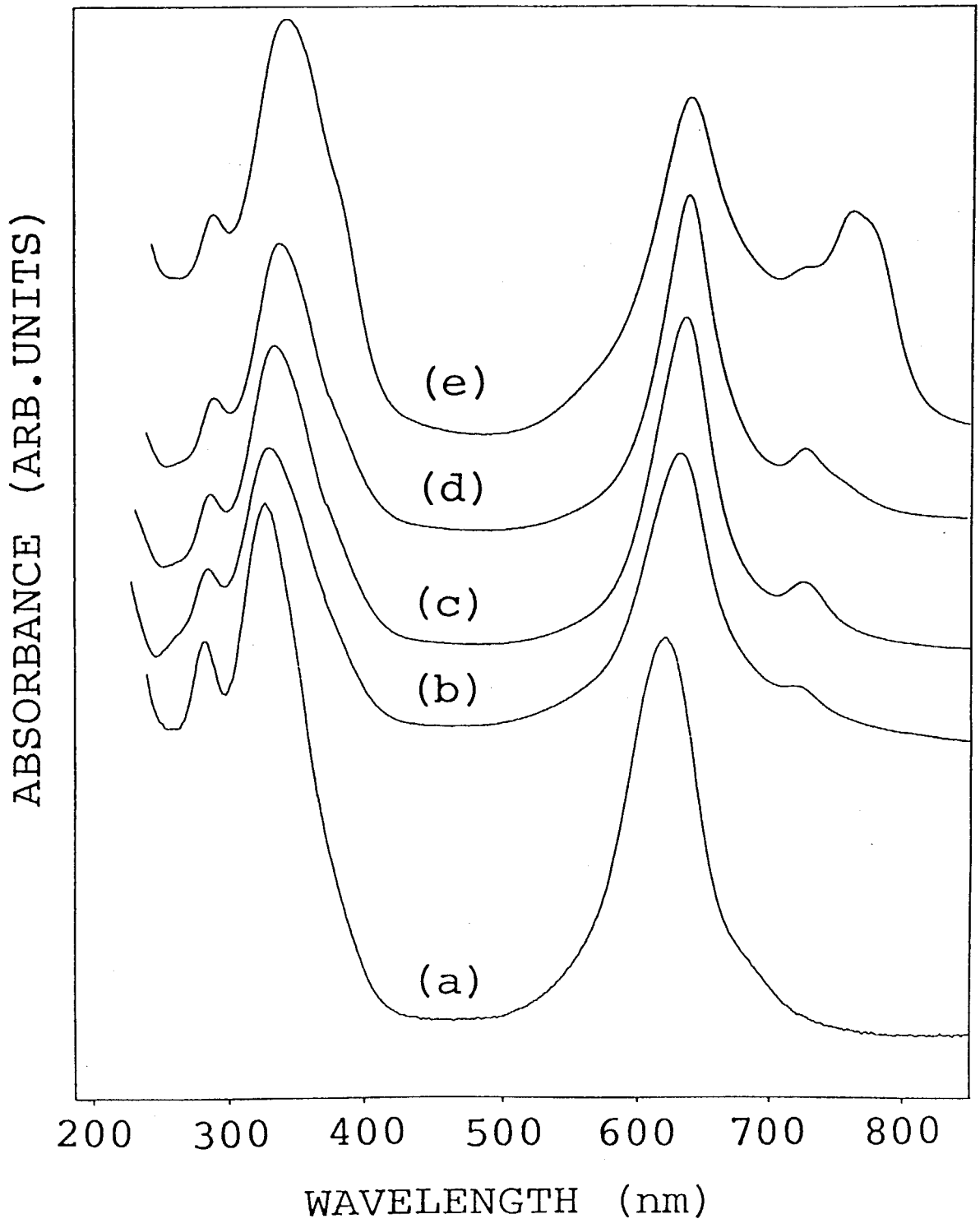

FIG. 3.2. The UV/visible spectra of 100-Å $(AlPcF)_n$/KCl deposited at various temperatures: (a) 200 °C, (b) 100 °C, (c) 70 °C, (d) 27 °C, and (e) -170 °C.

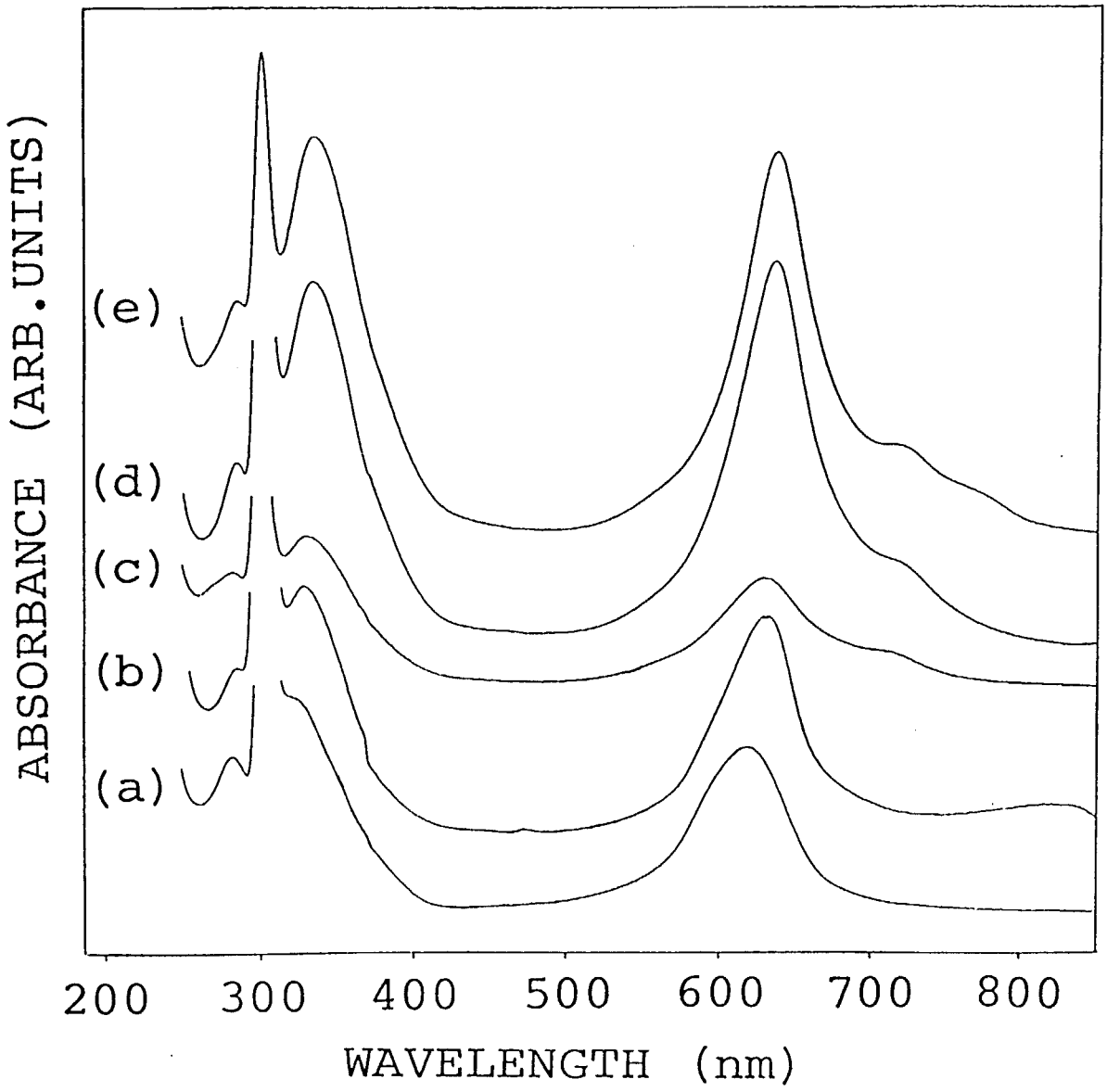

FIG. 3.3. The UV/visible spectra of 100-Å $(AlPcF)_n$/KBr deposited at various temperatures: (a) 200 °C, (b) 100 °C, (c) 70 °C, (d) 30 °C, and (e) -170 °C.

The substrate temperature dependence of structure has shown that films grown on low-temperature substrates are of very high continuity with small crystallite size, and the degree of epitaxy is good. In contrast, on higher temperature substrates, large crystallite island structures (1000 × 1000 $\mathring{A}^2$) are obtained, and continuity and the degree of epitaxy is low.[1] The appearance of the new absorption is thus linked to the quality of the film in terms of the continuity, crystallite order, and epitaxy.

C. Thickness dependence of the spectra

The spectra of films of various thickness deposited on KCl(100) at room temperature are shown in Fig. 3.4. The intensity of the 723-nm peak relative to the main Q band increases as the thickness is decreased. This effect is even more pronounced on low-temperature (-170 °C) substrates (Fig. 3.5). In this case the two extra peaks become of almost equal intensity with respect to the Q band in very thin films. The most favorable conditions to observe the new absorption is thus in thin films on low-temperature substrates. Temperature is more effective than thickness because a thin film (10 Å) on KCl at 200 °C does not show the new peaks.

D. The effect of annealing for the spectra

The TEM photos of Fig. 3.6 show the results of annealing a 100-Å film deposited on KBr(100) at -170 °C. This condition

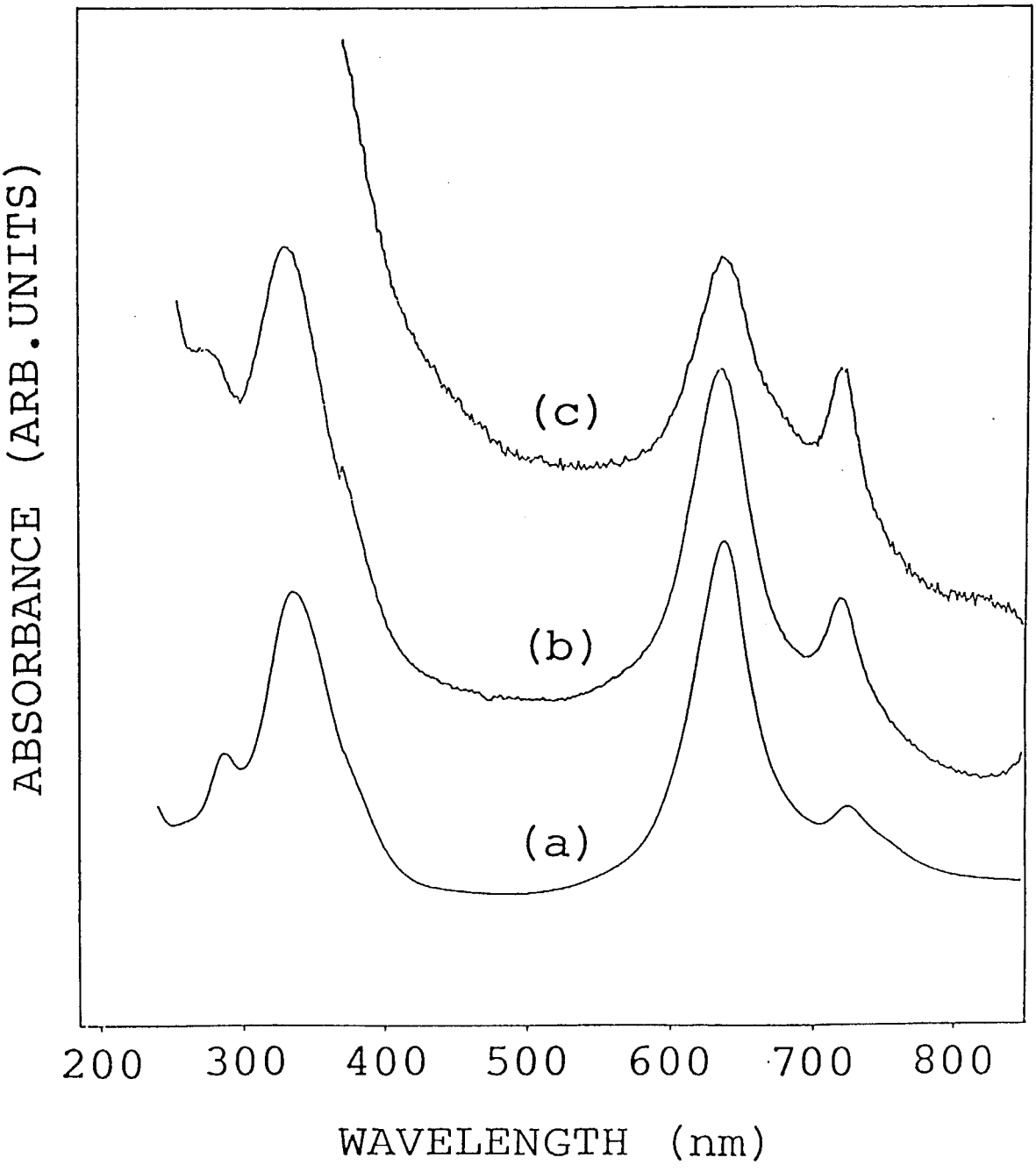

FIG. 3.4. The UV/visible spectra of $(AlPcF)_n$/KCl deposited at 28 °C and various thickness: (a) 100 Å, (b) 25 Å, and (c) 10 Å.

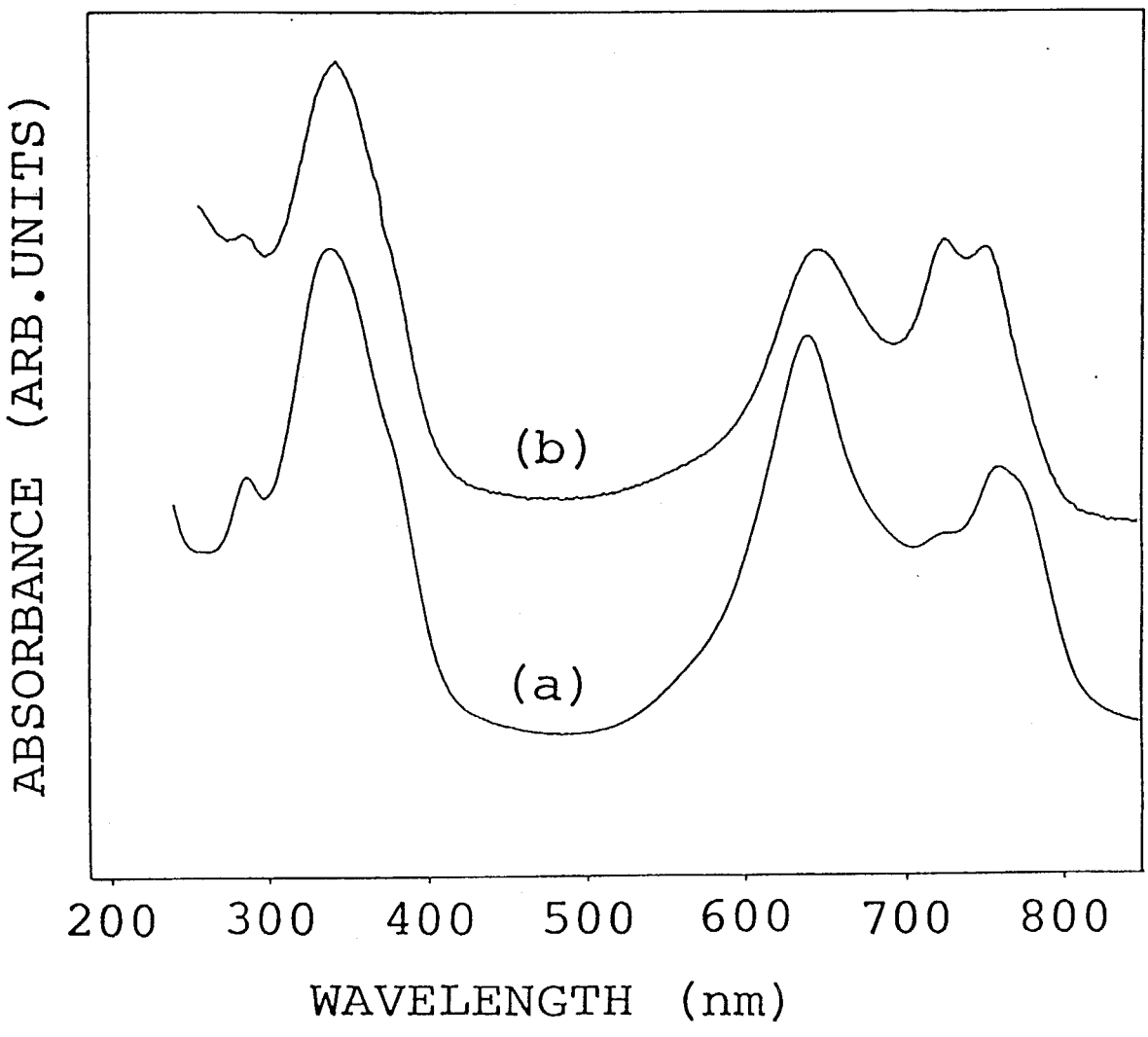

FIG. 3.5. The UV/visible spectra of $(AlPcF)_n$/KCl deposited at -170 °C and various thickness: (a) 100 Å and (b) 20 Å.

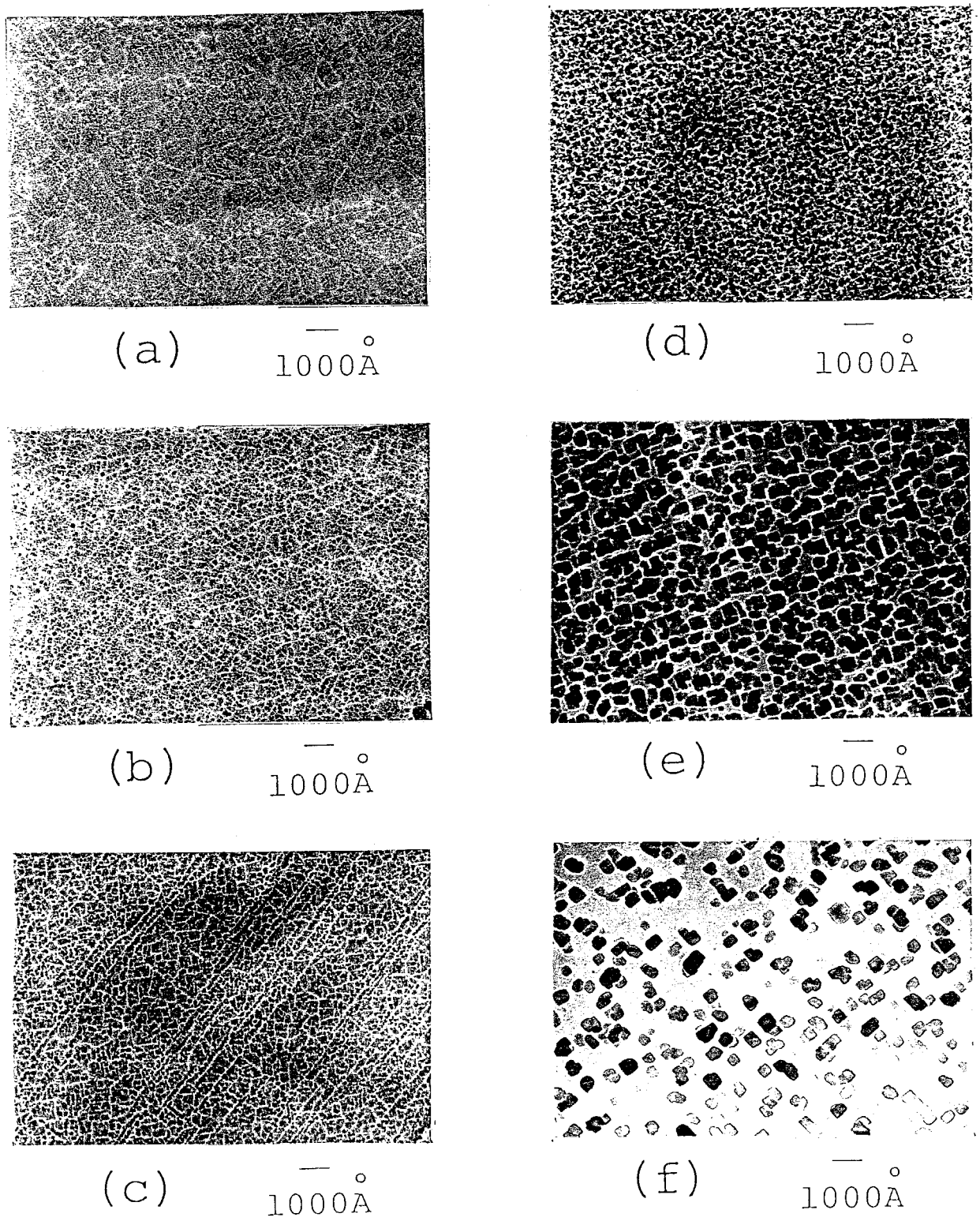

FIG. 3.6. The TEM images of 100-Å $(AlPcF)_n$/KBr deposited at -170 °C, then annealed at various conditions: (a) no anneal, (b) 70 °C, 10 h, (c) 140 °C, 10 h, (d) 170 °C, 10 h, (e) 200 °C, 2 h, and (f) 200 °C, 24 h.

is believed to be the most ideal for the preparation of the highest quality film since the crystallite orientation on the surface is unidirectional and continuity is excellent. At anneal temperatures of 140 °C or lower, there is no significant change in structure. However, at higher anneal temperatures the crystallite size becomes obviously larger until, in the case of a 200°C anneal for 2 h, island structures of average size 500 × 500 $Å^2$ are obtained. High-resolution studies show that the unidirectional orientation of lattice images is retained among each crystallite (Fig. 3.7).

The corresponding spectra are shown in Fig. 3.8. There is little change below 140°C, but the two new peaks on the red side of the Q-band region disappear if the anneal temperature is 170 °C or higher.

3-4. DISCUSSION

There were many suggestions as to the cause of the new absorption. It is known that upon partial charge transfer the spectra of $(AlPcF)_n$ normally shows a red-shifted shoulder on the Q band.[5] However, such an effect caused by atmospheric oxygen or water vapor would cause a similar change in the spectrum of all films regardless of substrate identity.

It is also known that in phthalocyanine crystals, Davydov splitting of the Q band results from dipole-dipole interactions in the solid state.[6] The new absorption cannot be ascribed to such effects since no splitting is observed on high-temperature substrates, even though good crystal islands are formed. The Q

FIG. 3.7. The TEM lattice image of 100-Å $(AlPcF)_n$/KBr deposited at -170 °C, then annealed at 200 °C, 2 h.

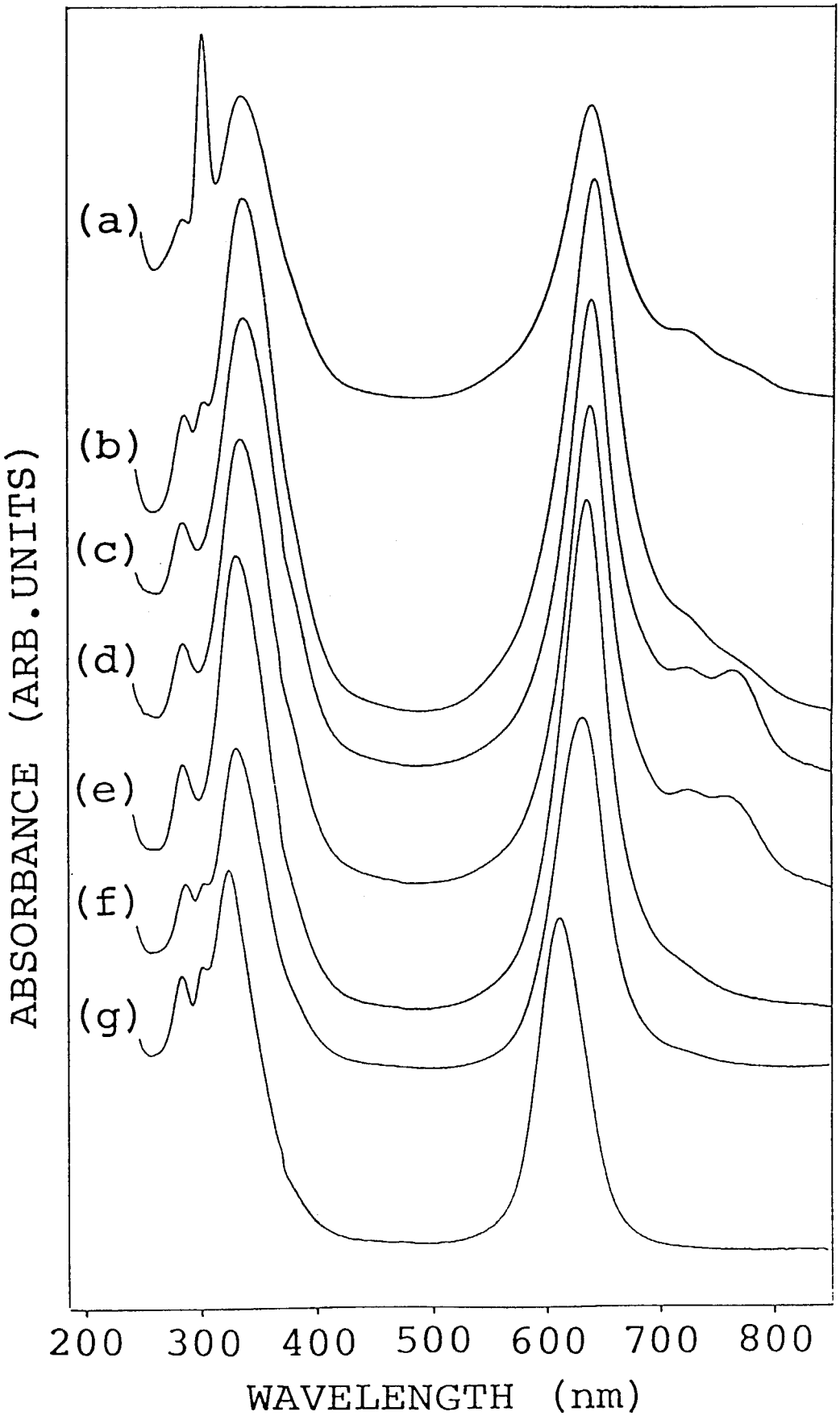

FIG. 3.8. The UV/visible spectra of 100-Å $(AlPcF)_n$/KBr deposited at -170 °C, then annealed at various conditions: (a) noanneal, (b) 70 °C, 10h, (c) 110 °C, 10 h, (d) 140 °C, 10 h, (e) 170 °C, 10 h, (f) 200 °C, 2h, and (g) 200 °C, 24 h.

band is not shifted as would be expected if splitting occurs. The new absorption is totally independent.

Qualitative interpretation of the accumulated results can be made if one assumes that a pseudomorphic layer region exists at the thin-film/substrate interface which arises as a consequence of epitaxial growth. The distance between neighboring molecules in the initial layer may be governed by the size of the substrate lattice. For example, on KCl(100) the next site for a neighboring molecule, bearing in mind the size of the phthalocyanine moiety, lies in the [012] or [021] direction. This distance is 14.074 Å. The bulk lattice constant of the $(AlPcF)_n$ film as derived from electron diffraction patterns is b = c = 12.7 Å. Thus, in the initial layer, the crystal structure will be different to the bulk.[1] As film thickness increases, this structure relaxes to that of the normal lattice to relieve the inherent strain of the system. An illustration of the subsequent structure of the film is shown in Fig. 3.9.

The molecules in the pseudomorphic layer will be under tensile stress due to the constraint imposed by the substrate and this may affect their electronic structure, thereby resulting in new absorption in the optical spectra.

It is well known for inorganic materials that a high-quality superlattice, which is called strained-layer superlattice, can be grown as a layer with lattice mismatch to the substrate up to about 7% if the layer thickness does not exceed a critical value, and the consequent large layer strains may shift bulk energy levels and split certain band

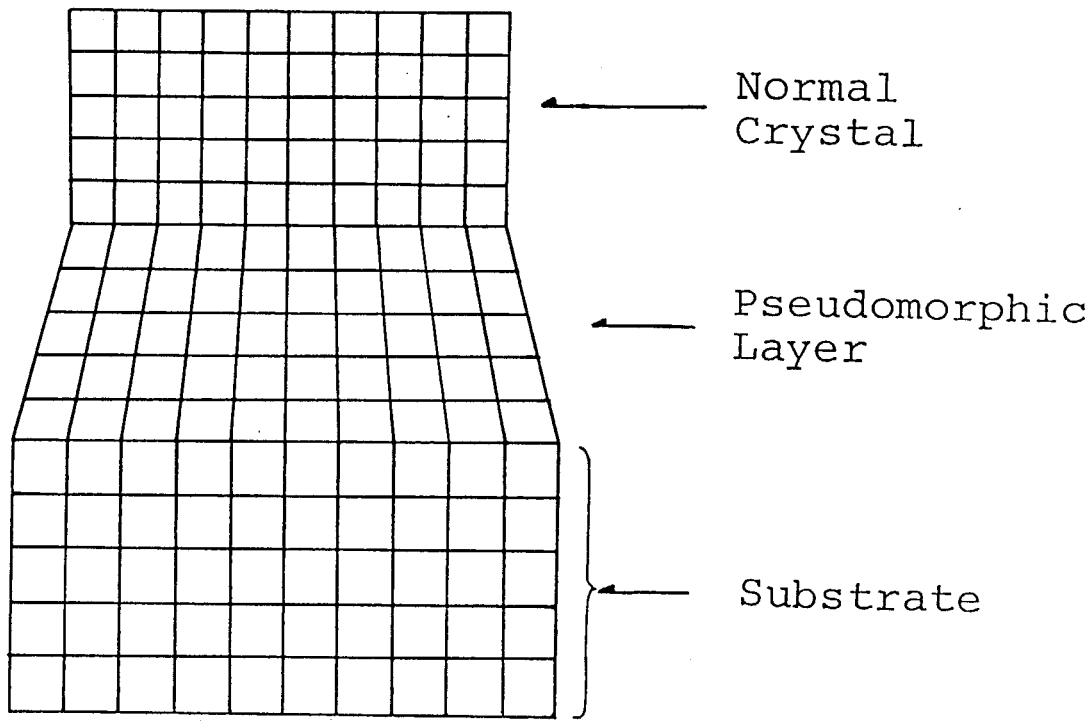

FIG. 3.9. A schematic model of pseudomorphic layer.

degeneracies.[7] Such studies for organic materials are rare, but a low-energy electron diffraction (LEED) investigation of CuPc, FePc, and H_2Pc films grown *in-situ* on copper (100) substrates clearly showed that they do not have surface structure characteristic of the normal bulk crystal, but rather have a surface unit mesh compatible with a single molecule per unit mesh, oriented parallel to the surface. This implies the existence of pseudomorphic structure which is stable up to a film thickness of 1000 Å.[8] The optical properties, however, were not observed.

The pseudomorphic model can easily explain the thickness dependence of the spectra. If the film is very thin, the pseudoregion is of a higher proportion to the bulk of the film, and so the new absorption is of higher intensity relative to the main Q band. Hence the new absorption does not apparently obey the Lambert-Beer law.

If higher temperature substrates are used, the formation of a pseudomorphic layer is not possible since the phthalocyanine admolecule mobility is very high, and islands of normal bulk crystal structure are formed. Consequently, no suitable junction is formed between substrate and admolecule via pseudomorphic layer, and the resultant films are of a low degree of epitaxy and high disorder.

The pseudomorphic layer which is formed at low temperatures is in a metastable state and therefore can be destroyed by thermal activation such as annealing. However, it seems that the destruction occurs in a small temperature range of between 140 and 170 °C. When the layer is destroyed, the

phthalocyanine units are free to migrate across the surface and form larger crystallite islands, and the new absorption also disappears. The admolecule accommodation on KBr is not so favorable as the case on KCl as shown in chapter 2, and consequently there may be a fair amount of misfitting domains on a low-temperature KBr substrate. If we anneal the film up to ~140 °C, the misfitted admolecule can migrate so as to obtain a stronger interaction with the substrate. Thus, in this temperature region, the absorption intensity of additional peaks may increase with raising the annealing temperature.

The effect of substrate identity is more subtle. The probability of pseudomorphic formation is governed by the degree of ionicity of the substrate. The order of the strength of interaction and thus the degree of epitaxy for different substrates follows the order KCl > KBr > KI.[1] The new absorption is thus of highest intensity in films on KCl. On KBr, the intensity is lower, and on KI it is not observed. Since films on silicon or quartz are not epitaxial, the pseudomorphic effect is not possible.

The electronic origin of the new absorption is not yet clear. The relatively strong interaction between admolecule and substrate may cause some distortion in the electronic structure of phthalocyanine molecule probably through a charge-transfer interaction. The next candidate for the origin is an occurrence of forbidden transition in the perfect crystal due to symmetry breaking in the pseudomorphic layer. It was reported that some of the Q-band excitons of phthalocyanine have negative dispersion in some branches.[9] Because of the

change in optical transition selectivity (k=0), the new absorption (k≠0) might appear at lower energy region (negative dispersion). Anyhow, in order to clarify the origin of new absorption further, more elaborative studies are required.

3-5. SUMMARY

It is concluded from this study that the formation of a pseudomorphic region is of advantage in the production of films with a high degree of epitaxial order. The spectroscopic method employed is very suitable for determining the strained interface layer effect on the electronic structure.

To further understand the origin of the new absorption, a more detailed *in-situ* investigation of the first few layers is required, possibly by reflection high-energy electron diffraction (RHEED) or other optical techniques. A complementary theoretical prediction of the effect by quantum-chemical calculations may also be possible.

This is the first report of such an effect in phthalocyanine films and was made possible by the excellent control of film growth which the MBE technique affords.

REFERENCES

[1]Chapter 2 in this thesis.

[2]L. Edwards and M. Gouterman, J. Mol. Spectrosc. 33, 292 (1970).

[3]B. H. Schechtman and W. E. Spicer, J. Mol. Spectrosc. 33, 28 (1970).

[4]E. Orti, J. L. Bredas, and C. Clarisse, J. Chem. Phys. **92**, 1228 (1990).

[5]A. J. Dann, M. R. Fahy, M. R. Willis, and C. Jeynes, Synth. Met. **18**, 581 (1987).

[6]E. A. Lucia and F. D. Verderame, J. Chem. Phys. **48**, 2674 (1968).

[7]G. C. Osbourn, IEEE J. Quantum Electron. **QE-22**, 1677 (1986).

[8]J. C. Buchholz and G. A. Somorjai, J. Chem. Phys. **66**, 573 (1977).

[9]Y. Iyechika, K. Yakushi, and H. Kuroda, Chem. Phys. **87**, 101 (1984).

CHAPTER 4 EPITAXIAL GROWTH OF ULTRATHIN FILMS OF LUTETIUM DIPHTHALOCYANINE

4-1. INTRODUCTION

In the previous chapters, the characterization and ultraviolet / visible spectroscopic study of MBE-grown thin films of the fluoro-bridged aluminum phthalocyanine polymer, $(AlPcF)_n$, were presented.[1,2] It was shown that on single-crystal alkali halide substrates the orientation of the polymer chains is perpendicular to the substrate and forms a square-lattice structure whose orientation has an epitaxial relation to the substrate. It was suggested that in order to obtain a high degree of epitaxy, the formation of a pseudomorphic layer at the thin-film-substrate interface is important and this can be controlled by the substrate type and the temperature during deposition. A lower substrate temperature during deposition resulted in a higher degree of epitaxy and continuity. It was assumed that the pseudomorphic layer is unstable under high temperature and this causes a lower degree of epitaxy. The degree of epitaxy was related to substrate type and followed the order KCl > KBr > KI. The pseudomorphic layer was assumed to be more stable on substrates of higher ionicity. The phthalocyanine square lattices were found to coincide with the substrate lattices whose vector lengths are approximately 14Å. In the case of KCl, the square lattice was along the [021] or [012] directions, and this causes a bidirectional square lattice (Fig. 4.1). This is $\sqrt{10}\times\sqrt{10}$-type epitaxy in reference

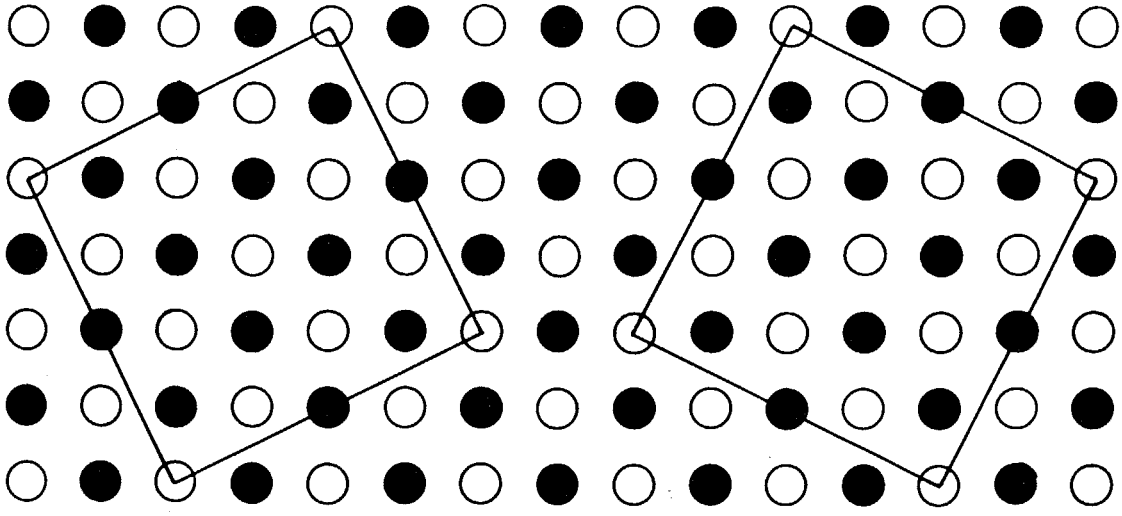

FIG. 4.1. The epitaxial structure AX(100)($\sqrt{10}\times\sqrt{10}$)R$\pm$27° on NaCl-type alkali halides AX. The AX ions are shown as open and solid circles.

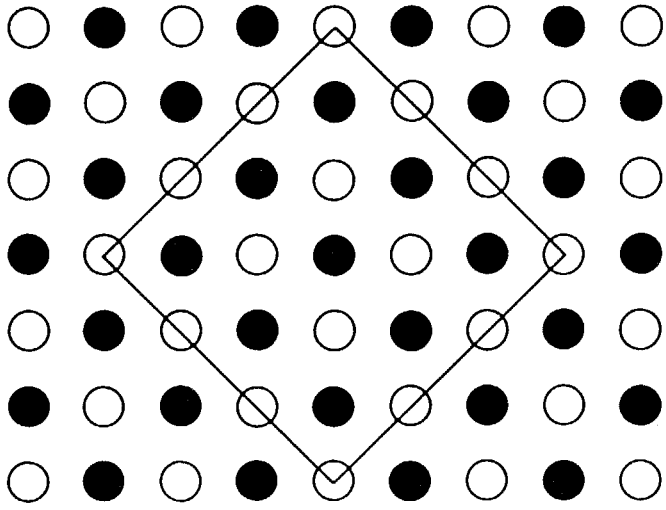

FIG. 4.2. The epitaxial structure AX(100)(3×3)R45° on NaCl-type alkali halides AX. The AX ions are shown as open and solid circles.

to the substrate lattice, which is denoted as KCl(100)($\sqrt{10}\times\sqrt{10}$)R$\pm$27°-$(AlPcF)_n$ in Wood's notation, where $\pm$27° corresponds to $\pm\tan^{-1}(1/2)$. In the case of KBr, the square lattice was along the [011] direction and a unidirectional square lattice was formed (Fig. 4.2). This is 3×3-type epitaxy, which is denoted as KBr(100)(3×3)R45°-$(AlPcF)_n$. In particular, a film grown on KBr at -170 °C was an almost perfect single crystal.

In this chapter, a different phthalocyanine system, lutetium diphthalocyanine ($LuPc_2$), is studied (Fig. 4.3). $LuPc_2$ is a stable radical and its film is known to show interesting electrochromic properties.[3] The structure of the $LuPc_2$ single crystal has been analyzed (Fig. 4.4).[4,5] Using transmission electron microscopy (TEM), Zhang *et al.* analyzed the structure of $LuPc_2$ films deposited on NaCl or KCl kept at 160 °C under a vacuum of 2×10^{-6} Torr.[6,7] According to their results, the $LuPc_2$ column stacks were perpendicular to the substrate and formed square lattices whose orientation had an epitaxial relation to the substrate. In particular, the orientation in the film of $LuPc_2$/KCl was $\sqrt{10}\times\sqrt{10}$-type epitaxy, which is the same as that in $(AlPcF)_n$/KCl. This analogous behavior of $(AlPcF)_n$ and $LuPc_2$ films on KCl motivated the present study. In order to control the orientation of a $LuPc_2$ film, two types of substrates are used in this experiment. The first is a KBr substrate, because the orientation in $(AlPcF)_n$/KBr is different from that on KCl, and it is unidirectional 3×3-type epitaxy. The second one is the $(AlPcF)_n$ film predeposited on KBr. The growth condition of

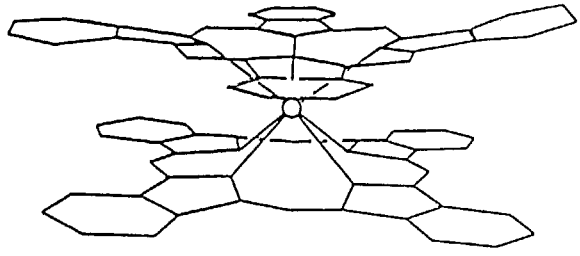

FIG. 4.3. Molecular structure of $LuPc_2$.

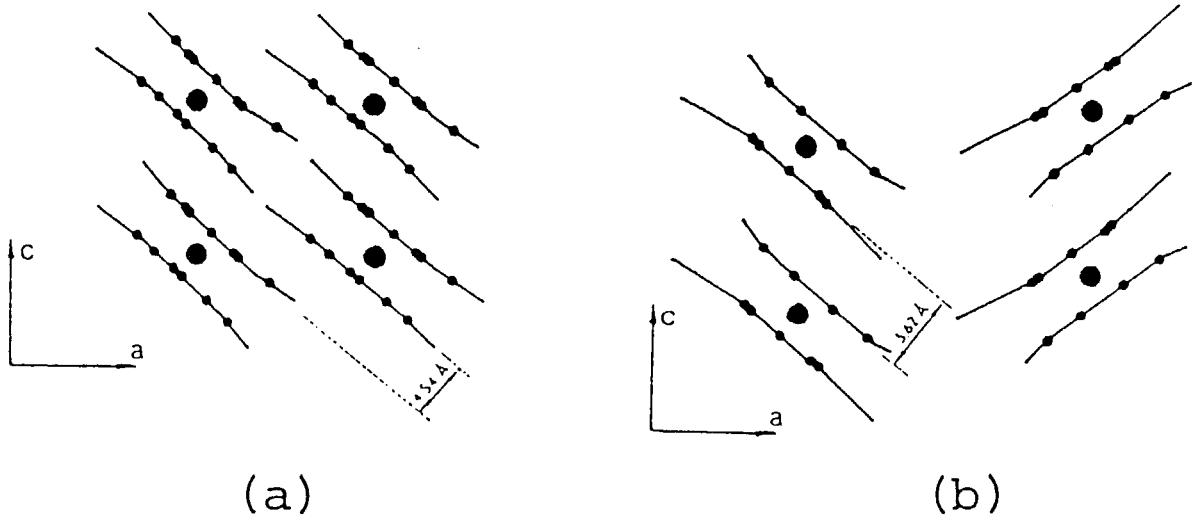

FIG. 4.4. The crystal structures of $LuPc_2$ cited from ref. 5: (a) $LuPc_2$ and (b) $LuPc_2 \cdot CH_2Cl_2$.

high-quality films of $(AlPcF)_n$/KBr has already been established,[1,2] and the growth of different phthalocyanine on a phthalocyanine is interesting from the viewpoint of the preparation of highly ordered organic multilayer systems. In this chapter, the study of the film structure of $LuPc_2$/KBr and $LuPc_2/(AlPcF)_n$/KBr by TEM and scanning electron microscopy (SEM) is reported.

4-2. EXPERIMENT

The $LuPc_2 \cdot CH_2Cl_2$ material was synthesized by the established method of De Cian *et al.*[4] This gave highly pure material as confirmed by microanalysis: Mass % calculated for $Lu(C_{32}H_{16}N_8)_2 \cdot CH_2Cl_2$- C,60.7; H,2.6; N,17.4; found- C,60.76; H,2.81; N,17.23. Outgassing of CH_2Cl_2 from the source material was detected by a mass spectrometer at a Knudsen cell temperature of 170 °C or lower. After finishing outgassing completely, $LuPc_2$ was sublimed at about 430 °C. The MBE growth conditions were similar to those in chapter 2. A double-layer film was prepared through two successive *in situ* steps of deposition. The first step is the deposition of $(AlPcF)_n$ on KBr kept at -170 °C followed by the second step of deposition of $LuPc_2$ at the substrate temperature of 22 and 140 °C. The microscope observation of phthalocyanine films has been well established[8] and was undertaken in a similar manner as in chapter 2.

4-3. RESULTS AND DISCUSSION

The SEM and TEM images of 100-Å $LuPc_2$ film on KBr deposited at 27 °C are shown in Fig. 4.5. The film is made of small crystallites (about 200×200 $Å^2$), and the porous regions between them are so obvious that the continuity was poorer than in the $(AlPcF)_n$ case. The high-resolution TEM lattice image of the same film is shown in Fig. 4.6, which revealed that each crystallite consists of highly ordered square lattices. Detailed examination for the lattice image shows that the relative orientation of the square lattices of different crystallites is definitely controlled by the nature of the substrate. It was noted that on KBr a mutual angle of 37° between the square-lattice images of neighboring crystallites is found over the entire film. This was also confirmed by the electron diffraction pattern (EDP), which consists of two sets of four spots with an angle of 37° between them (Fig. 4.7). These features are the same as those in the reported structure of $(AlPcF)_n$/KCl (Ref. 1) and $LuPc_2$/KCl (Refs. 6 and 7). Thus, the orientation of $LuPc_2$/KBr can be explained by the $\sqrt{10}\times\sqrt{10}$-type epitaxy, KBr(100)($\sqrt{10}\times\sqrt{10}$)R±27°-$LuPc_2$ (Fig. 4.1).

The reported lattice constant of $LuPc_2$/KCl was a = 13.5 Å.[6] If the following lattice constants of the substrates are considered, KCl($\sqrt{10}\times\sqrt{10}$) = 14.07 Å, KBr($\sqrt{10}\times\sqrt{10}$) = 14.75 Å and KBr(3×3) = 13.99 Å, KBr(3×3) should be more favorable than KBr($\sqrt{10}\times\sqrt{10}$) from the viewpoint of lattice mismatch. Actually in the case of $(AlPcF)_n$, preferential selection of KBr(3×3) was observed, and so the selection of KBr($\sqrt{10}\times\sqrt{10}$) in $LuPc_2$/KBr

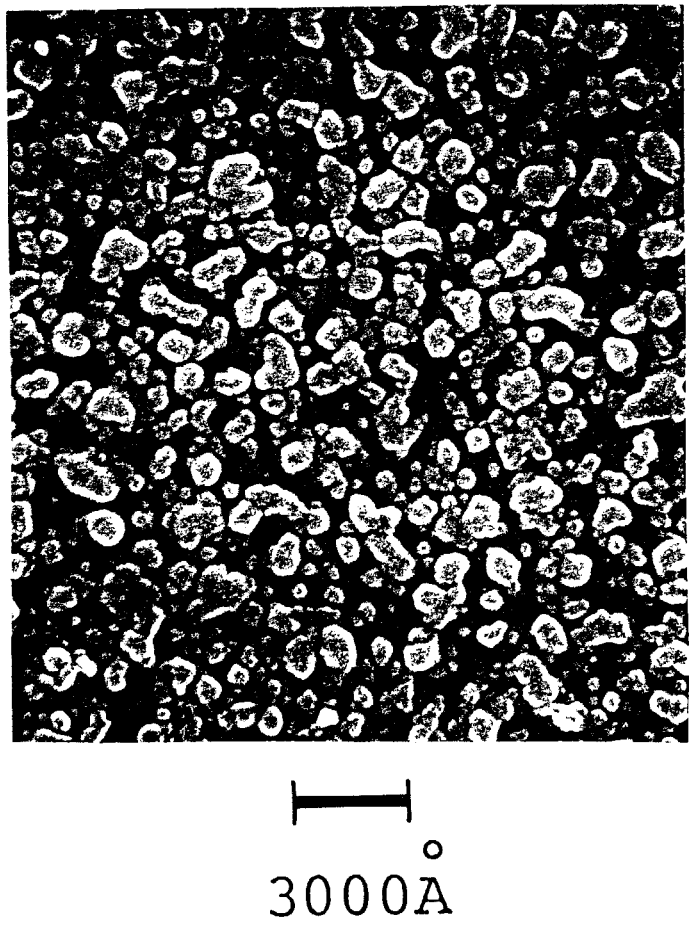

FIG. 4.5. The SEM image of a 100-Å $LuPc_2$/KBr deposited at 27 °C.

FIG. 4.6. The TEM lattice image of a 100-Å $LuPc_2$/KBr deposited at 27 °C.

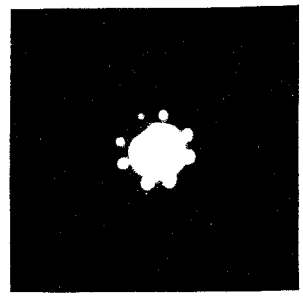

FIG. 4.7. The EDP of a 100-Å $LuPc_2$/KBr deposited at 27 °C.

looks strange. A qualitative explanation is possible by considering the interactions at the interface, $LuPc_2$-$LuPc_2$ interaction and $LuPc_2$-substrate interaction. The essential nature of the epitaxial growth should be determined by the interaction between $LuPc_2$ and substrate ions. However, intermolecular interaction is also important in the growth of crystalline film. First, let us consider the $LuPc_2$-$LuPc_2$ interaction. If a hard-body model of $LuPc_2$ is assumed, in which two phthalocyanines are fixed in the staggered form by 45° and the shape is determined by the van der Waals radius of each atom, it can be shown that the nearest central site of the neighboring $LuPc_2$ is angle dependent as shown in Fig. 4.8 and the minimum value 13.6 Å is achieved at θ = 22.5°, where θ is the angle from the line connecting the center and coordinated nitrogen. Another mechanism may also work to favor θ = 22.5°. In Fig. 4.9 two square units were formed by assuming θ = 22.5° and 67.5°. This corresponds to the model of top and bottom phthalocyanines since two phthalocyanines are known to be staggered by 45°. One remarkable feature of θ = 22.5° is the existence of mirror symmetry between these two units, so the energy of two square units should be equivalent, and this configuration will correspond to the potential energy minimum and stabilize the structure. Second, let us consider the $LuPc_2$-substrate interaction. For simplification let us consider only the bottom phthalocyanine part. According to Ashida,[9] the most probable orientation of phthalocyanine on an alkali halide substrate is the one shown in Fig. 4.10. By taking this orientation, the electrically negative nitrogen

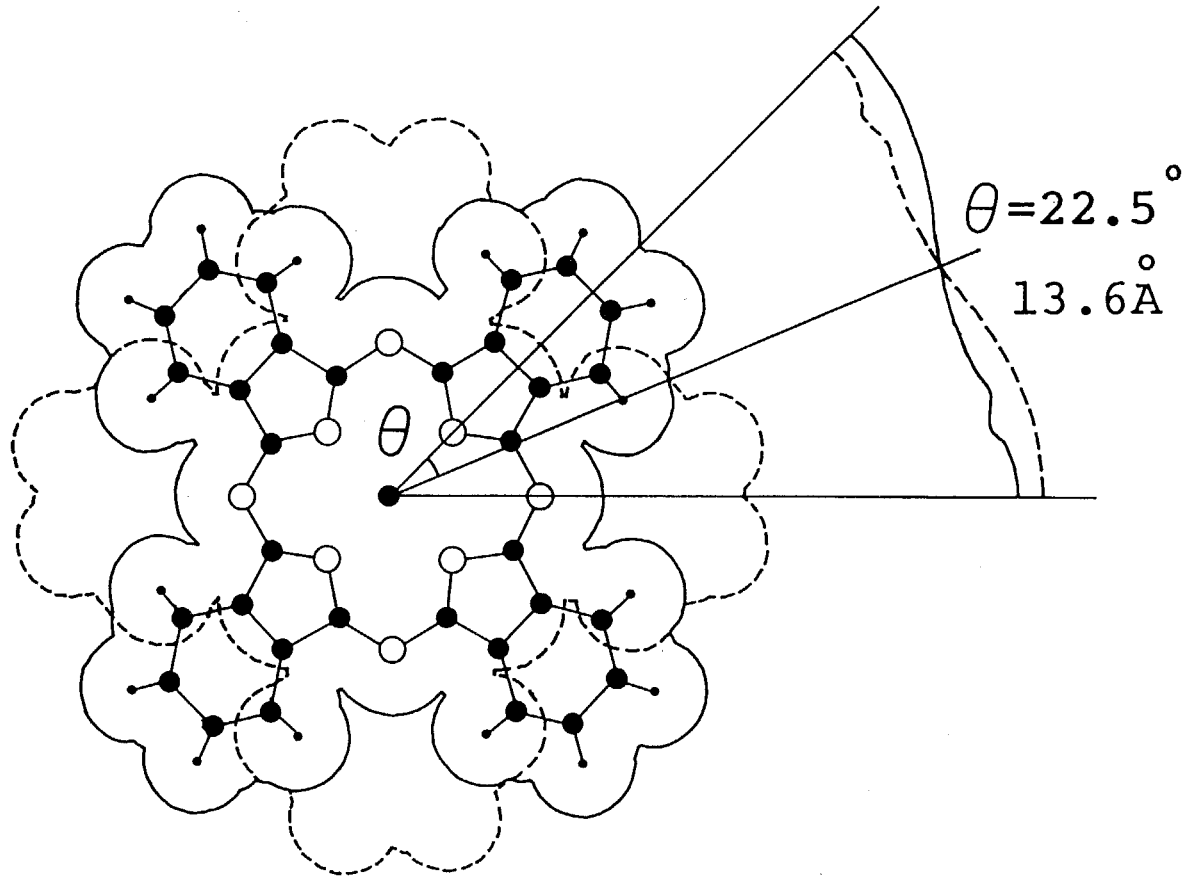

FIG. 4.8. A hard-body model of $LuPc_2$ in which the shape is determined by van der Waals radii of atoms. Two phthalocyanine molecules are drawn by solid and broken lines, and they are staggered by 45°. The traces of possible center positions of nearest-neighboring phthalocyanine molecules are also shown by corresponding lines.

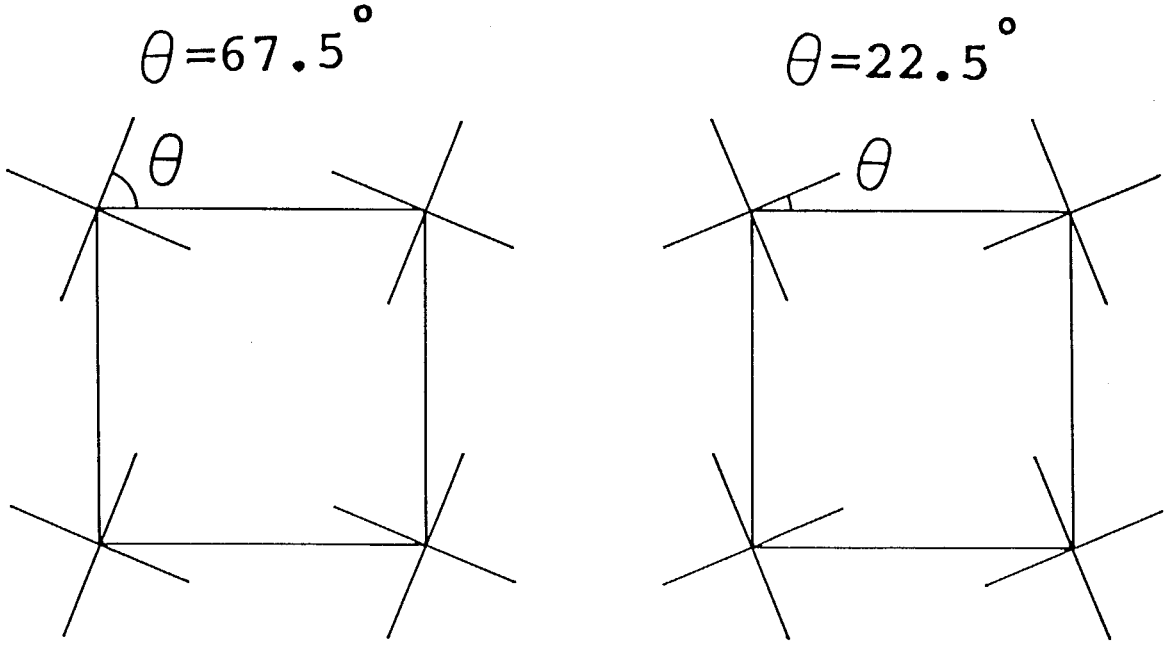

FIG. 4.9. Two possible square units by assuming the orientation of θ = 22.5° and 67.5°.

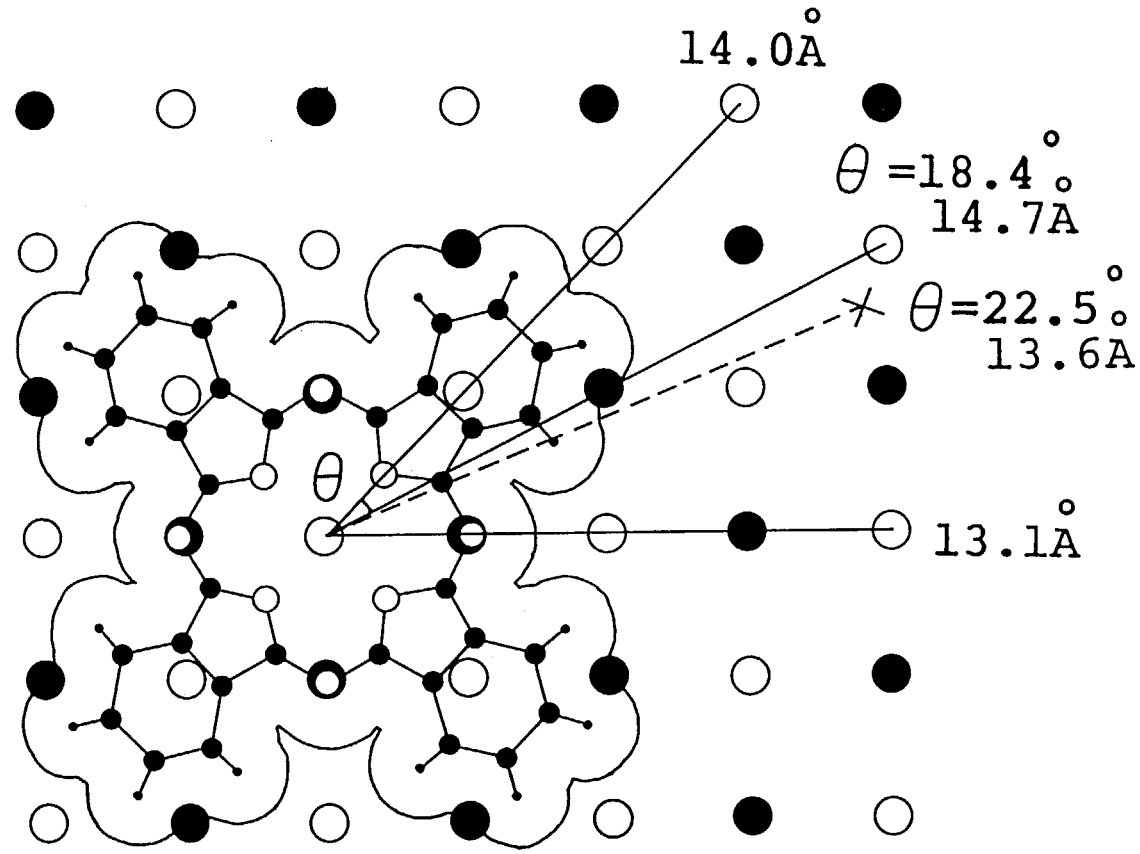

FIG. 4.10. The most probable orientation of phthalocyanine on an alkali halide substrates. The position of neighboring phthalocyanine is also shown based on the assumption of θ = 22.5° and distance 13.6 Å. The nearest corresponding ion site is found at the position of θ = 18.4° and distance 14.7 Å, which is in the [021] direction.

atoms are on the K^+ ions. If one phthalocyanine is fixed like this, it is evident that the most probable site of the next phthalocyanine is in the [021] direction (Fig. 4.10). Figure 4.11 presents the molecular packing model of a square unit according to the above discussion. This reveals good packing with no van der Waals overlap between phthalocyanines.

The SEM images of the double-layer system, 150 Å $LuPc_2$ / 15 Å $(AlPcF)_n$ / KBr, are shown in Figs. 4.12 and 13. The first layer, 15 Å $(AlPcF)_n$ on KBr, was deposited at -170 °C. This condition is believed to be the most ideal for the preparation of the highest-quality film since continuity is excellent and the crystallite orientation on the surface is unidirectional 3×3-type epitaxy (Fig. 4.2).[1] The second layers, 150 Å $LuPc_2$, were deposited under various conditions. One was at 22 °C (Fig. 4.12) and the other one was at 140 °C (Fig. 4.13). The picture reveals that the first layer, $(AlPcF)_n$, consists of small crystallites (100×100 $Å^2$), and continuity seems to be good. It is known that the annealing of $(AlPcF)_n$ on KBr at 140 °C can retain the pseudomorphic layer structure.[2] Thus the observed results about the first layer were the same as the previous results.[1,2] However, the second layer consists of island structures with bigger crystallites (1000×1000 $Å^2$ at 140 °C) and poor continuity. The ordering of the second-layer crystallites seems to be better at 140 °C. It suggests the possibility of epitaxy that allows the rectangular shaped crystallites to grow along the two perpendicular axes.

The TEM lattice image of this film is shown in Fig. 4.14. This picture reveals that the crystallites are dominantly

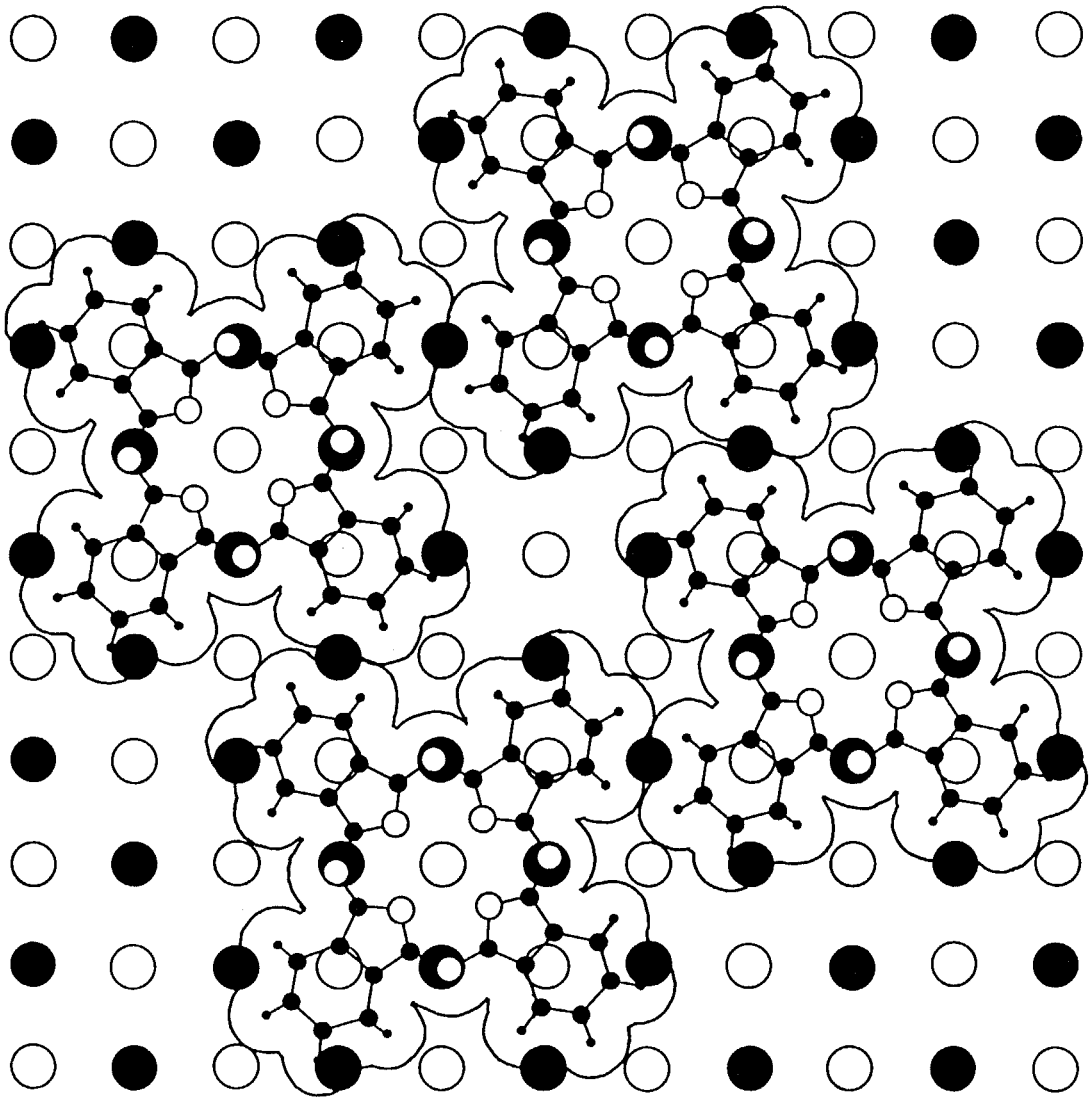

FIG. 4.11. A packing model of the lower molecular plane square unit on KBr.

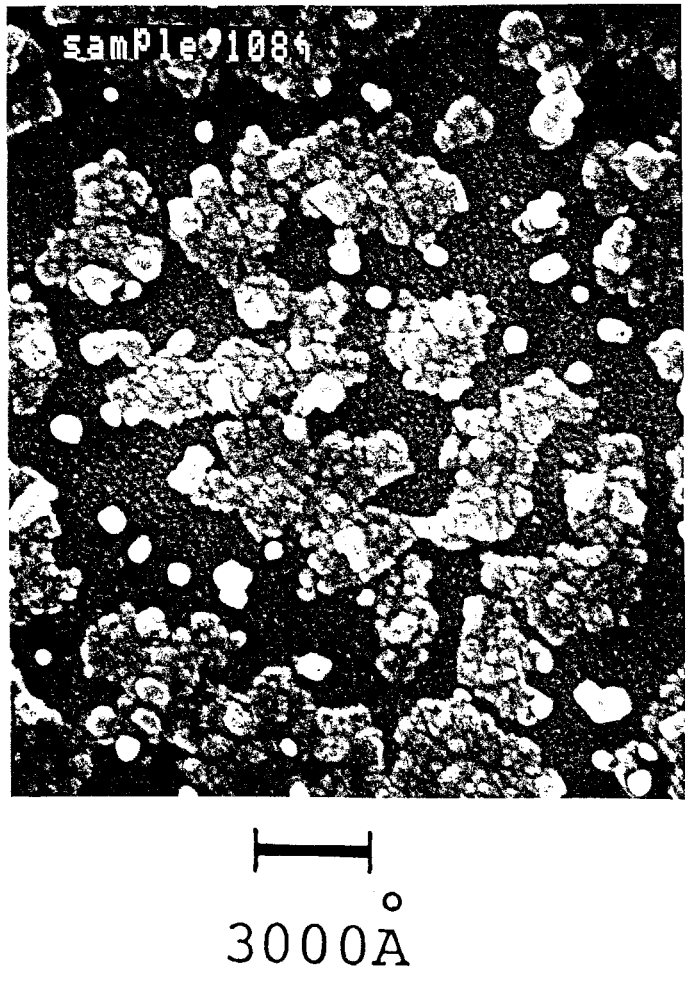

FIG. 4.12. The SEM image of a 150-Å $LuPc_2$/ 15-Å $(AlPcF)_n$/ KBr. $(AlPcF)_n$ and $LuPc_2$ were deposited at -170 and 22 °C, respectively.

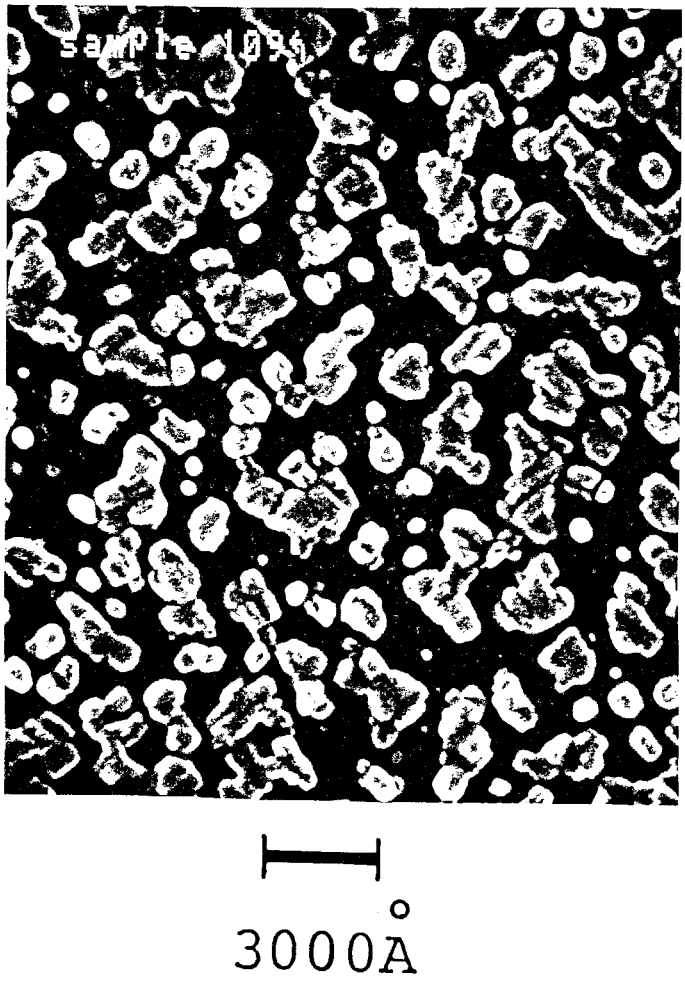

FIG. 4.13. The SEM image of a 150-Å $LuPc_2$/ 15-Å $(AlPcF)_n$/ KBr. $(AlPcF)_n$ and $LuPc_2$ were deposited at -170 abd 140 °C, respectively.

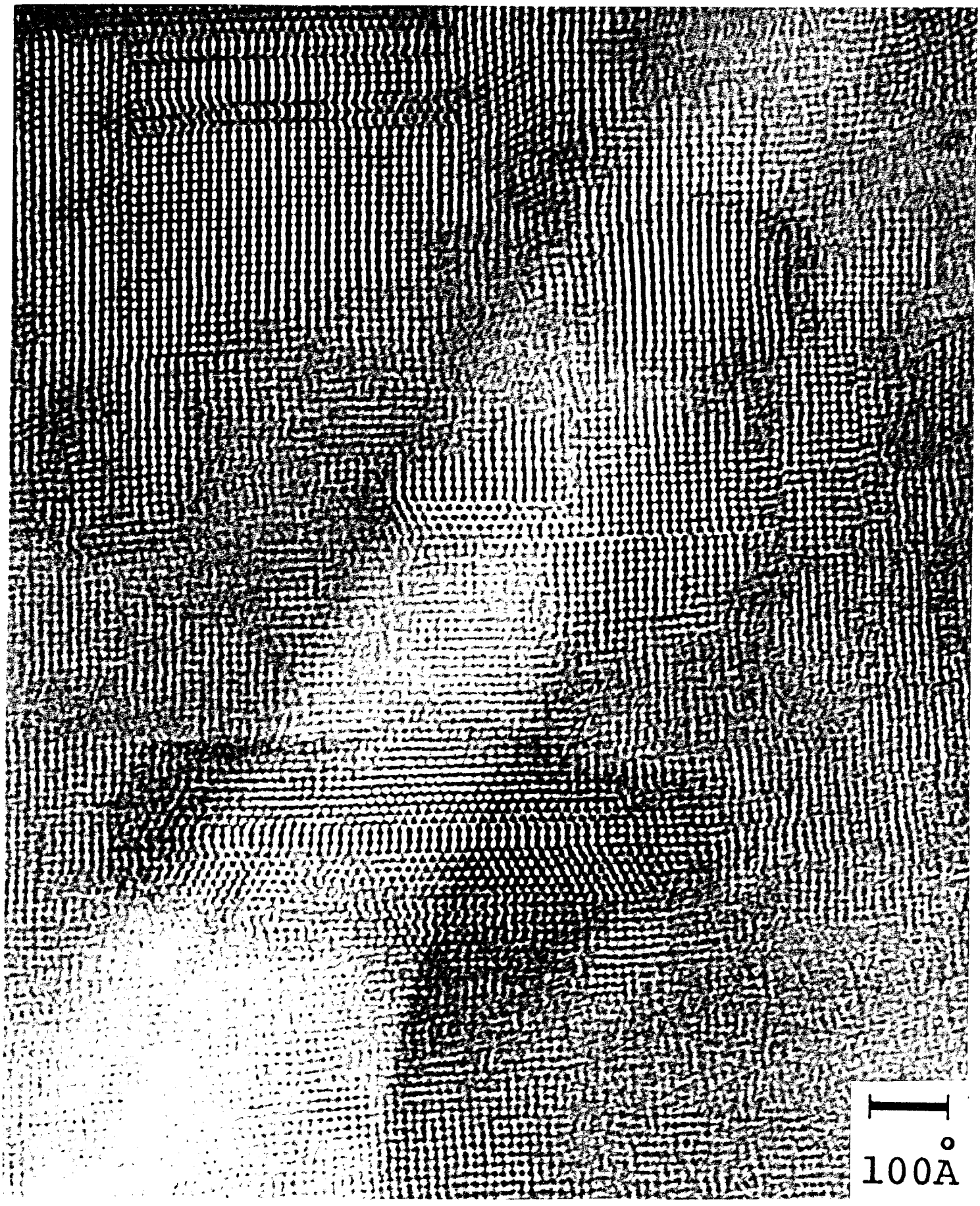

FIG. 4.14. The TEM lattice image of a 150-Å $LuPc_2$/ 15-Å $(AlPcF)_n$/ KBr. $(AlPcF)_n$ and $LuPc_2$ were deposited at -170 and 140 °C, respectively.

composed of unidirectional tetragonal square lattices, and consequently their growth is in 3×3-type epitaxy. The lattice constant of this tetragonal phase was known to be a = 13.4 Å from the observed EDP. It is known that the first layer of $(AlPcF)_n$ on KBr has 3×3-type epitaxy, but the observed structure does not necessarily correspond to the first layer. Because the first layer is very thin, 15 Å, and the second layer is 10 times thicker than the first layer, then it is reasonable to interpret the observed images as due to the $LuPc_2$ layer and the growth of the second layer to be in 3×3-type epitaxy. The result by SEM also supports the unidirectional epitaxy of the second layer. In the previous discussion on $LuPc_2$/KBr it was assumed that the $LuPc_2$-KBr interaction at the interface plays an important role for the preferential selection of KBr √10×√10-type epitaxy. In the present case, however, $LuPc_2$ does not interact with KBr but with the intermediate $(AlPcF)_n$ layer, and so the 3×3-type epitaxy is now possible and preferable since the $(AlPcF)_n$ layer is in 3×3 type.

The TEM lattice image in Fig. 4.14 reveals that small amounts of orthorhombic phase are also present, as seen in the figure. There is a mutual angle of 27° or 63° between the diagonal of the orthorhombic lattice and the side of the tetragonal lattice. This feature can be explained by assuming such epitaxy about the orthorhombic phase as shown in Fig. 4.15. The packing density in the plane of the orthorhombic phase is the same as that of tetragonal phase. This is $(AlPcF)_n$(100)C(2×1)-$LuPc_2$ or equivalently KBr(100)C(6×3)R45°-

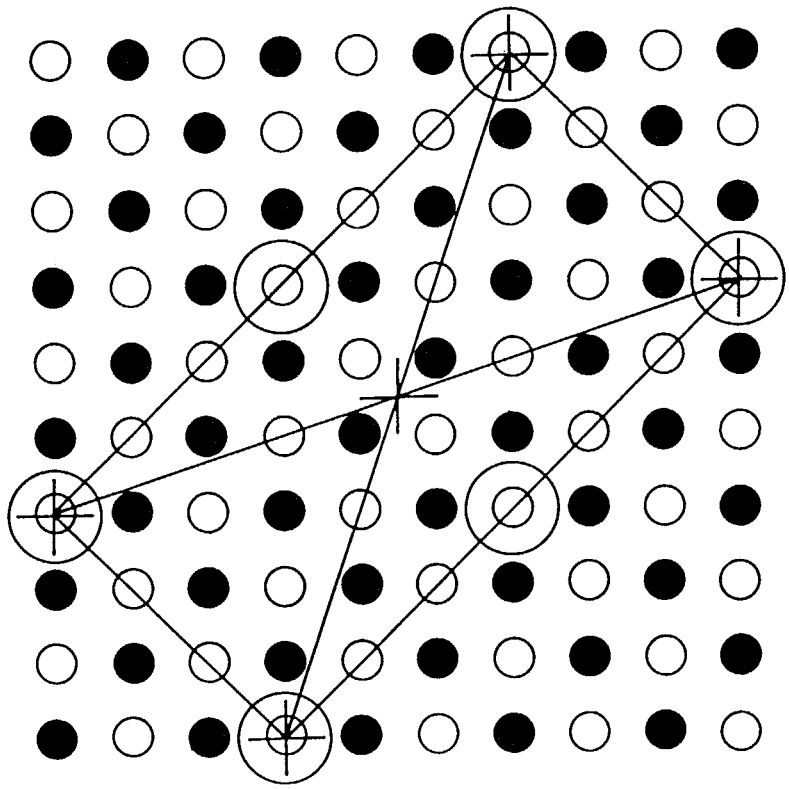

FIG. 4.15. The epitaxial structure AX(100)C(6×3)R45° of $LuPc_2$ on NaCl-type alkali halides AX(×). The AX ions are shown by small open and solid circles. The large open circles situated at AX(100)(3×3)R45° represent the $(AlPcF)_n$ molecules.

$LuPc_2/(AlPcF)_n$. The C(6×3) epitaxial lattices are bidirectional and make an angle of 90° to each other. The EDP of the same film is shown in Fig. 4.16. The reciprocal-lattice points drawn by assuming 3×3- and C(6×3)-type epitaxy are shown in Fig. 4.17, and they are in good agreement with the EDP. In Fig. 4.17, the reciprocal-lattice points corresponding to {20} of √10×√10-type epitaxy are also indicated since weak corresponding spots were found in the EDP (Fig. 4.16). This reveals the coexistence of small amounts of √10×√10-type epitaxy. This structure may occur by the direct contact of $LuPc_2$ with KBr through pinholes that may exist in the very thin $(AlPcF)_n$ layer.

4-4. SUMMARY

Epitaxial films of $LuPc_2$ were obtained on KBr and $(AlPcF)_n$/KBr. In the film of $LuPc_2$/KBr, a √10×√10-type bidirectional tetragonal phase was obtained, and it was explained on the basis of the $LuPc_2$-$LuPc_2$ interaction and $LuPc_2$-substrate interaction. In the film of $LuPc_2/(AlPcF)_n$/KBr, a 3×3-type unidirectional tetragonal phase was obtained. It was also seen that in the film of $LuPc_2/(AlPcF)_n$/KBr, small amounts of C(6×3)-type bidirectional orthorhombic phase were included.

From the viewpoint of the control of the film structure, this study revealed the feasibility of obtaining high-quality $LuPc_2$ films by using $(AlPcF)_n$/KBr as a substrate since the crystallites are mainly of unidirectional tetragonal phase.

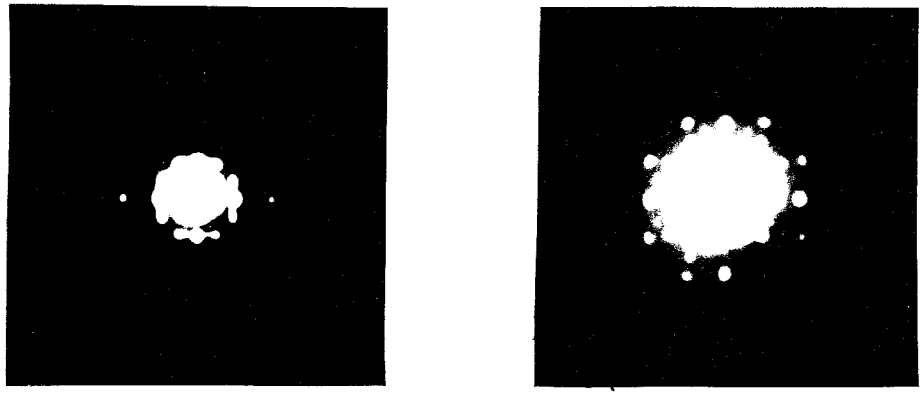

FIG. 4.16. The EDP of a 150-Å $LuPc_2$/ 15-Å $(AlPcF)_n$/ KBr. $(AlPcF)_n$ and $LuPc_2$ were deposited at -170 and 140 °C, respectively. Two pictures are shown to clarify the inside and outside patterns.

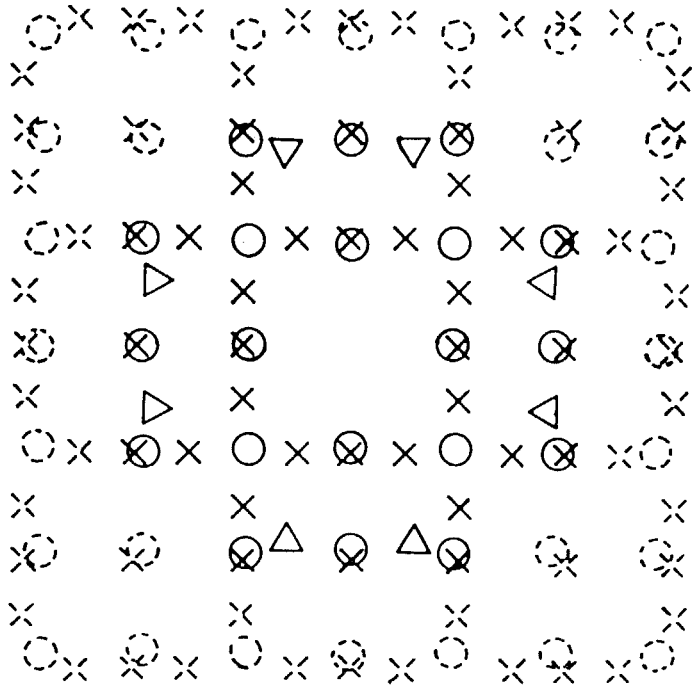

FIG. 4.17. The reciprocal-lattice points drawn by assuming the epitaxy of KBr(100)(3×3)R45°-$LuPc_2$/$(AlPcF)_n$ (○), and KBr(100)C(6×3)R45°-$LuPc_2$/$(AlPcF)_n$, (×). The {20} points corresponding to KBr(100)(√10×√10)R±27° are also shown by Δ. The points drawn by broken lines are not seen in the EDP because their intensities may be too weak.

The next step is to obtain higher continuity and to remove the orthorhombic phase. The effect of temperature and thickness should be examined, and the physical properties of this type of film may be interesting.

REFERENCES

[1]Chapter 2 in this thesis.

[2]Chapter 3 in this thesis.

[3]P. N. Moskalev and I. S. Kirin, Russ. J. Phys. Chem. **46**, 1019 (1972).

[4]A. De Cian, M. Moussavi, J. Fischer, and R. Weiss, Inorg. Chem. **24**, 3162 (1985).

[5]P. Petit, Ph. Turek, J. J. Andre, R. Even, J. Simon, R. Madru, M. Al Sadoun, G. Guillaud, and M. Maitrot, Synth. Met. **29**, F59 (1989).

[6]W. P. Zhang, K. H. Kuo, Y. F. Hou, and J. Z. Ni, J. Solid State Chem. **74**, 239 (1988).

[7]W. P. Zhang, K. H. Kuo, Y. F. Hou, and J. Z. Ni, J. Solid State Chem. **75**, 373 (1988).

[8]T. Kobayashi, Y. Fujiyoshi, and N. Uyeda, J. Cryst. Growth **65**, 511 (1983).

[9]M. Ashida, Bull. Chem. Soc. Jpn. **39**, 2632 (1966).

CHAPTER 5 EPITAXIAL GROWTH OF ULTRATHIN FILMS OF LITHIUM PHTHALOCYANINE

5-1. INTRODUCTION

In the previous chapters, epitaxial growth of fluoro-bridged aluminum phthalocyanine polymer, $(AlPcF)_n$, and lutetium diphthalocyanine, $LuPc_2$, has been realized by using the MBE technique. The study has shown that one-dimensional Pc column stacks form epitaxial square lattices perpendicularly to alkali halide (100) surface. At present, 3×3 and √10×√10 types of epitaxy are known (Fig. 5.1). Unidirectional 3×3 was found in $(AlPcF)_n$/KBr[1] and this single-crystalline film was used to prepare a new Pc multilayer system.[3] Bidirectional √10×√10 was found in $(AlPcF)_n$/KCl,[1] $LuPc_2$/KCl,[2] and $LuPc_2$/KBr.[3] These two types of epitaxy caused the author to study a different Pc system to know more about the nature of the epitaxy on KBr.

In this chapter, the finding of an unusual epitaxy in lithium phthalocyanine (LiPc) on KBr(100), LiPc/KBr is reported. LiPc is known to be a stable radical and the molecular structure is shown in Fig. 5.2. In single crystals, planar LiPc forms one-dimensional column stacks, where two adjacent molecules are rotated by 38.7°, and the columns form square lattices (Fig. 5.3).[4,5] Vacuum-sublimed LiPc films have been prepared,[6] but their structure not determined.

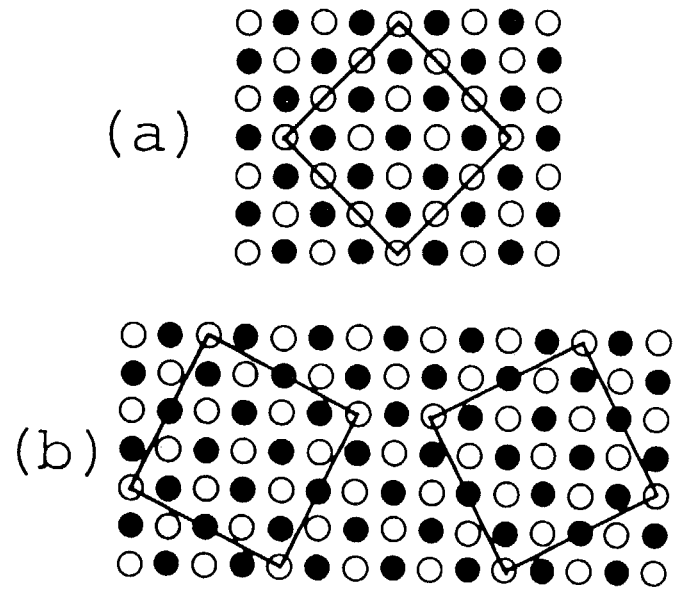

FIG. 5.1. Epitaxial structure (a) AX(100)(3×3)R45°-Pc, and (b) AX(100)(√10×√10)R±27°-Pc on NaCl-type alkali halides AX. The AX ions are shown as open and solid circles.

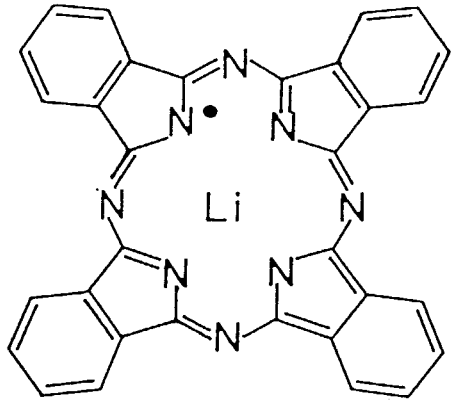

FIG. 5.2. Molecular structure of LiPc.

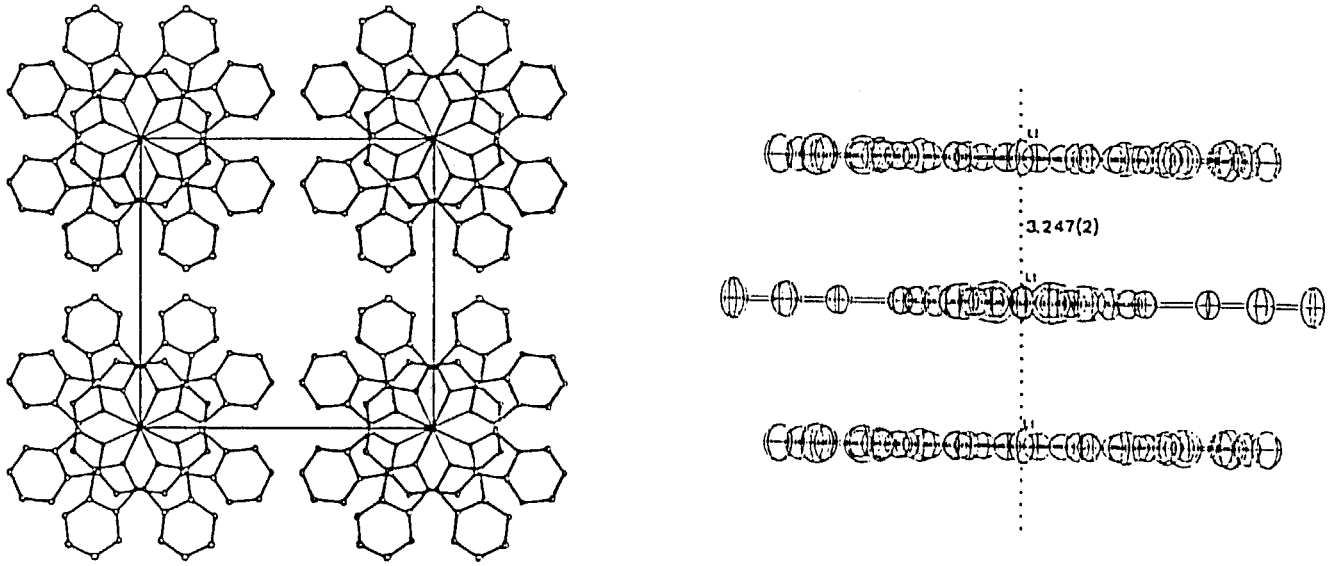

FIG. 5.3. The crystal structure of LiPc cited from ref. 5.

5-2. EXPERIMENT

In this experiment, LiPc was synthesized[4] and used for the MBE growth. The growth conditions and the observation method by transmission electron microscopy (TEM) are similar to those in chapter 2.

5-3. RESULTS AND DISCUSSION

The TEM lattice image of the film is shown in Fig. 5.4. The lattices correspond to the column stacks, so they are perpendicular to the substrate. It also shows the presence of tetragonal and monoclinic phases. In bulk single crystals, only tetragonal and orthorhombic phases are known,[5] so the new monoclinic phase forms only in a film. The mixed phases are also evident from the electron diffraction pattern (EDP) (Fig. 5.5). This EDP can be reconstructed by assuming two types of epitaxy. For the tetragonal phase, bidirectional $\sqrt{10}\times\sqrt{10}$ epitaxy was assumed [Fig. 5.1(b)]. For the monoclinic phase, a new type of tetradirectional $\sqrt{10}\times\sqrt{12.5}$ epitaxy was assumed [Fig. 5.6(a)]. Another four congruent unit meshes shown in Fig. 5.6(b) were derived from those in Fig. 5.6(a), since the same nets are formed. The reciprocal lattice points based on these epitaxies are shown in Fig. 5.7, which agree well with the EDP. Therefore, the assumed epitaxy agrees with this model.

In the preceding chapter[3] the reason why $LuPc_2$/KBr prefers $\sqrt{10}\times\sqrt{10}$ to 3×3 was explained based on the interactions at the

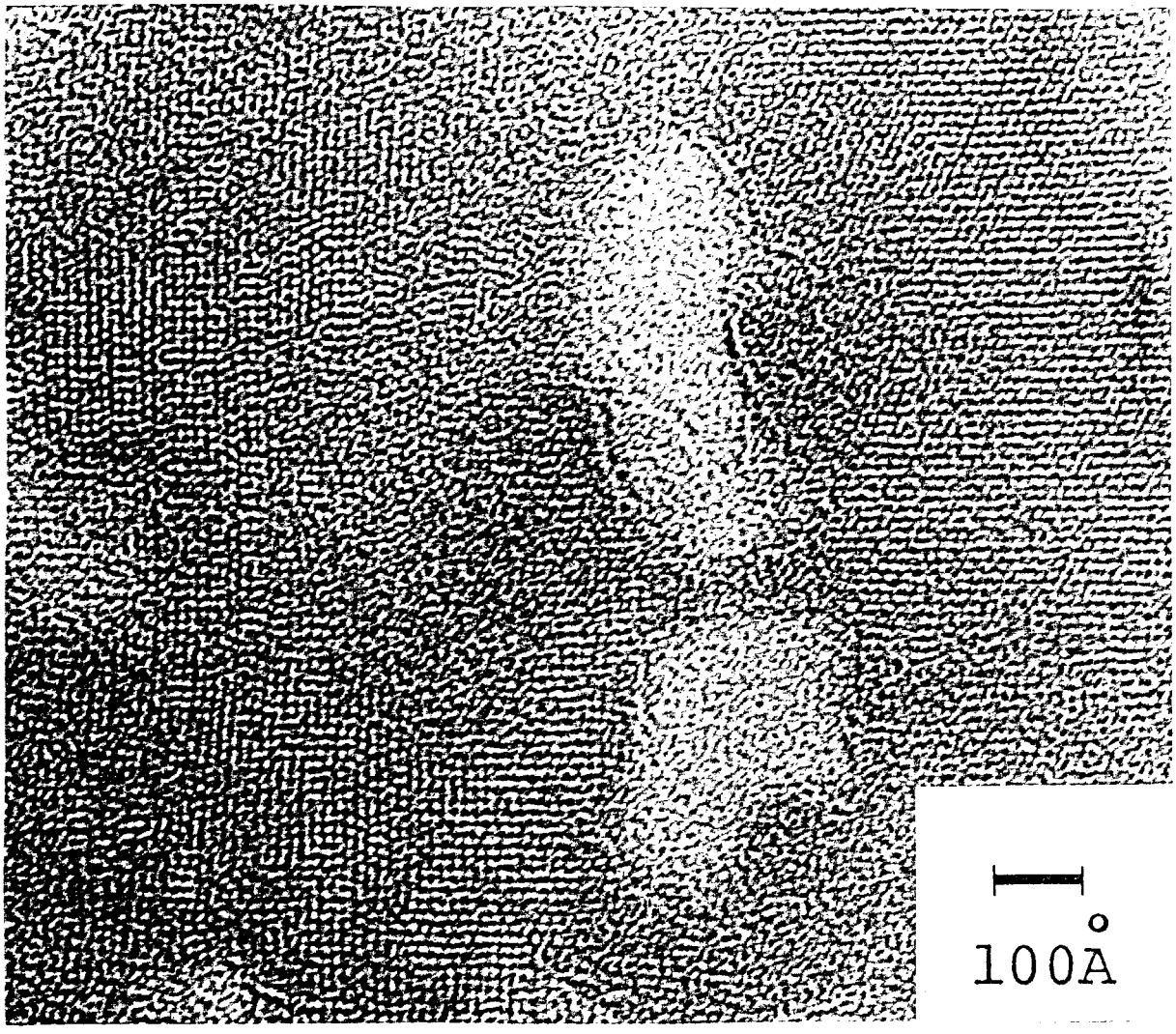

FIG. 5.4. The TEM lattice image of a 430-Å LiPc/KBr deposited at 28 °C.

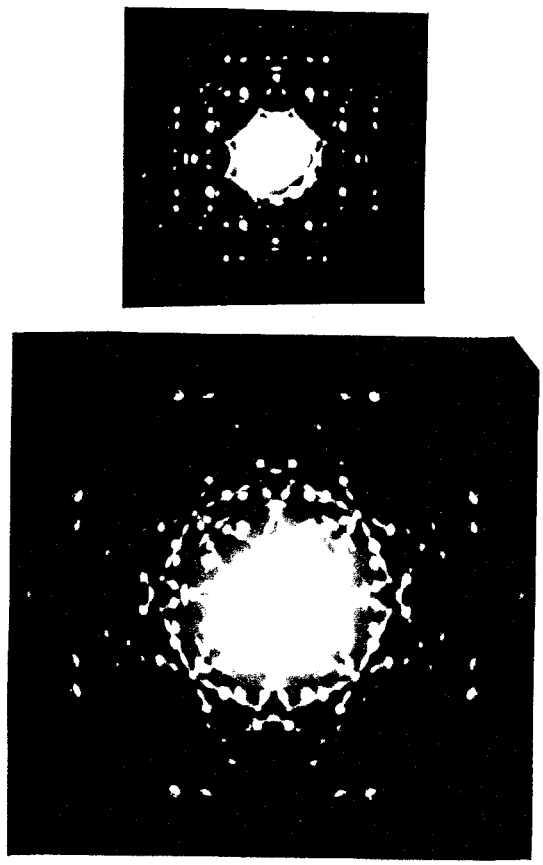

FIG. 5.5. The EDP of a 430-Å LiPc/KBr deposited at 28 °C. Two pictures are shown to clarify the inside and outside patterns.

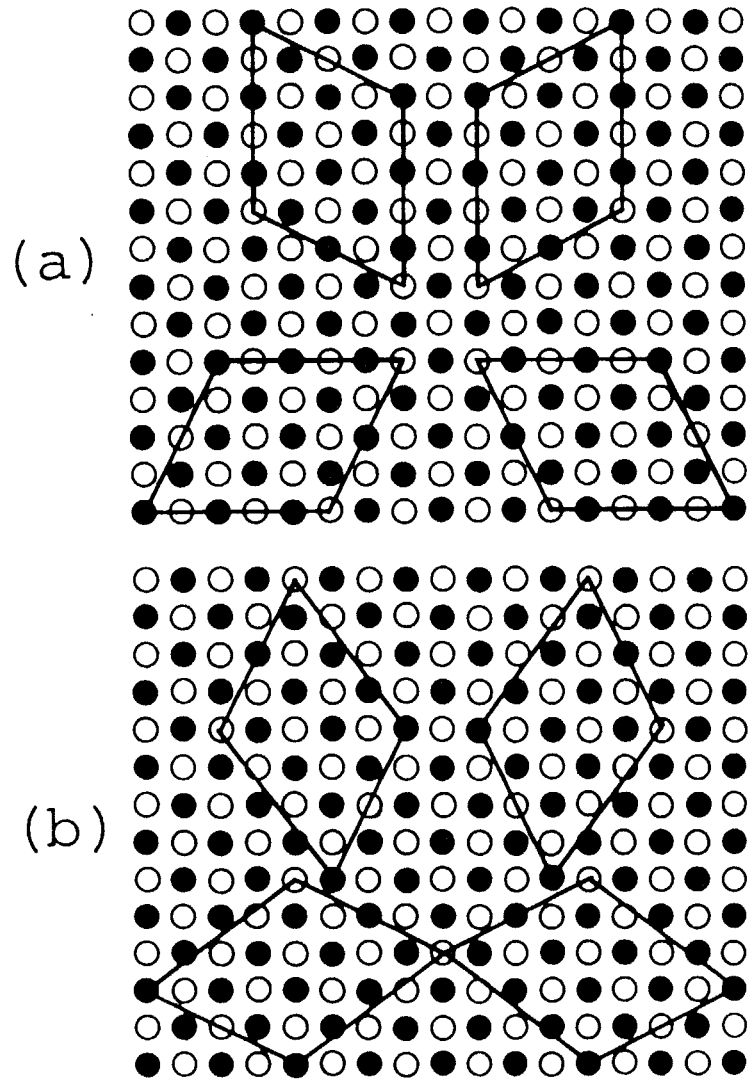

FIG. 5.6. (a) Four unit meshes for √10×√12.5-type epitaxy on KBr(100), and (b) other four unit meshes that depend on (a).

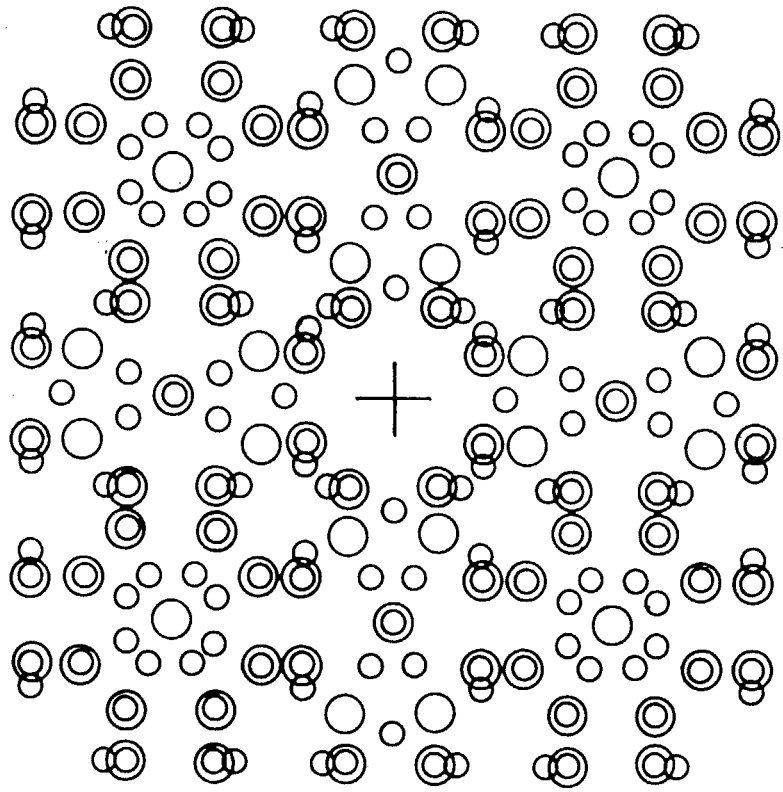

FIG. 5.7. The reciprocal-lattice points drawn by assuming $\sqrt{10}\times\sqrt{10}$-type epitaxy (large open circles) and $\sqrt{10}\times\sqrt{12.5}$-type epitaxy (small open circles) on KBr(100).

interface; Pc-substrate and Pc-Pc interactions. For the former interaction, Ashida's model was applied, which considers the electrostatic interaction and assumes that the Pc metal center is located on the substrate halogen ion and the Pc nitrogen atoms coordinated to the metal center are located on the substrate alkali metal ions.[7] For the latter interaction, which determines the next Pc position, a hard-body model was applied. In this model, the molecular shape of $LuPc_2$, which is rotated by 45°, characterizes the anisotropic van der Waals interaction and the most favorable direction is [021] or [012], which corresponds to $\sqrt{10}\times\sqrt{10}$ epitaxy. This is also applicable to LiPc since 38.7° rotated $(LiPc)_2$ has similar shape of $LuPc_2$. Thus, LiPc also prefers $\sqrt{10}\times\sqrt{10}$ to 3×3.

On the other hand, in unusual $\sqrt{10}\times\sqrt{12.5}$ epitaxy, Li center is located on both K^+ and Br^-, so Ashida's model cannot be simply applied. At present two interpretations are possible. One is the contribution of a bond between Li and K, whose nature is unknown, but a similar bond may appear in the epitaxy of metal-Pc on Cu.[8] The other interpretation is the growth of pseudomorphic layers, where the first layer is grown as $\sqrt{10}\times\sqrt{8}$ and/or $\sqrt{10}\times\sqrt{18}$ epitaxy shown in Fig. 5.8. After a few layers growth, it relaxes to $\sqrt{10}\times\sqrt{12.5}$. In this case, Ashida's model is retained, however, the convergence to $\sqrt{12.5}$ is accidental.

5-4. SUMMARY

This study has revealed the unusual epitaxy in LiPc/KBr. Two epitaxial phases are found in this system. One is

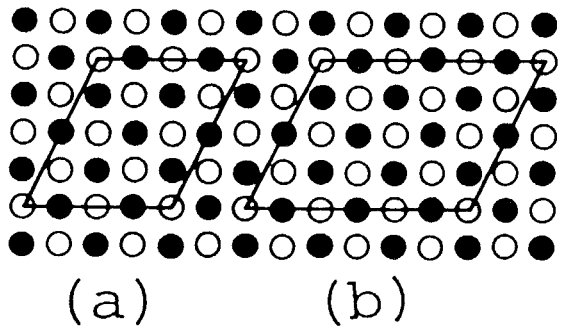

FIG. 5.8. (a) One example of unit meshes for √10×√8-type epitaxy, and (b) √10×√18-type epitaxy on KBr(100).

bidirectional tetragonal phase ($\sqrt{10}\times\sqrt{10}$). The other is a new type of tetradirectional monoclinic phase ($\sqrt{10}\times\sqrt{12.5}$), in which LiPc lattices match with both K^+ and Br^- ions, which form unusual unit meshes. For further understanding, the nature of the first layer Pc should be studied.

REFERENCES

[1]Chapter 2 in this thesis.

[2]W. P. Zhang, K. H. Kuo, Y. F. Hou, and J. Z. Ni, J. Solid State Chem. 75, 373 (1988).

[3]Chapter 4 in this thesis.

[4]H. Sugimoto, M. Mori, H. Masuda, and T. Taga, J. Chem. Soc., Chem. Commun. 1986, 962.

[5]The crystal structure of LiPc is tetragonal at 22 °C (a = 13.846 Å, c = 6.488 Å) and orthorhombic at different temperatures. H. Masuda, in Abstract of the 58th Spring Meeting of Japan Chem. Soc. Kyoto, 1989, Vol. 1, p. 943.

[6]P. Turek, P. Petit, J.-J. Andre, J. Simon, R. Even, B. Boudjema, G. Guillaud, and M. Maitrot, J. Am. Chem. Soc. 109, 5119 (1987).

[7]M. Ashida, Bull. Chem. Soc. Jpn. 39, 2632 (1966).

[8]J. C. Buchholz and G. A. Somorjai, J. Chem. Phys. 66, 573 (1977).

CHAPTER 6 EPITAXIAL GROWTH OF ULTRATHIN FILMS OF CHLOROALUMINUM AND VANADYL PHTHALOCYANINES

6-1. INTRODUCTION

Epitaxy is an important condition to prepare a highly ordered film on a substrate and it is a basis of preparation of artificial superlattice systems. Because of their potential applications in optical or electrical devices, organic films are becoming important. Recent finding of the epitaxy in the system of phthalocyanine (Pc) on alkali halide substrates has enabled us to obtain high-quality Pc films by the molecular-beam epitaxy (MBE) technique.[1-6] These studies showed that one-dimensional Pc column stacks are perpendicular to alkali halide (100) surfaces and form epitaxial lattices. Single-crystalline films were obtained in fluoro-bridged aluminum phthalocyanine polymer, $(AlPcF)_n$, on KBr, $(AlPcF)_n$/KBr, where epitaxial square lattices are unidirectional 3×3-type (Fig. 6.1)[1], and this type of film was used to prepare a new Pc double-layer system.[4] On the other hand, in $(AlPcF)_n$/KCl, epitaxial square-lattices are bidirectional $\sqrt{10}\times\sqrt{10}$-type (Fig. 6.2).[1] In the different Pc systems, lutetium diphthalocyanine ($LuPc_2$)/KCl[3] or KBr[4], lithium phthalocyanine (LiPc)/KBr[5], and vanadyl phthalocyanine (VOPc)/KCl[6], $\sqrt{10}\times\sqrt{10}$-type was also found, but the unidirectional epitaxy has not been realized. This bidirectional epitaxy is unfavorable to obtain a continuous single-crystalline film, and the dominating factor to realize the unidirectional epitaxy should be determined.

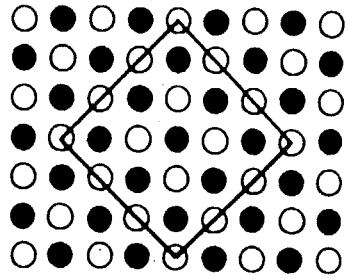

FIG. 6.1. The epitaxial structure AX(100)(3×3)R45° on NaCl-type alkali halides AX. The AX ions are shown as open and solid circles.

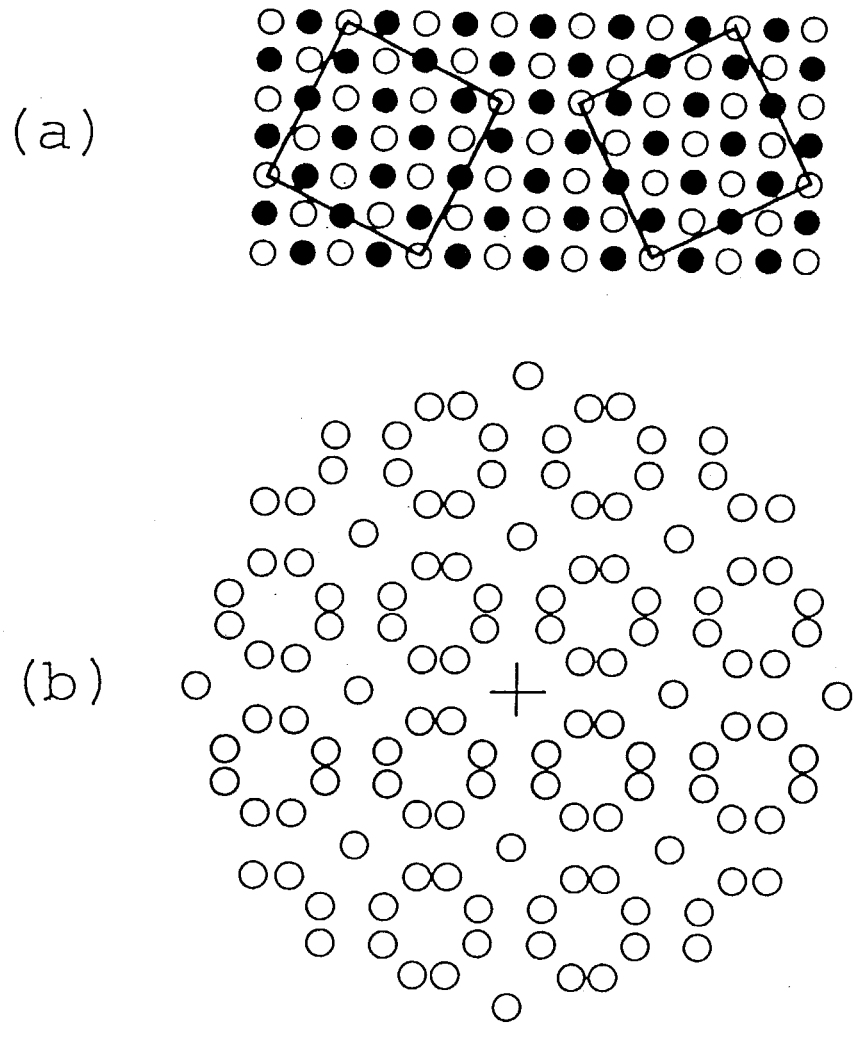

FIG. 6.2. (a) The epitaxial structure AX(100)($\sqrt{10}\times\sqrt{10}$)R$\pm$27° on NaCl-type alkali halides AX. The AX ions are shown as open and solid circles and (b) its reciprocal-lattice points.

In this chapter, chloroaluminum phthalocyanine (AlPcCl) (Fig. 6.3) and VOPc (Fig. 6.4) are studied with the intention of obtaining unidirectional epitaxy. Films of VOPc[6-8] and AlPcCl[9,10] have been already studied by several researchers, and Tada *et al.* presented $\sqrt{10}\times\sqrt{10}$-type epitaxy model on VOPc/KCl based on reflection high-energy electron diffraction (RHEED) patterns,[6] however, no unidirectional epitaxy has been realized in these compounds. Unidirectional epitaxy is realized only in the case of $(AlPcF)_n$.[1] AlPcCl and VOPc have protrudent chlorine and oxygen atoms, respectively, and their molecular structures are similar to that of the monomer form of $(AlPcF)_n$, so a unidirectional epitaxial film of AlPcCl or VOPc is expected to be obtained. AlPcCl and VOPc films were prepared on alkali halide (100) surfaces by the MBE method and their details of morphology and epitaxy were studied by scanning electron microscopy (SEM) and transmission electron microscopy (TEM). AlPcCl is known as saturable absorber[11] and similar compounds, $(AlPcF)_n$ and GaPcCl, is known to show large optical nonlinearity.[12] VOPc is also known to show large optical nonlinearity.[8] Thus, the epitaxial films are expected to have large nonlinear optical activity.

6-2. EXPERIMENT

The AlPcCl and VOPc materials were purchased from Eastman Kodak Company and purified by sublimation. The base pressure in the MBE vessel was about 2×10^{-9} Torr and the film-growth condition was similar to that in chapter 2. The microscope

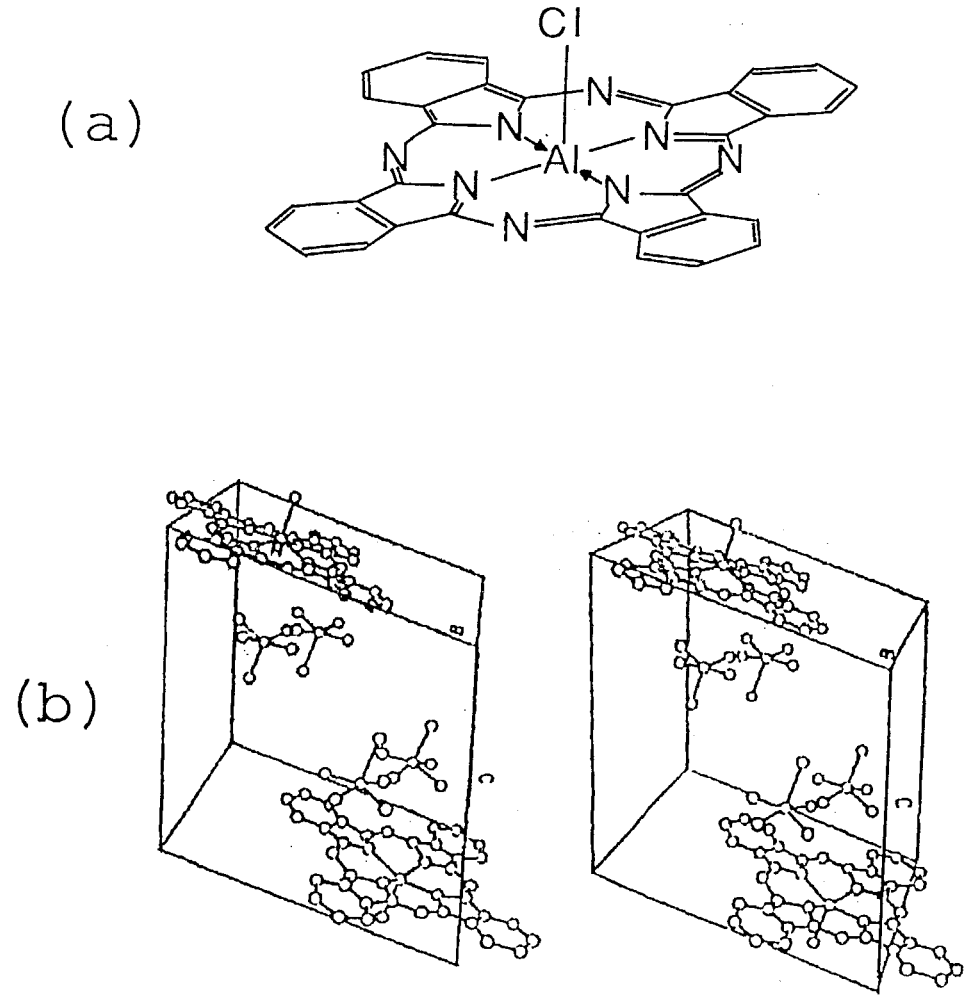

FIG. 6.3. (a) Molecular structure and (b) crystal structure of AlPcCl cited from ref. 14.

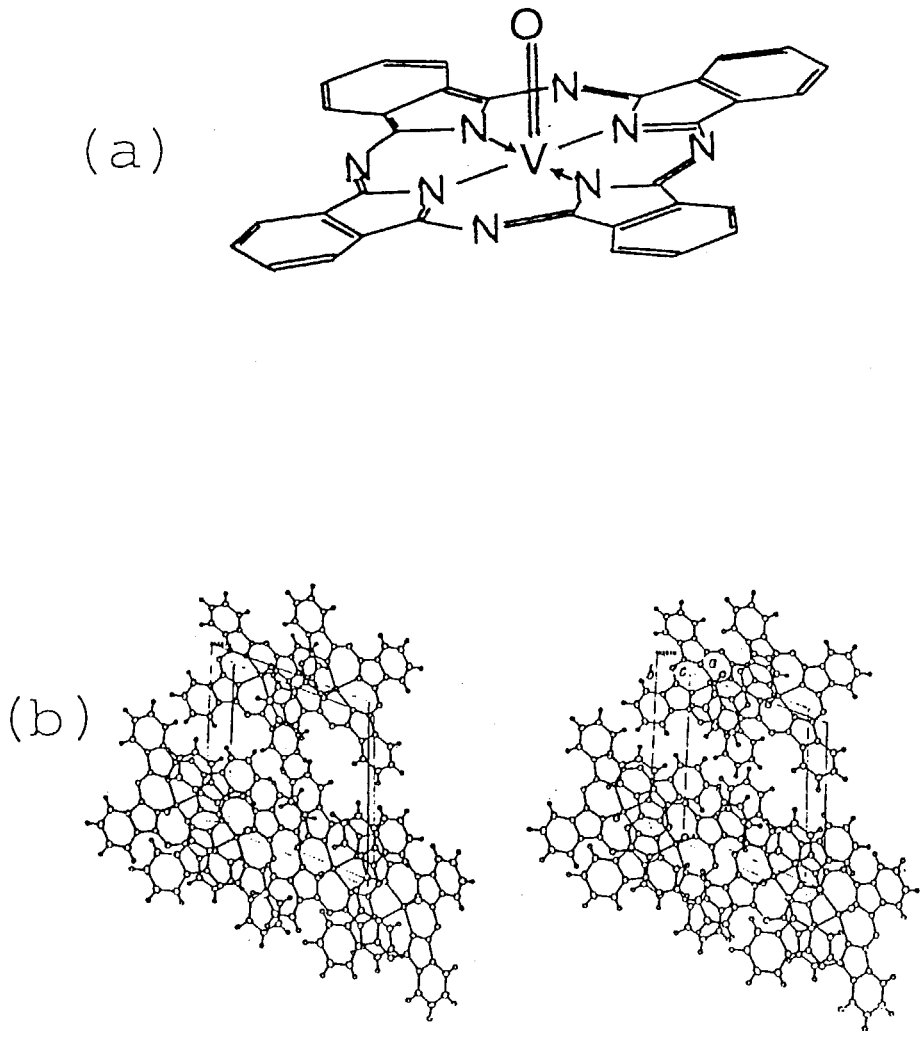

FIG. 6.4. (a) Molecular structure and (b) crystal structure of VOPc cited from ref. 16.

observation of Pc films has been established[13] and was undertaken in a similar manner as in chapter 2. A new technique for TEM sample preparation, coupled sample technique, was introduced to determine the epitaxial lattice direction. The process in this method was as follows: Two AlPcCl films deposited on different substrates were coated with carbon by evaporation and each was cleaved into a small piece using a razor blade. The two pieces with the different substrates were combined by a sticking tape to fix each piece as shown in Fig. 6.5. After the substrates were removed by the wet stripping, the coupled films were mounted on a TEM mesh and finally the tape was removed. These two films should hold the same lattice direction of the substrates. If a standard epitaxial film whose epitaxial lattice direction is known is coupled to the other film in question, the direction of the substrate lattice can be assigned. Thus, the epitaxial lattice direction in question can be determined.

6-3. RESULTS

A. Morphology

The SEM image of 100-Å AlPcCl film on NaCl deposited at 31 °C is shown in Fig. 6.6. Similar structure was also found in the films on KCl, KBr, and KI substrates. The film is continuous and made of densely packed crystallites (about 500×500 $Å^2$), which are bigger than those in $(AlPcF)_n$ films deposited at room temperature.[1] The continuity is as good as

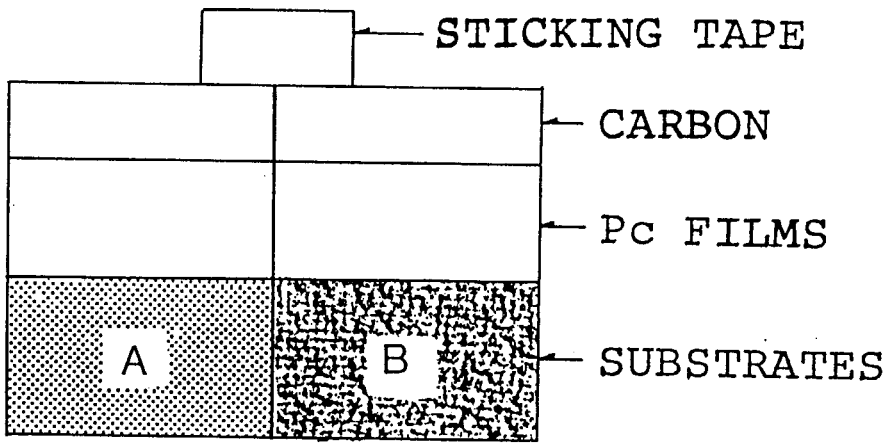

FIG. 6.5. Preparation of coupled films.

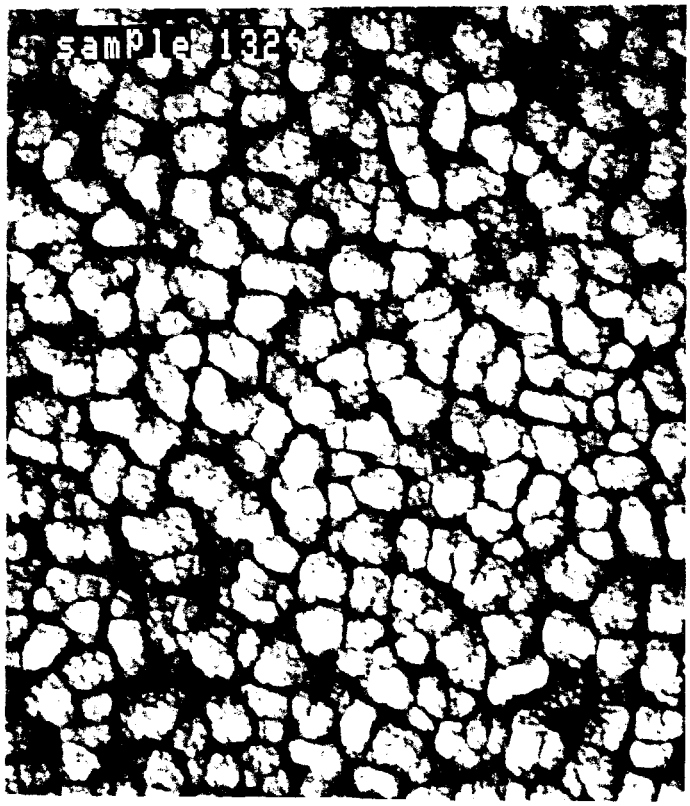

FIG. 6.6. The SEM image of 100-Å AlPcCl/NaCl deposited at 31 °C.

that of $(AlPcF)_n$ films deposited at room temperature (Ref.1) and better than that of $LuPc_2$ films (Ref.4).

The TEM images of 100-Å VOPc films on KCl and KBr are shown in Figs. 6.7 and 8. The films were also continuous and consisted of densely packed crystallites (about 500×500 $Å^2$). Thus, good continuity is found in the Pc systems, $(AlPcF)_n$, AlPcCl, and VOPc that have the protrudent atoms.

The effect of substrate temperature during deposition was studied in the case of AlPcCl/KI. The SEM images of 100-Å AlPcCl films on KI deposited at 31 and -170 °C are shown in Fig 6.9. On the lower-temperature substrate, smaller crystallites (about 300×300 $Å^2$) are grown. A similar behavior was observed in $(AlPcF)_n$ films.[1]

B. Epitaxy

1. AlPcCl

The TEM lattice image of 100-Å AlPcCl film on KI deposited at 31 °C is shown in Fig. 6.10. The lattices correspond to the column stacks, so they are perpendicular to the substrate. The electron diffraction pattern (EDP), whose electron-beam sampling diameter is 5 μm, shows that the film is predominantly made of unidirectional tetragonal phase (Fig. 6.11). It seems that the crystallinity of this film is better than that of the reported films[10] prepared by the conventional evaporation method. In bulk single crystals, only triclinic phase is known, where the unit cell consists of four AlPcCl molecules and two of them are disordered [Fig. 6.3(b)].[14] Thus, the

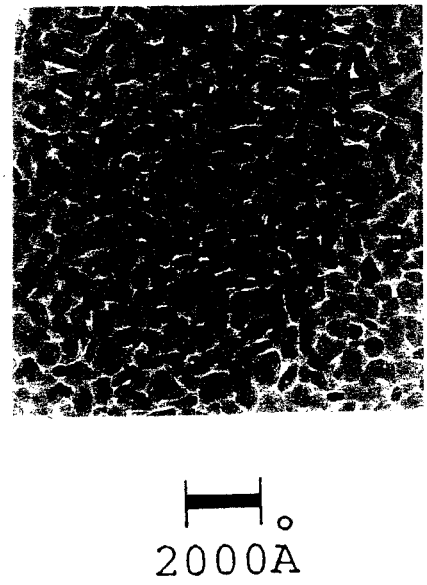

FIG. 6.7. The TEM image of 100-Å VOPc/KCl deposited at 32 °C.

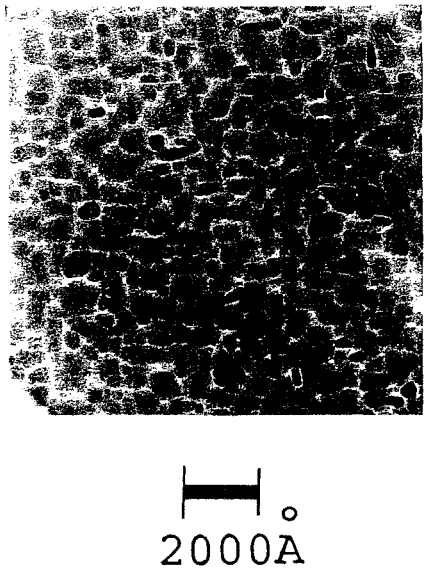

FIG. 6.8. The TEM image of 100-Å VOPc/KBr deposited at 29 °C.

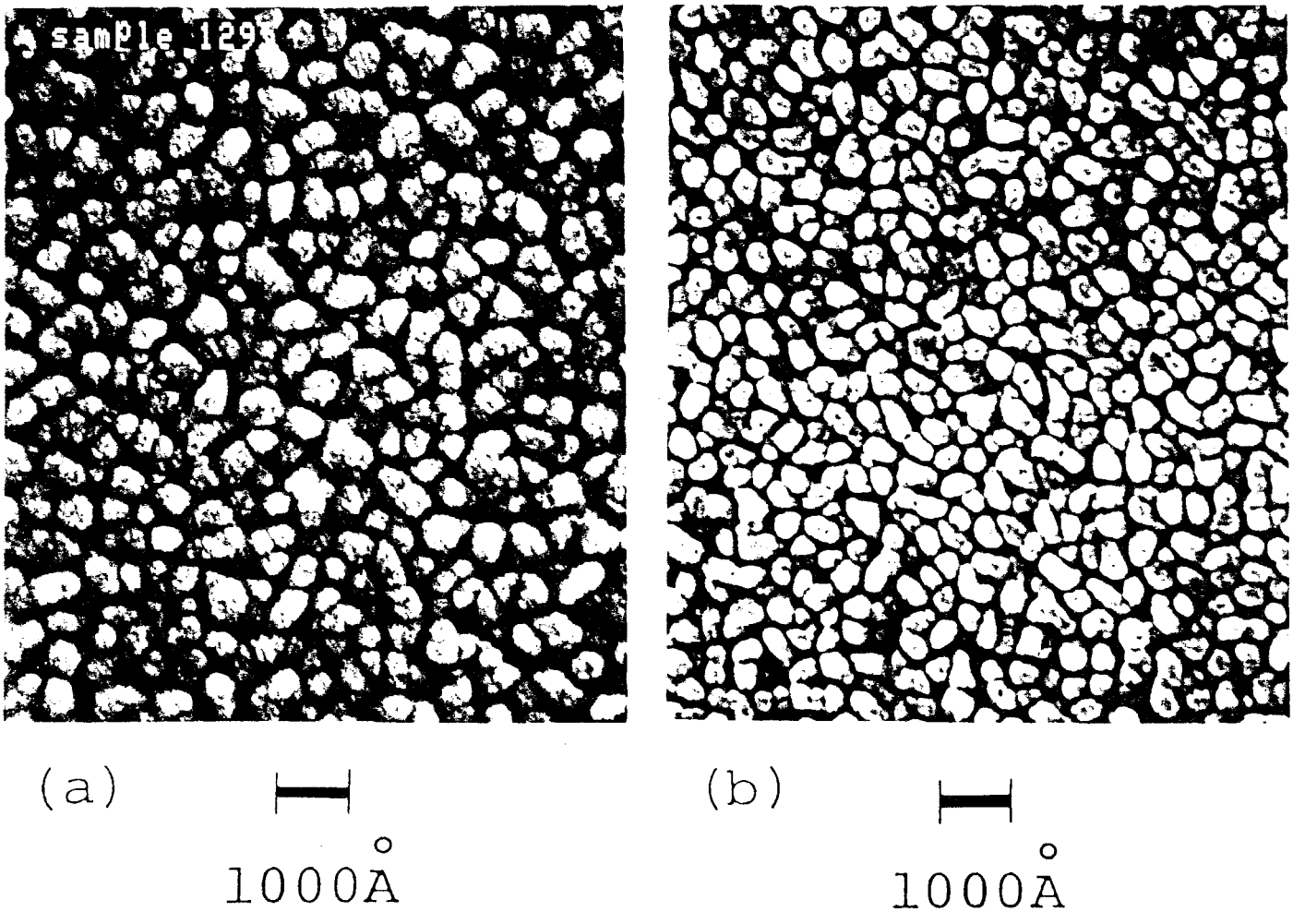

FIG. 6.9. The SEM images of 100-Å AlPcCl/KI deposited at (a) 31 °C and (b) -170 °C.

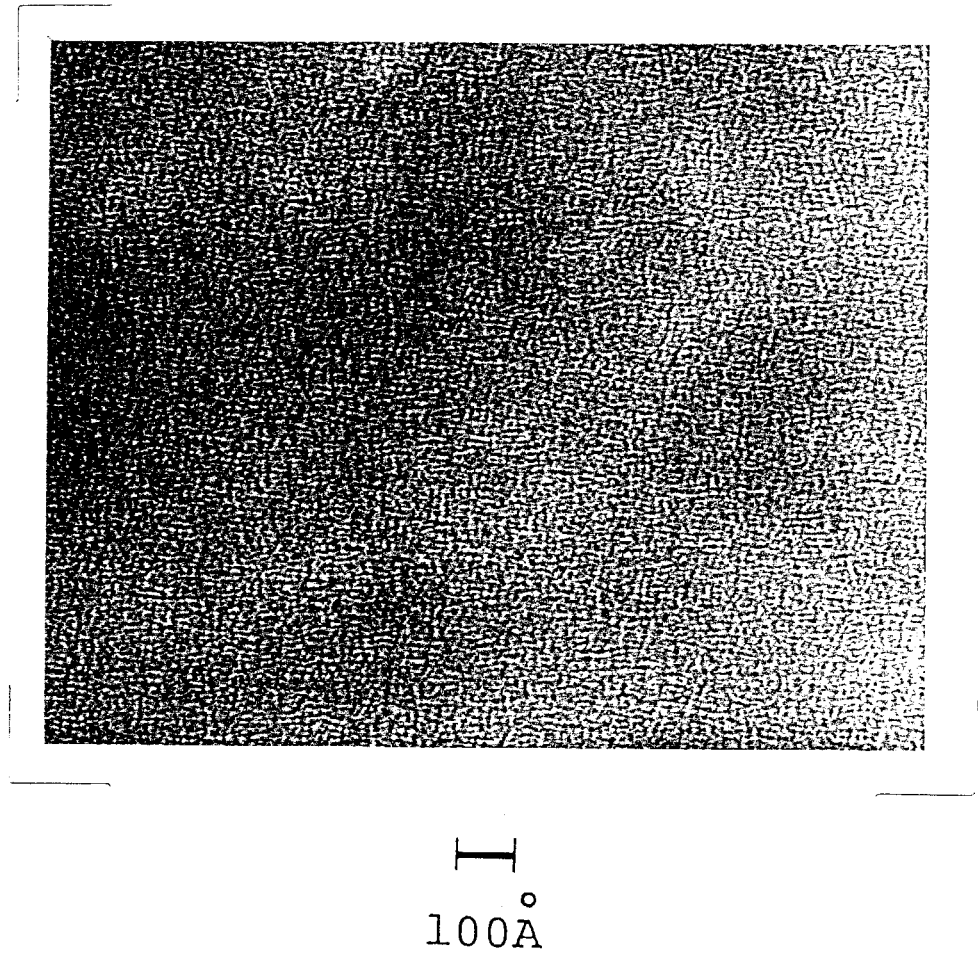

FIG. 6.10. The TEM lattice image of 100-Å AlPcCl/KI deposited at 31 °C.

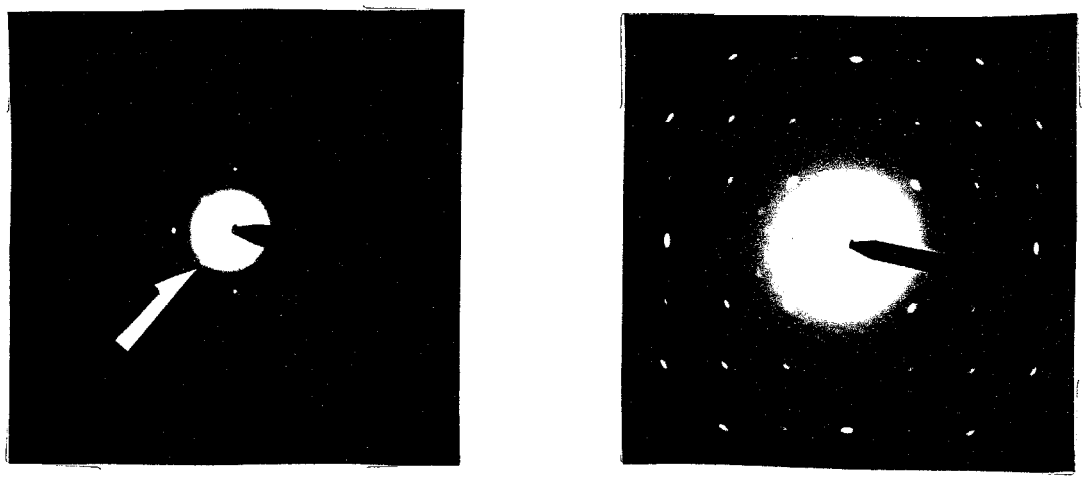

FIG. 6.11. The EDP of 100-Å AlPcCl/KI deposited at 31 °C. Two pictures are shown to clarify the inside and outside patterns. They are coupled to the EDP of Fig. 6.13. The white arrow indicates the one of the most inside spots.

tetragonal phase was newly identified in this film. The presence of additional weak diffraction spots and the weak traces of rings corresponding to the tetragonal lattices in the EDP indicates that the degree of crystal order is a little poorer than that of $(AlPcF)_n$/KBr film.[1] Unidirectional tetragonal epitaxy is also known in $(AlPcF)_n$/KI, whose degree of epitaxy is lower than that of $(AlPcF)_n$/KBr.[1] The epitaxial lattice direction of AlPcCl/KI was determined by the coupled sample technique where AlPcCl/KCl was used as a standard. The result is described after the discussion of AlPcCl/KCl.

The EDP of the 100-Å films on KBr and KCl deposited at 31 and 29 °C are shown in Figs. 6.12 and 13. They were assigned to $\sqrt{10}\times\sqrt{10}$-type epitaxy since the reciprocal-lattice points for $\sqrt{10}\times\sqrt{10}$-epitaxy (Fig. 6.2) agree well with the EDP. The type of the epitaxy in AlPcCl/KBr is different from that of $(AlPcF)_n$/KBr. The former is $\sqrt{10}\times\sqrt{10}$ and the latter is 3×3. This leads to the conclusion that both KBr and KI substrates may be useful to obtain a unidirectional epiatxial film.

For the unidirectional tetragonal phase found in AlPcCl/KI, two possible types of epitaxy, 3×3 (Fig. 6.1) and $\sqrt{8}\times\sqrt{8}$ (Fig. 6.14) were considered. The epitaxial lattice direction was determined by the coupled sample technique. The coupled films were prepared by using AlPcCl/KCl as a standard. A rod was fixed in front of a negative film for the TEM picture. During observation, the sample was translated but never rotated. The results are shown in Figs. 6.11 and 13, where the position of the rod is fixed. We can determine KCl [010] direction from the EDP of AlPcCl/KCl (Fig. 6.13) since

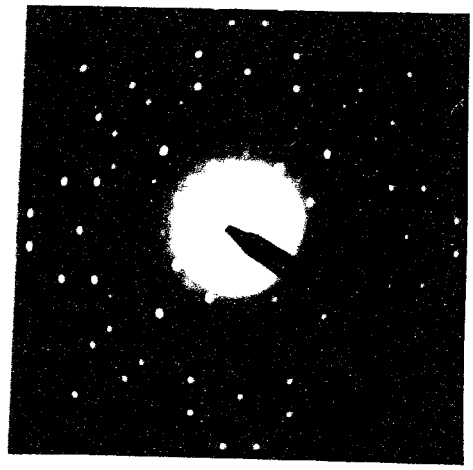

FIG. 6.12. The EDP of 100-Å AlPcCl/KBr deposited at 31 °C.

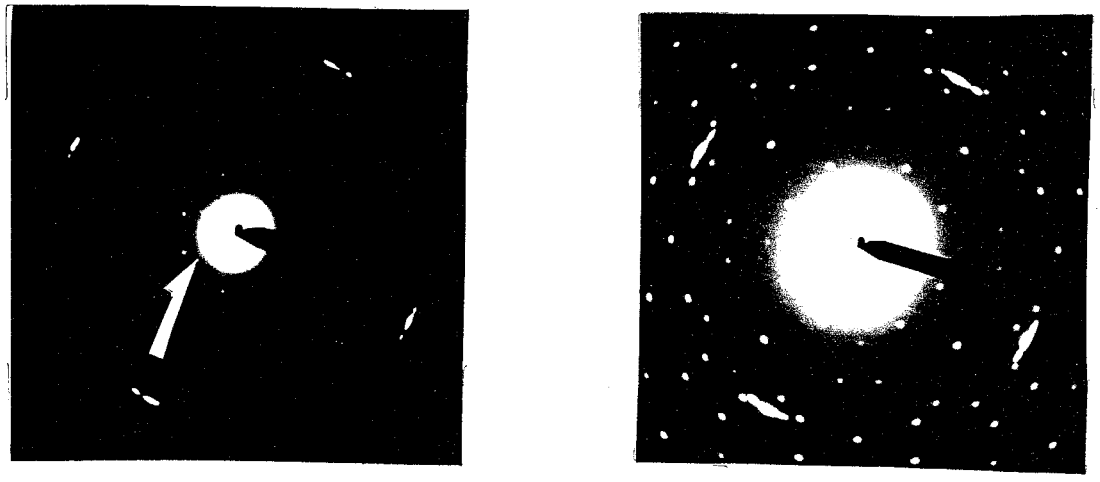

FIG. 6.13 The EDP of 100-Å AlPcCl/KCl deposited at 29 °C. Two pictures are shown to clarify the inside and outside patterns. They are coupled to the EDP of Fig. 6.11. The white arrow indicates the one of the most inside spots.

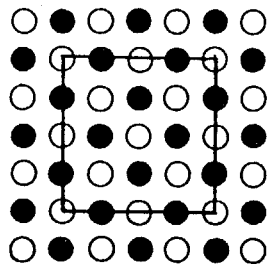

FIG. 6.14. The epitaxial structure AX(100)($\sqrt{8}\times\sqrt{8}$) on NaCl-type alkali halides AX. The AX ions are shown as open and solid circles.

the type of the epitaxy on KCl is $\sqrt{10}\times\sqrt{10}$. By using the rod as a standard direction, we can also determine KI [010] direction in AlPcCl/KI sample (Fig. 6.11). In this way, we found that the AlPcCl square lattices are in the KI [011] direction, which leads to the conclusion that this is 3×3-type epitaxy. To determine the epitaxial lattice direction, this technique is more reliable than semistripped method,[1] since semistripped method often gives scattered results because of the destruction of the substrate in the stripping process. The EDP shows the epitaxial order over the electron-beam sampling area (5 μm). However, if the epitaxy does not occur over the entire film, the coupled sample technique cannot be applied. Thus, good reproducibility of this technique indicates that the epitaxy occurs over the entire film. The additional weak spots found in the EDP of AlPcCl/KI indicate the presence of additional phase, which is not determined since their intensities are too weak.

The EDP of the 100-Å AlPcCl film on NaCl deposited at 31 °C is shown in Fig. 6.15. It is evident that new bidirectional $\sqrt{13}\times\sqrt{13}$-type epitaxy, NaCl(100)($\sqrt{13}\times\sqrt{13}$)R±11°-AlPcCl, where ±11° corresponds to $\pm\tan^{-1}(1/5)$, is realized since the corresponding reciprocal-lattice points agree well with the EDP (Fig. 6.16). Besides predominant $\sqrt{13}\times\sqrt{13}$-type epitaxy, few additional spots are found in the EDP, which are not assigned at present since they are too few to determine the phase.

2. VOPc

The TEM lattice image of VOPc/KBr is shown in Fig. 6.17.

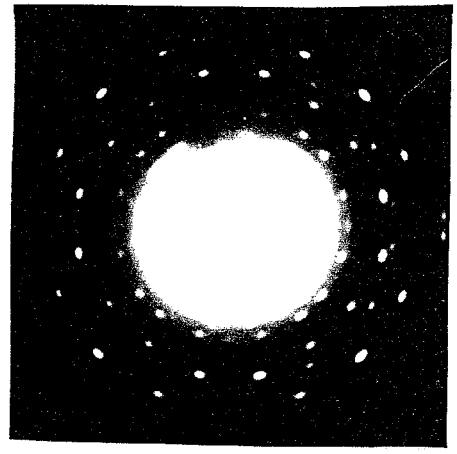

FIG. 6.15. The EDP of 100-Å AlPcCl/NaCl deposited at 31 °C.

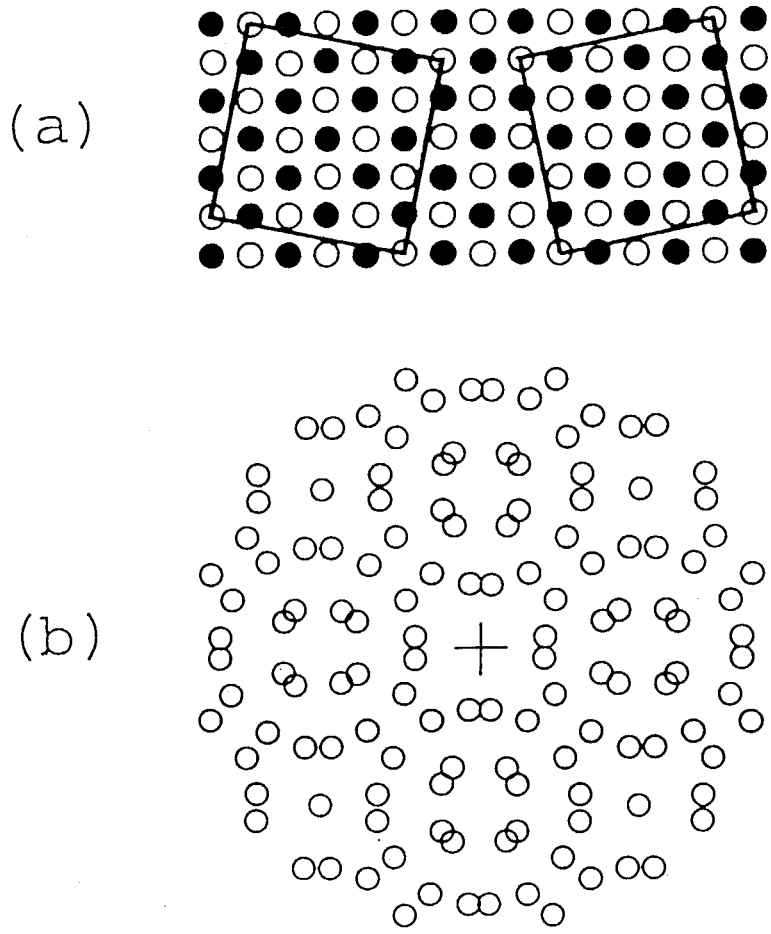

FIG. 6.16. (a) The epitaxial structure AX(100)($\sqrt{13}\times\sqrt{13}$)R$\pm$11° on NaCl-type alkali halides AX. The AX ions are shown as open and solid circles and (b) its reciprocal-lattice points.

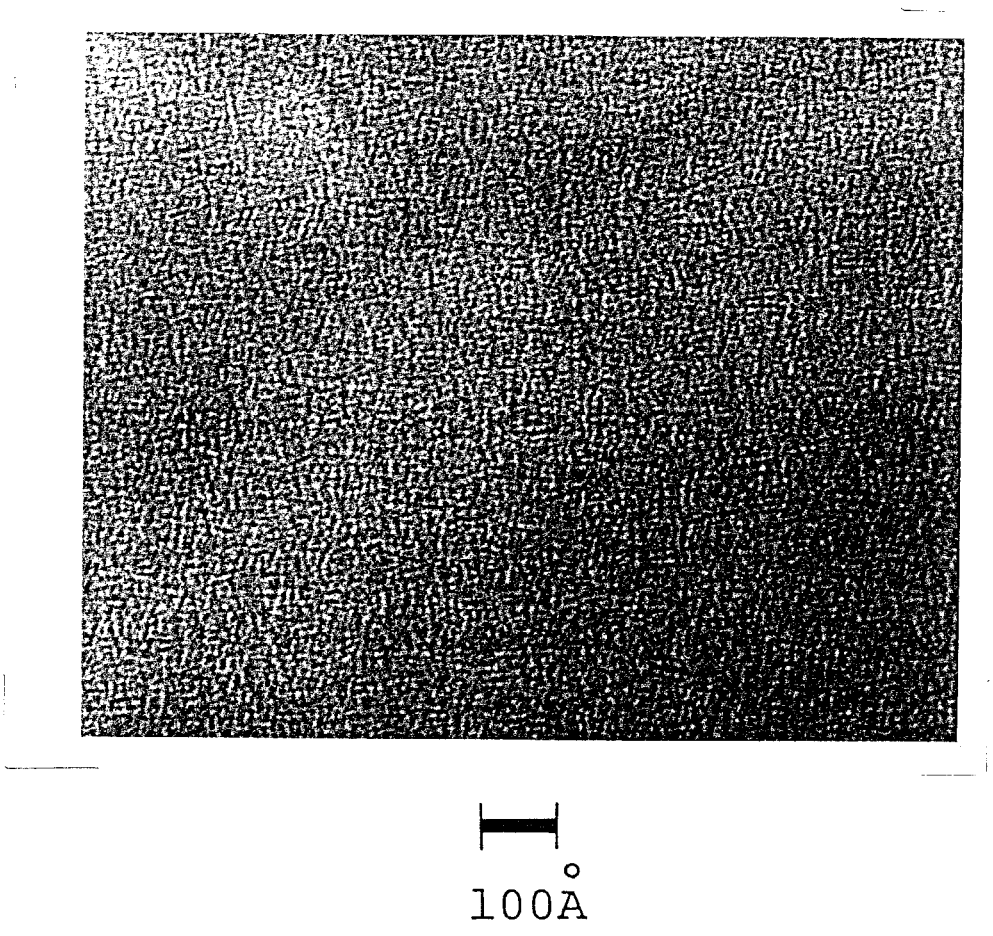

FIG. 6.17. The TEM lattice image of 100-Å VOPc/KBr deposited at 29 °C.

The lattices correspond to the stacked columns that are perpendicular to the substrate. The EDP in Fig. 6.18 shows that the film is made of unidirectional tetragonal phase. This feature is the same as the reported structure of $(AlPcF)_n/KBr$[1] and AlPcCl/KI, so the epitaxy of VOPc/KBr can be explained by 3×3-type epitaxy (Fig. 6.1). In bulk crystals, three phases are known [Fig. 6.4(b)],[15,16] but the tetragonal phase has not been identified yet.

The EDP of VOPc/KCl is shown in Fig. 6.19. This is assigned to √10×√10-type epitaxy, since the reciprocal-lattice points for √10×√10-epitaxy (Fig. 6.2) coincide well with the EDP. This result is consistent with the reported model by Tada *et al.* based on RHEED patterns.[6]

6-4. DISCUSSION

Table 6.1 shows the unit lattice lengths of the substrates and the cases in which epitaxy was found in this study. This table reveals the importance of lattice matching since all observed types of the epitaxy in this study are found in the range from 14 to 15-Å of the unit lattice lengths, though it is difficult to predict the epitaxy uniquely. On the basis of these findings, it may be possible to make an assumption that this simple behavior could be derived from the protrudent atoms of the Pcs. If the interaction between the protrudent atom of the Pc and the alkali metal ion of the substrate dominates the epitaxial growth, the distance between the Pc ring and the substrate will be longer. According to Ashida, the nitrogen

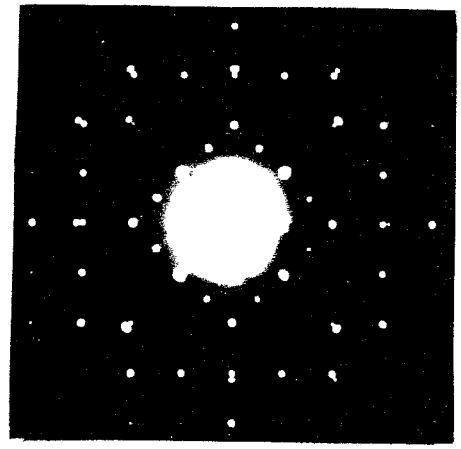

FIG. 6.18. The EDP of 100-Å VOPc/KBr deposited at 29 °C.

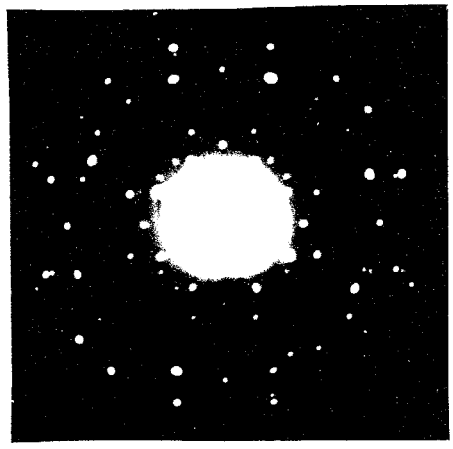

FIG. 6.19. The EDP of 100-Å VOPc/KCl deposited at 32 °C.

TABLE 6.1. Unit lattice lengths of the square epitaxial nets of the substrates. The epitaxial lattices are found in the underlined cases in this table.

epitaxy	Unit lattice length (Å)			
	NaCl	KCl	KBr	KI
√8×√8				14.132
3×3		13.352	<u>13.992</u>[b]	<u>14.989</u>[a]
√10×√10	12.611	<u>14.074</u>[a,b]	<u>14.749</u>[a]	15.800
√13×√13	<u>14.379</u>[a]	16.047	16.817	

[a] AlPcCl

[b] VOPc

atoms of the Pc ring are assumed to interact with the metal ions of alkali halide substrate, and such interaction results in rather fixed orientation of the Pc ring on the substrate.[17] This fixing effect and Pc-Pc van der Waals interaction lead to the preference of $\sqrt{10}\times\sqrt{10}$-type epitaxy in the staggered Pc.[4] Actually $\sqrt{10}\times\sqrt{10}$ is the predominant epitaxy of staggered $LuPc_2$ even on KI substrate.[18] If the protrudent atom of the Pc dominates the interaction with the substrate, Ashida's fixing effect will be reduced and the Pc ring can be rotated from the fixed orientation on the substrate. 3×3-type epitaxy will be realized under this condition since van der Waals repulsion makes 3×3-type epitaxy difficult under the fixing effect (Fig. 6.20). In this case, the epitaxial lattice direction will be simply determined by the degree of lattice matching between Pc and the substrate and this might be the case of $(AlPcF)_n$, AlPcCl, and VOPc. The occurrence of unidirectional epitaxy and good continuity in $(AlPcF)_n$, AlPcCl, and VOPc films suggests the possibility that the nature of Pc-substrate interaction of these Pcs might be different from that of $LuPc_2$. More extensive studies such as low-energy electron diffraction,[19] RHEED,[6,20] and scanning-tunneling microscopy[21] should be done to reveal the orientation of the first layer and to ascertain this hypothetical mechanism for the unidirectional epitaxy.

6-5. SUMMARY

The MBE technique was successfully applied to obtain epitaxial AlPcCl films on NaCl, KCl, KBr and KI(100) and VOPc

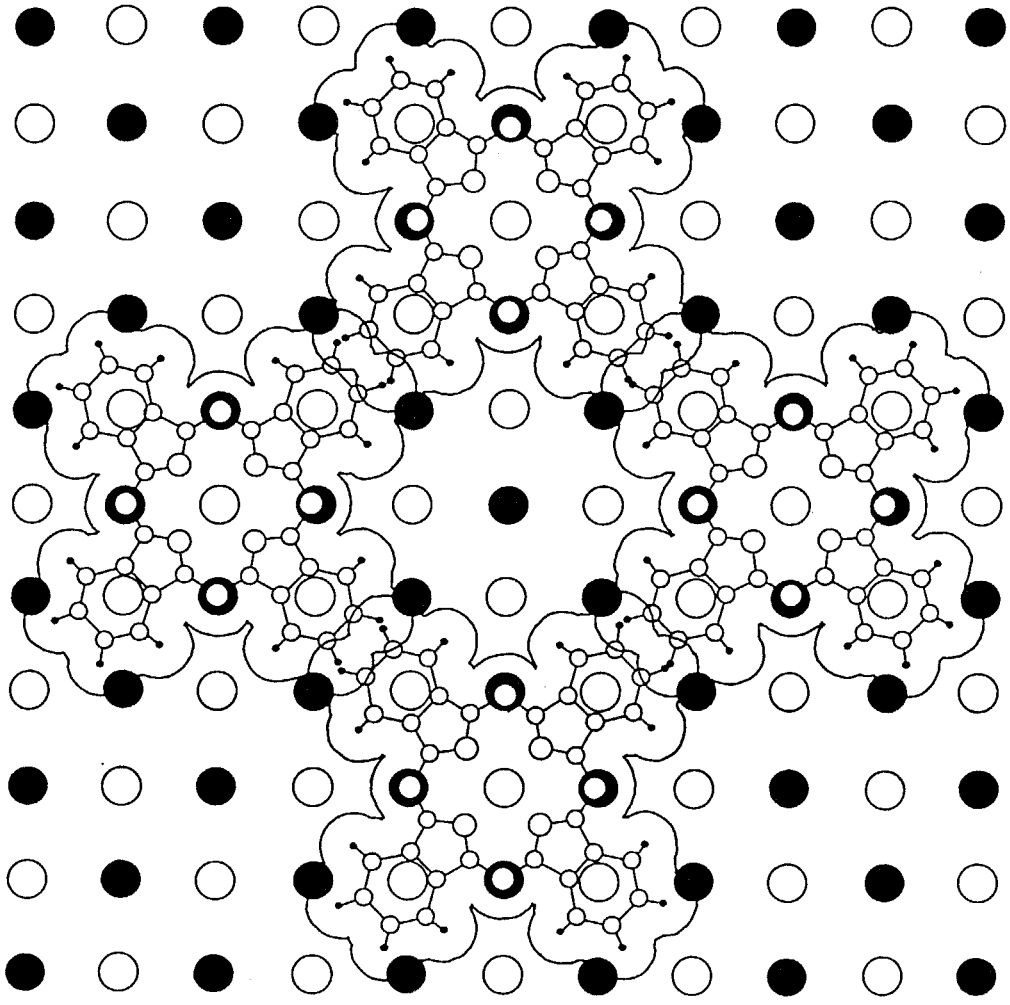

FIG. 6.20. A molecular packing model for 3×3-type epitaxy on KI substrate under the assumption of Ashida's constraint.

films on KCl and KBr(100). The films were continuous and made of tetragonal phase that is different from the phases in the single crystals. The predominant epitaxy of AlPcCl/NaCl was newly found bidirectional $\sqrt{13}\times\sqrt{13}$. The epitaxy of AlPcCl/KCl and VOPc/KCl was bidirectional $\sqrt{10}\times\sqrt{10}$. The epitaxy of AlPcCl/KBr was bidirectional $\sqrt{10}\times\sqrt{10}$, while that of VOPc/KBr was unidirectional 3×3. The predominant epitaxy of AlPcCl/KI was unidirectional 3×3, which was determined by the newly introduced coupled sample technique. The epitaxy found suggests the importance of the lattice matching and the protrudent atoms of the Pc molecules.

REFERENCES

[1]Chapter 2 in this thesis.

[2]Chapter 3 in this thesis.

[3]W. P. Zhang, K. H. Kuo, Y. F. Hou, and J. Z. Ni, J. Solid State Chem. **75**, 373 (1988).

[4]Chapter 4 in this thesis.

[5]Chapter 5 in this thesis.

[6]H. Tada, M. Sakurai, K. Saiki, and A. Koma, in Abstract of the 37th Spring Meeting of Japan Appl. Phys. Soc. Saitama, 1990, Vol. 3, p. 999.

[7]T.-H. Huang, J. Phys. Soc. Jpn. **56**, 1213 (1987).

[8]T. Wada, S. Yamada, Y. Matsuoka, C. H. Grossman, K. Shigehara, H. Sasabe, A. Yamada, and A. F. Garito in *Nonlinear Optics of Organics and Semiconductors*, edited by T. Kobayashi (Springer, Berlin, 1989), p. 292.

[9]D. Guay, J. P. Dodelet, R. Cote, C. H. Langford, and D.

Gravel, J. Electrochem. Soc. **136**, 2272 (1989).

[10]D. Guay, G. Veilleux, R. G. Saint-Jacques, R. Cote, and J. P. Dodelet, J. Mater. Res. **4**, 651 (1989).

[11]See, for example, A. Zunger and K. Bar-Eli, IEEE J. Quantum Electron. **QE-10**, 29 (1974).

[12]Z. Z. Ho, C. Y. Ju, and W. M. Hetherington III, J. Appl. Phys. **62**, 716 (1987).

[13]See, for example, T. Kobayashi, K. Yase, and N. Uyeda, Acta Crystallogr. Sect. **B40**, 263 (1984).

[14]K. J. Wynne, Inorg. Chem. **23**, 4658 (1984).

[15]C. H. Griffiths, M. S. Walker, and P. Goldstein, Mol. Cryst. Liq. Cryst. **33**, 149 (1976).

[16]R. F. Ziolo, C. H. Griffiths, and J. M. Troup, J. Chem. Soc. Dalton 2300 (1980).

[17]M. Ashida, Bull. Chem. Soc. Jpn. **39**, 2632 (1966).

[18]It seems that tetragonal and orthorhombic phases are present in $LuPc_2$/KI. Strong electron diffraction spots corresponding to the tetragonal phase are seen near the reciprocal-lattice points for $\sqrt{10}\times\sqrt{10}$-type epitaxy, though their correspondence is imperfect. H. Hoshi, A. J. Dann, and Y. Maruyama (unpublished).

[19]J. C. Buchholz and G. A. Somorjai, J. Chem. Phys. **66**, 573 (1977).

[20]M. Hara, H. Sasabe, A. Yamada, and A. F. Garito, Jpn. J. Appl. Phys. **28**, L306 (1989).

[21]P. H. Lippel, R. J. Wilson, M. D. Miller, Ch. Wöll, and S. Chiang, Phys. Rev. Lett. **62**, 171 (1989).

CHAPTER 7 CONCLUSION

As described in chapter 1, this study has started with the aim of looking for the condition that provides high-quality ultrathin organic films by using the MBE technique. At starting point, the following questions have arisen.

Is epitaxial growth possible ?

If possible, what is the condition ?

This study has shown that the epitaxial growth can be realized in the system of phthalocyanines on alkali halide substrates. The following types of epitaxy have been found.

KCl(100) ($\sqrt{10}\times\sqrt{10}$) R$\pm$27°-$(AlPcF)_n$ and KBr(100) (3×3) R45°-$(AlPcF)_n$ in chapter 2.

KBr(100) ($\sqrt{10}\times\sqrt{10}$) R$\pm$27°-$LuPc_2$, KBr(100) (3×3) R45°-$LuPc_2$ / $(AlPcF)_n$, and KBr(100) C(6×3)-$LuPc_2$ / $(AlPcF)_n$ in chapter 4.

KBr(100) ($\sqrt{10}\times\sqrt{10}$) R$\pm$27°-LiPc and KBr(100) ($\sqrt{10}\times\sqrt{12.5}$)-LiPc in chapter 5.

NaCl(100) ($\sqrt{13}\times\sqrt{13}$) R$\pm$11°-AlPcCl, KCl(100) ($\sqrt{10}\times\sqrt{10}$)R$\pm$27°-AlPcCl, KBr(100) ($\sqrt{10}\times\sqrt{10}$) R$\pm$27°-AlPcCl, KI(100) (3×3)R45°-AlPcCl, KCl(100) ($\sqrt{10}\times\sqrt{10}$)R$\pm$27°-VOPc, and KBr(100) (3×3)R45°-VOPc in chapter 6.

In particular, single-crystalline unidirectional epitaxy (3×3) has been realized in $(AlPcF)_n$ / KBr, AlPcCl / KI, and VOPc / KBr.

Strange behavior of ultrathin films has been found in the uv / visible spectra of $(AlPcF)_n$ as described in chapter 3.

The author believes that further development of this technique promises to make progress in the study of ultrathin

organic films.